Vibration Attenuation of the NASA Langley Evolutionary Structure Experiment Using H_∞ and Structured Singular Value (μ) Robust Multivariable Control Techniques

Midyear Report

NASA Contract: NASA/NAG-1-1254

Gary J. Balas
Aerospace Engineering and Mechanics
107 Akerman Hall
University of Minnesota
Minneapolis, MN 55455
612.625.6857

9 March, 1992

1 Introduction

This report investigates the use of active control to attenuate structural vibrations of the NASA Langley Phase Zero Evolutionary Structure due to external disturbance excitations. H_∞ and structured singular value (μ) based control techniques are used to analyze and synthesize control laws for the NASA Langley Controls-Structures Interaction (CSI) "Evolutionary Model" (hereon denoted by CEM) [Bel91,LimB]. The CEM structure experiment provides an excellent test bed to address control design issues for large space structures. Specifically, control design for structures with numerous lightly damped, coupled flexible modes, collocated and noncollocated sensors and actuators and stringent performance specifications. The performance objectives are to attenuate the vibration of the structure due to external disturbances, and minimize the actuator control force.

The control design problem formulation for the CEM Stucture uses a mathematical model developed and refined by NASA researchers with finite element techniques. A reduced order state space model for the control design model is formulated from the finite element model. It is noted that there are significant variations between the design model and the experimentally derived transfer function data. These model inaccuracies or *uncertainties* take the form of unknown parameter values, natural frequencies, damping levels, and unmodeled high frequency dynamics. Control laws are designed which accounted for these uncertainties and it is seen that the incorporation of errors between the physical system and its mathematical models into the design process is essential to achieve the desired performance objectives.

2 CSI Evolutionary Model

The structure shown in figure 1 is the CEM structure located at NASA Langley Research Center. The main section of the truss is approximately 50 feet long to which are attached two vertical appendages. Mounted on the short appendage is a 16 ft. diameter reflector with a circular mirror attached to its center. A laser beam whose source is attached to the end of a vertical appendage is pointed at the mirror. The laser beam reflection from the mirror is detected by a spatially fixed optical detector array (target plant) mounted approximately 60 ft. above the structure.

A finite element model of the CEM structure was developed by NASA Langley researchers. The model contained 86 modes corresponding to all of the CEM structural

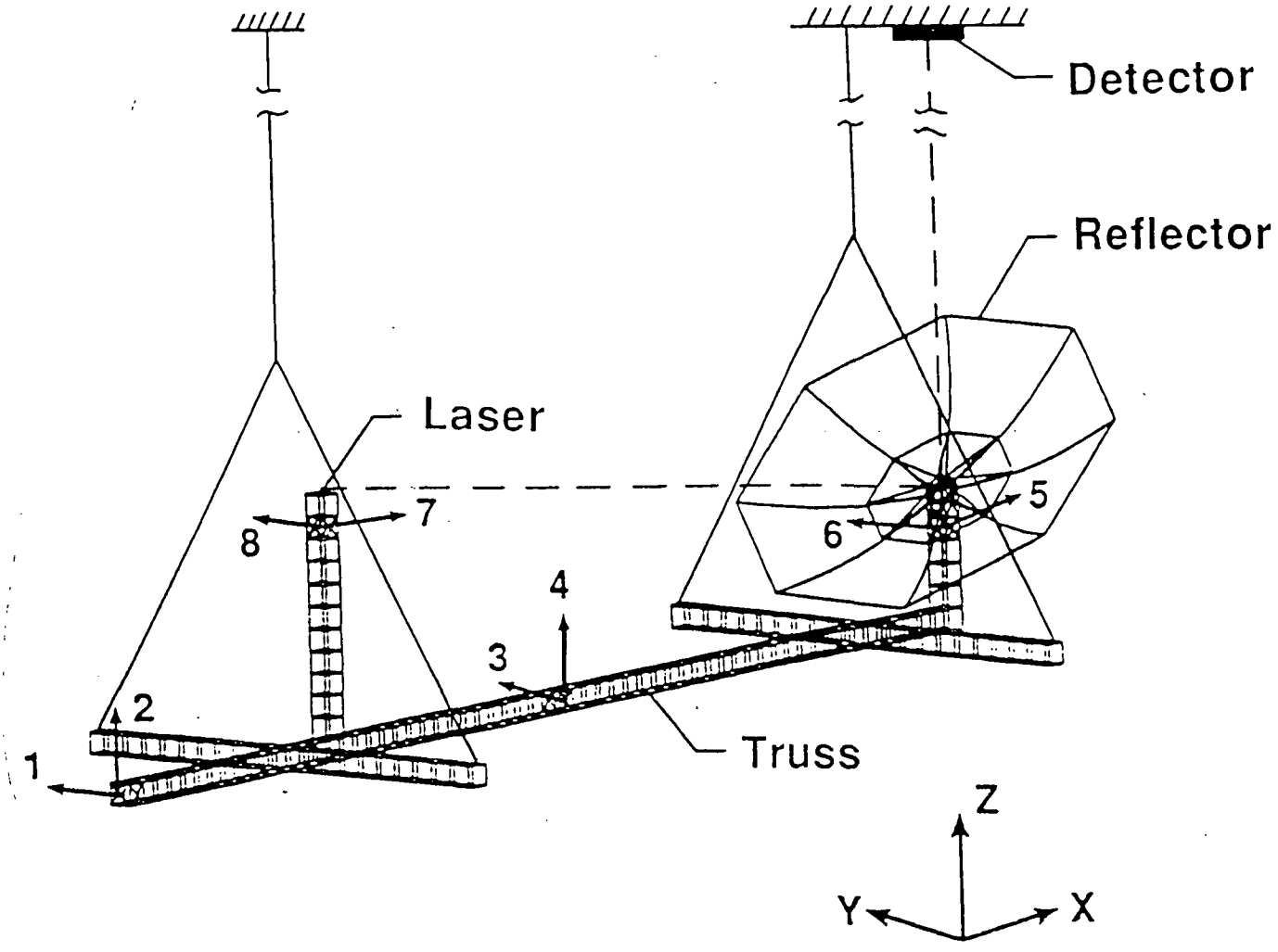

Figure 1: Schematic of the NASA Langley Controls-Structures Interaction (CSI) Evolutionary Structure (CEM)

Mode	Frequency (rad/s)	Mode	Frequency (rad/s)
1	0.924	2	0.937
3	0.975	4	4.587
5	4.699	6	5.491
7	9.258	8	10.921
9	11.831	10	14.460
11	17.835	12	25.225
13	25.335	14	26.425
15	27.595	16	34.566
17	38.827	18	39.149
19	40.658	20	41.908
21	46.322	22	52.108
23	56.337	24	78.451
25	105.89		

Table 1: CEM Modes and Natural Frequencies

modes under 50 Hz. A 25 mode reduced order model of the structure, based on the 86 mode finite element model, is obtained through a controllability and observability analysis. These 25 modes correspond to the set of modes below 20 Hz that significantly contribute to the measured accelerations and LOS displacements. The first six lowest frequency modes are the pseudo rigid body modes (pendulum modes) which range from 0.14 Hz to 0.87 Hz, the seventh and eight modes are the first horizontal and vertical plane bending modes respectively. Table 1 contains the natural frequency of each mode in the CEM reduced order control design model.

For this study, the eight air actuators are used for control and the eight nearly collocated accelerometers are the measurements used for feedback (see Fig. 1). A $50th$ order, 8 input and 8 output, state-space model of the CEM structure, denoted as `mod25`, is constructed from the 25 mode reduced order finite element model for control analysis.

Model of the air actuators are taken as a constant gain in all the problem formulations since the bandwidth of the actuators are $50Hz$, which is significantly higher than design model. Similarly, the accelerometers, which have a bandwidth of $200Hz$, are treated as constant gains in the control designs. For further details on the evolutionary structure one is referred to References [Bel91].

3 Control Design Models for the CEM Structure

A measure of the accuracy of the control design model or alternatively a measure of the model error is needed in the control analysis and synthesis process. Transfer functions between the CEM control actuators and sensors were derived experimentally via Fourier Transform techniques by NASA researchers to access the accuracy of the control design model. Significant differences were noted between the experimental transfer function data and the $50th$ state-space model, `mod25`, above 4 Hz. Figures A1, A2, A3, A4, A5 and A6 in Appendix A contain plots of the experimentally derived transfer functions and `mod25` transfer functions between air actuator 2 and acceleroemeter 2, air actuator 2 and accelerometer 4, air actuator 3 and accelerometer 3, air actuator 4 and accelerometer 4, air actuator 6 and accelerometer 6, and air actuator 8 and accelerometer 6.

The variation between the experimentally derived transfer functions and the design model are accounted for in the control design process via unstructured uncertainty models. An additive uncertainty model is used to account for neglected structural modes in the design model. An actuator input uncertainty model is used to incorporate any errors between the experimental data and the $50th$ state-space model which occur within the control bandwidth. Alternatively, these modeling inaccuracies could have been described by parametric uncertainty in the natural frequencies, damping values and mode shapes of the control design state-space model. Initially, the uncertainty models in the control problem formulation are restricted to unstructured multiplicative input uncertainty and additive uncertainty. Describing the modeling errors as parametric uncertainty in the natural frequencies, damping values and mode shapes of the control design model is addressed in the paper on design of controllers to achieve line-of-sight (LOS) performance requirements for the CEM structure [LimB].

The additive uncertainty weight is selected such that the magnitude of the its transfer function description bounds the peaks of the neglected structural modes. Hence, the additive uncertainty weight is highly dependent on the level of damping assumed in the design model. The damping values associated with the structural modes of the CEM are difficult to predict, therefore based on estimates by engineers at NASA Langley, a value of 0.5% damping is assumed for all of the flexible modes in the control design model. The additive uncertainty weights are chosen accordingly.

Eight additive uncertainty weights are formulated based on the variation between the control design model and the experimentally derived transfer function data. Each weight corresponds to the input/output relationship between an air actuator and the eight accelerometer measurements. The additive uncertainty weights are varied in the design

process to determine their effect on the closed-loop robustness and performance of the controllers synthesized with the μ-framework.

Three models of the CEM structure are used in the control design problem formulation. All of these models have 8 actuator inputs and 8 sensor outputs. `mod25r` is a 22 state model of the CEM structure, containing the first eleven structural modes between 0 and 4 Hz. The 14 modes between 4 and 10 Hz, which are in the 50 state model `mod25` but not `mod25r`, are treated as unmodeled dynamics along with all of the higher frequency structural modes not included in the $50th$ order design model. `mod25r` is the design model used in the control problem formulations 1 through 4.

Design model `mod25r2` consists of the first eleven modes of the CEM structure along with the next ten structural modes, for a total of 42 states. This model describes the CEM structure between 0 and 6.8 Hz. As before, the neglect structural modes and higher frequency modes are accounted for in the control problem formulation via additive uncertainty models. The goal of this model is to increase the bandwidth of the controller to attenuate vibrational modes of the CEM structure up to 6.8 Hz. `mod25r2` is the model of the CEM structure used in control problem formulations 6 through 8. Design model `mod25z` consists of the first 15 modes of the CEM structure. The first eleven modes are the same as `mod25r` with modes 12 through 15 at 25.2, 25.3, 26.4 and 27.6 rad/sec. The additional modes of the structure are included near the bandwidth of the closed-loop system to evaluate their effect on the robustness properties of the control design. Control problem formulation 9 uses `mod25z` in the control design process.

All of the controllers synthesized with the three models of the CEM structure are simulated with the $50th$ order state-space model and implemented on the real CEM structure.

4 The Structured Singular Value (μ) Framework

The structured singular value (μ) framework is used to analyzes the robustness of model sets to structured and unstructured uncertainties and synthesize controllers which achieve desired robust performance objectives. The model sets are constructed for the each control problem formulation by introducing perturbations, of the appropriate magnitude, in all uncertain parameters associated with the design model. The new design model encompasses a set of uncertain systems defined by a model whose parameters lie in the set plus the norm-bounded unstructured uncertainty.

The μ-framework is used to analyze and synthesize controller for the Evolutionary Phase

Zero Structure. It provides a quantitative way of measuring robustness and performance in the same framework. The generic model structure, figure 2, is based on linear fractional transformations (LFT). Any linear interconnection of inputs, outputs and commands along with perturbations and a controller can be viewed in this context and rearranged to match this diagram [Doy1]. Figure 3 (a) is a diagram of the control analysis problem. The analysis problem assumes a controller K has been provided and the bottom loop of the augmented plant P has been closed. The goal is to determine the stability of the closed-loop system in the presence of the norm-bounded uncertainty block Δ. The controller synthesis problem is shown in figure 3 (b). The goal is to design a controller K which minimizes the size of the output errors e' due to a set of norm-bounded input v' in the sense of the structured singular value, μ.

The following are references that provide the background on μ-analysis and synthesis techniques [Doy1, Doy2, Pack, Mutools, Balas, BalDoy1, BalDoy2, DoyLP].

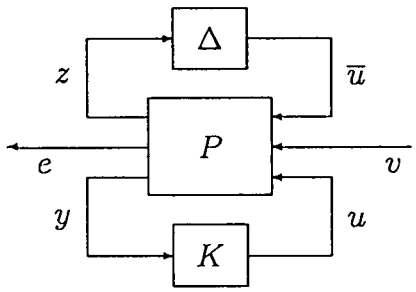

Figure 2: General Interconnection Structure

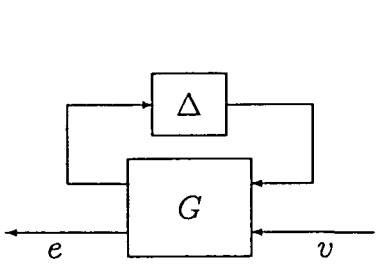

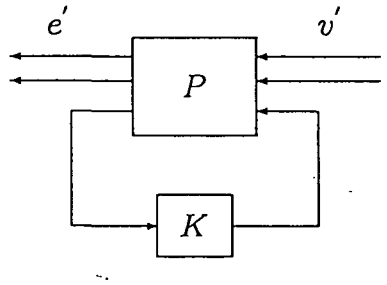

Figure 3: (a) Analysis and (b) Synthesis Problem

5 Control Objectives

The performance objective is to attenuate the sensed vibration at accelerometer locations 1 through 8. These sensors are nearly collocated with air actuators 1 through 8. The disturbances used to excited the structure enter at air thruster 1, 2, 6, and 7. The performance criteria is defined as minimizing the $||\cdot||_\infty$ norm of the transfer function from the input disturbances to accelerometers 1 through 8. In problem formulations 1 and 3, the performance objective is to attenuate only the structural modes which affect sensors 1, 2, 7, and 8. The input disturbances are modeled in the control problem formulation as white noise inputs to the air actuators. It was decided not to use filtered white noise in the problem formulation to reduce the number of states in the control design.

Approximation of the input signals as white noise is based on H_∞ norm requirement to attenuate the resonant peaks of the disturbance to error transfer function. The highest resonance peak will receive the most attention from the controller since it corresponds to the largest gain from input to output. The resonance peaks of the CEM structure are two order of magnitude larger than the steady state gain of the transfer function at high frequency. Therefore, filtering the input or performance weight isn't required since the high frequency gain of the system is a factor of 100 lower than the resonant peaks. To verify this control design 6 through 8 filter the performance weight, which has little effect on the performance of the controllers.

6 Control Problem Formulation

The control problem formulation interconnection structure is shown in figure 4. The problem formulation is the same for the eight control designs with the additive uncertainty weight, *Addunc*, input multiplicative uncertainty weight, *actu*, and performance weight $perfwt$ varying with each design. The goal of the control design is to minimize the low frequency vibration of the accelerometers due to input disturbances entering at air actuators 1, 2, 6 and 7. The controllers are tested by inputting a disturbance signal into the air thrusters for 9 seconds, terminating the disturbance signal and allowing the CEM structure to vibrate in the open-loop configuration for one second, on implementing the controller which uses the air thrusters to attenuate the induced vibrations.

Four input disturbances are used to excite the CEM structure experimentally. Disturbance signal 1, $2\sin(9.24t)$, is input to air thruster 1 to excite the first X-Y bending

mode, disturbance signal 2, $0.5\sin(10.93t)$ is input to actuator 2 to excite the first X-Z bending mode, disturbance signal 3, $2\sin(.974t)$, is input to actuator 7 to excite the yaw pendulum mode and the fourth disturbance signal, $0.5\sin(.924t)$, is input to actuator 8 to excite the X pendulum mode. The disturbance signals are treated as pure white noise inputs into the system.

The uncertainty descriptions in the control design problem formulation defined the set of plant models in which the actual CEM structure is assumed. The performance weights are used to define the vibration attenuation requirements at each accelerometer location.

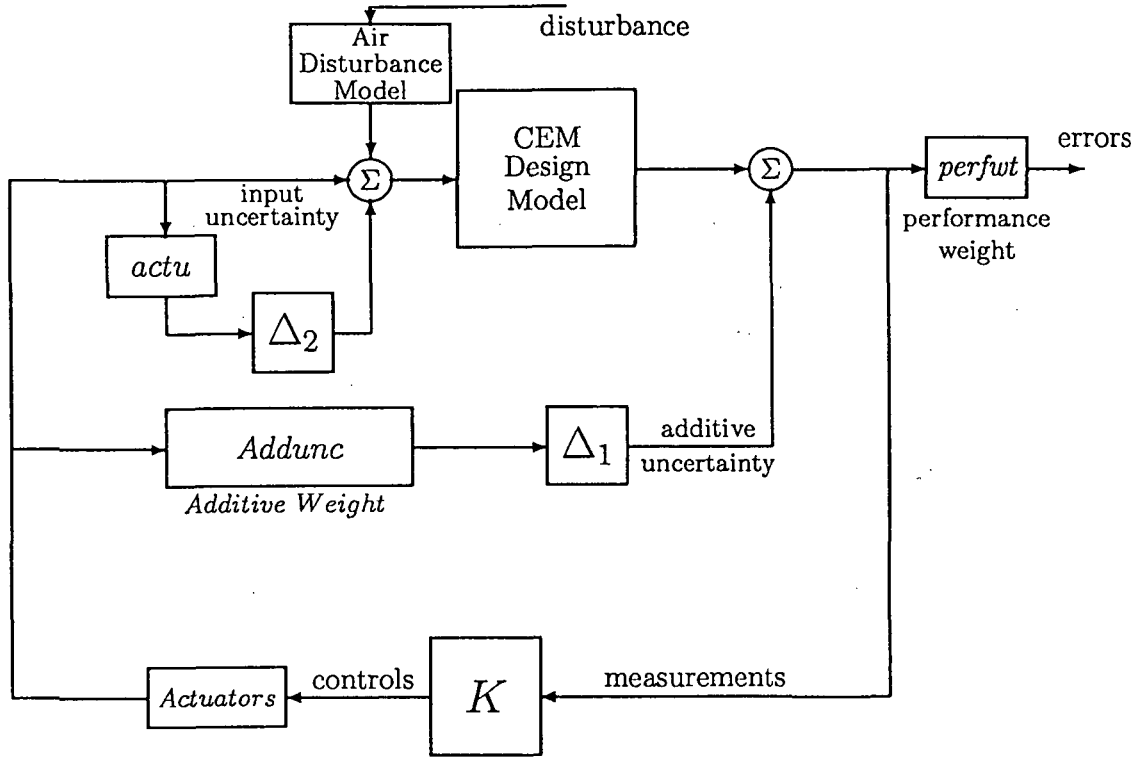

Figure 4: CEM Control Problem Formulation

7 Uncertainty Models

Two types of uncertainty are used to account for modeling errors between the design model and experimentally derived transfer functions. An input multiplicative uncertainty accounts for variations between the model and the real structure within the con-

trol bandwidth and an additive uncertainty model accounts for unmodeled dynamics. The additive uncertainty ensures that the controller will not destablize the unmodeled modes of the structure, provided the nominal structural model and the additive uncertainty description accurately represent the dynamics of the CEM structure.

The input multiplicative uncertainty weight is selected to be a constant in first seven of the eight control designs. The reasoning behind this is that the input uncertainty weight is only important within the control bandwidth. Outside the control bandwidth the additive uncertainty weight dominates the control problem and it is difficult to determine the differences in the modeling error of the pendulum modes as compared with the first bending modes, hence the same level of uncertainty is selected for both. Another approach to account for the modeling error is to include parametric uncertainty in the natural frequency and damping coefficients in the control design model. This is the approach taken to design controllers to minimize LOS errors due to external disturbances excitations [LimB].

Experimental results have indicated that as long as some input uncertainty is included in the problem formulation, the controllers will be robust to errors within and the performance will not be significantly degraded [Balas, BalDoy2]. Determining the correlation between a minimal level of uncertainty and a large amount of uncertainty is an area of research which will be pursued this year by the principal investigator.

Table 2 contains the actuators, sensors, uncertainty weights and performance weights used in the control problem formulations to synthesize the eight controllers. Note that there is no control design 5. μ-synthesis techniques based on $D-K$ iteration are used to design the controllers to achieve robust performance for the given problem formulation. The eight controller designed all had on the order of 80 states prior to being reduced. The large number of states is due to the order of the conrol design model, additive uncertainty weights and D-scaling used in the $D-K$ iteration process. The reduced order controllers for each design, the controller order reduction is done using balanced realization techniques, are listed in Table 2.

8 Control Design Results

All eight of the controllers designed using the μ-synthesis techniques resulted in a stable closed-loop system and performed very well when implemented on the experimental CEM structure. Control design 9 achieved the best performance of any controller previously tested. These results indicate that the μ-framework is ideally suited for the analysis

Design	Model	Sensors	Actuators	Input Uncertainty	Additive Uncertainty	Performance Weight	Controller Order
1	mod25r	1,2,7,8	1,2,7,8	10%	addwt 1,2,7,8	10:1	28
2	mod25r	$1 \rightarrow 8$	$1 \rightarrow 8$	10%	addwt $1 \rightarrow 8$	10:1	36
3	mod25r	1,2,7,8	1,2,7,8	2%	addwt 1,2,7,8	10:1	30
4	mod25r	$1 \rightarrow 8$	$1 \rightarrow 8$	1%	addwt $1 \rightarrow 8$	10:1	40
6	mod25r2	$1 \rightarrow 8$	$1 \rightarrow 8$	1%	addwt $1 \rightarrow 8$	10:1, filters	50
7	mod25r2	$1 \rightarrow 8$	$1 \rightarrow 8$	10%	addwt $1 \rightarrow 8$	8:1, filters	50
8	mod25r2	$1 \rightarrow 8$	$1 \rightarrow 8$	$\frac{100(s+20)}{s+2000}$	addwt $1 \rightarrow 8$	8:1, filters	38
9	mod25z	$1 \rightarrow 8$	$1 \rightarrow 8$	10%	addwt $1 \rightarrow 8$	perfwt9	44

Table 2: Control Problem Formulation Uncertainty and Performance Weights

and synthesis of controllers for flexible structures with numerous, lightly damped modes and multiple actuators and sensors. Experimental results of open-loop system and the eight controllers are located in Appendix A, figures A7 to A42. The experiments on the CEM structure use four disturbance signals input to actuator 1, 2, 7 and 8 to excite the structure. The open-loop accelerometer responses of sensor 1 through 8 and actuator 1 through 8 inputs are shown in figures A7 through A10.

Controller 1 was designed using only four of the eight air actuators available. It was implemented on the actual CEM structure and performed as well as the previous best controller. Controller 2, used the same uncertainty and performance weights as control design 1, employed all eight actuators and sensors for control. The improvement in performance was limited, although only one set of disturbance excitations were used in the experiments. The most notable improvement with controller 2 was the attenuation of vibration at accelerometers 3 and 6. This is to be expected since accelerometers 3 and 6 are almost collocated with air actuators 3 and 6, which were used in control design 2 but not in control design 1.

The role the input multiplicative uncertainty level plays is evident when comparing the performance of controller 1 with that of controller 3. Controller 3 is designed the same as controller 1 except that the input multiplicative weight is selected to be 2% uncertainty compared with 10% uncertainty. The performance of controller 3 at all of the accelerometer locations is slightly improved. The increase in performance comes at the expense of increased actuator force, most notably from air thrustor 1 and 8. Results from the implementation of controllers 1 and 3 indicate that the uncertainty models used in the problem formulations accurately represent the physical CEM structure. The theoretical results for each design parallel the experimental data exactly.

Controller 4 uses the same problem formulation as control design 2 with the input multiplicative uncertainty weight choosen to be 1% as opposed to 10%. Similar results are obtained to controller 1 and 3. Controller 4 has increased the attenuate of low frequency virbation at the accelerometer locations at the expense of increased actuator control forces. It is interesting to note the high frequency content in the accelerometer 3 signal. The increased controller bandwidth in design 4 causes several high frequency modes to be excited.

The problem formulation used to synthesize controller 6 uses a higher order design model, different additive uncertainty models reduced in magnitude from designs 1 through 4 and first order filters on the performance weights. The performance of controller 6 is similar to controller 1, though controller 6 has significantly more high frequency content in the accelerometer signals. The additive uncertainty models used in design 6, allowed the controller to have a higher bandwidth leading to increased high frequency accelerometer signals. The higher bandwidth controller lead to poor robustness characteristics for controller 6. Similar problems were noted in control design 7. The input multiplicative uncertainty problem formulation was modified to 10% to account for the change in the additive uncertainty models. The results indicate that accounting for unmodeled dynamics via input multiplicative is not a good approach to the control design problem for lightly damped flexible structures. Based on intuition, one would expect that a very large multiplicative uncertainty weight would be required on the actuator in the neighborhood of an unmodeded flexible mode of the structure. A level of 10% multiplicative uncertainty would be inadequate to assure stability of the unmodeled flexible modes. Controller 7 appears to have destabilized a structural mode of the system around $7Hz$.

Control design 9 represents the controller with the highest level of performance. A high order model of the structure is used in the design process, with the goal to attenuate the structural mode at $7Hz$. The performance weight $perfwt$ is modified to reflect this goal and the additive uncertainty weight is modified accordingly. The controller attenuates the low frequency modes of the CEM structure quickly with little high frequency content to the acceleroemeter signals. Unfortunately, due to the limited accuracy of the control design model above $4Hz$, the modeling errors between the design model and experimentally derived transfer function data can be seen in Appendix A figures A1 through A6, controller 9 is unable to attenuate the structural mode at $7Hz$. In spite of this shortcoming, controller 9 achieved the high level of performance of any controller implemented on the experimental CEM structure.

It is of interest to noted that all of the controllers implemented were obtained using balanced realization model reduction techiques. Although the original controllers were

on the order of 80 states, the controllers implemented were reduce to approximately 40 states prior to implementation. This indicates that a number of states are not necessary in the control designs. It would be of interest to invesitgate how the controller order effect the achievable performance given the same problem formulation.

9 Summary

H_∞ and structured singular value (μ) based control design methods are used to analyze and synthesize control laws for the NASA Langley Controls-Structures Interaction (CSI) "Evolutionary Model." The CEM structure had numerous lightly damped, coupled flexible modes, collocated and noncollocated sensors and actuators and stringent performance specifications which lead to a difficult control problem. The control design problem was further complicated by the model errors noted between the model used for control design and experimentally derived transfer function data. These model inaccuracies or *uncertainties* are accounted for in the control design process via unstructured uncertainty models in addition to the performance specifications on the attenuation of structural vibration due to external disturbances. Eight controllers are synthesized for a variety of input multiplicative uncertainty, additive uncertainty and performance weights.

The controllers exhibited excellent correlation between the theoretically predicted and experimentally achieved results especially associated with the low frequency modes of the CEM structure. This was expected due to the error between the design model and experimenta at frequenies above $4Hz$. The μ-synthesis techniques resulted in controllers which traded off between robustness and performance given the specific problem formulation and achieved outstanding performance when implemented on the CEM structure. It was seen that unstructured uncertainty models of the modeling error were more than adequate in the control problem formulation.

10 Research in Progress

Parameteric uncertainty models of variation in natural frequency and damping levels is explored in detail by Dr. Kyong Lim at NASA Langley and myself in the paper [LimB]. The same H_∞ and structured singular value techniques are applied to the CEM structure to minimize the LOS error due to external disturbances. It was found that because the

CEM structure is very lightly damped, the robust performance for fine pointing was highly dependent on the accuracy of the structural frequencies. This was not unexpected since small variations in natural frequencies lead to large gain and phase variations in the neighborhood of those natural frequncies in lightly damped systems. These results were not verified on the experimental structure due to the controllers being synthesized after the CEM structure was disassembled. Modeling of system with parametric uncertainty in structural natural frequencies and damping values is currently being pursued by Dr. Kyong Lim and myself and will be an main area of research in the coming year.

Two Ph.D. graduate students at the University of Minnesota, Richard Lind and Arun Kumar are being support by this NASA grant. They are pursuing research topics applicable to the area of control of flexible space structures. Mr. Lind has developed realtime control software for a DSP processor which is housed within a Macintosh FX. The Macintosh has 16 A/D channels and 8 D/A channels for realtime control. The realtime control can be implemented at 2 kHz while input and output channels are graphically on the Macintosh screen. A two mass, three spring experiment has been developed to test out the realtime software. This experiment is being used by Mr. Kumar to investigate the tradeoff between collocated and noncollated control. Mr. Lind is also doing theoretical research on calculating optimal constant D scalings for the μ upper bound via convex optimization. This work may have a significant impact in the synthesis of optimal μ controllers for the full information control design problem.

Mr. Kumar is investigating the tradeoff between collocated and noncollocated control design. The idea is to develop a quantitative relationship between the degree of uncertainty in a system and the need for collocated control for robustness purposes. Mr. Kumar has spent a majority of this concentrating on coursework will be spending the spring quarter primarily doing research.

We are in the process of building a large flexible structure experiment in the Aerospace Controls Lab at the University of Minnesota. The structure will investigate modeling, system identification, model validation and control analysis and synthesis issues for flexible structures. The structure will have a slewing component which will introduce nonlinearities into the problem formulation. This experiment will be used to investigate control design issues for flexible structures prior to testing these ideas on the CEM structure at NASA Langley.

11 References

[Balas] G.J. Balas, "Robust control of flexible structures: theory and experiments," Ph.D. Thesis, California Institute of Technology, Pasadena, 1989.

[BalChuD] G.J. Balas, C.C. Chu, J.C. Doyle, "Vibration damping and robust control of JPL/AFAL experiment using μ-synthesis," 28^{st} CDC, Tampa, FL, December, 1989.

[BalDoy1] G.J. Balas and J.C. Doyle, "Identification and robust control for flexible structures," accepted for publication in *IEEE Control Systems Magazine*, November, 1989.

[BalDoy2] G.J. Balas and J.C. Doyle, "Robust control of flexible modes in the controller crossover region", ACC, Pittsburgh, PA, June, 1989.

[BalLDD] G.J. Balas, M. Lukich, R.L. Dailey and J.C. Doyle, "Robust control of a truss experiment," AIAA Guidance and Control Conference, Minneapolis, MN, August, 1988.

[Bev91] K.W. Belvin, et. al., "Langley's CSI Evolutionary Model: Phase 0," NASA TM 104165, November, 1991.

[Dora] P. Dorato, editor, *Robust Control*, IEEE Press, New York, 1987.

[DGKF] J.C. Doyle, K. Glover, P. Khargonekar and B.A. Francis, "State-space solutions to standard H_2 and H_∞ control problems," IEEE Transactions on Automatic Control, Vol. 34, No. 8, August, 1989, pp 831-847.

[Doy1] J.C. Doyle, "Analysis of feedback systems with structured uncertainties," Proc. IEE-D 129, 1982, pp 242-250.

[Doy2] J.C. Doyle, *Lecture notes on advances in multivariable control*, ONR/Honeywell Workshop on Advances in Multivariable Control, Minneapolis, MN, October, 1984.

[DoyLP] J.C. Doyle, K Lenz, A.K. Packard, "Design examples using μ-synthesis: Space shuttle lateral axis FCS during reentry," NATO ASI Series Vol. F34, Springer-Verlag Berlin Heidelberg, 1987.

[Francis]B.A. Francis, *A Course in H_∞ Control Theory*, Springer-Verlag, Berlin, 1987.

[**GlovDoy1**] K. Glover and J.C. Doyle, "State-space formulae for all stabilizing controllers that satisfy an H_∞-norm bound and relations to risk sensitivity," Systems & Control Letters 11, 1989, pp 167-172.

[**LimB**] K.B. Lim and G.J. Balas, "Line-of-sight control of the CSI evolutionary model: μ control," American Control Conference, Chicago, IL, June, 1992.

[**Mutools**] G.J. Balas, J.C. Doyle, K. Glover, A.K. Packard, and R. Smith, *μ Analysis and Synthesis Toolbox User's Guide*, MUSYN Inc., May 1991.

[**Pack**] A.K. Packard, "What's new with μ: structured uncertainty in multivariable control," Ph.D. Thesis, University of California at Berkeley, 1988.

Appendix A

Experimental Results

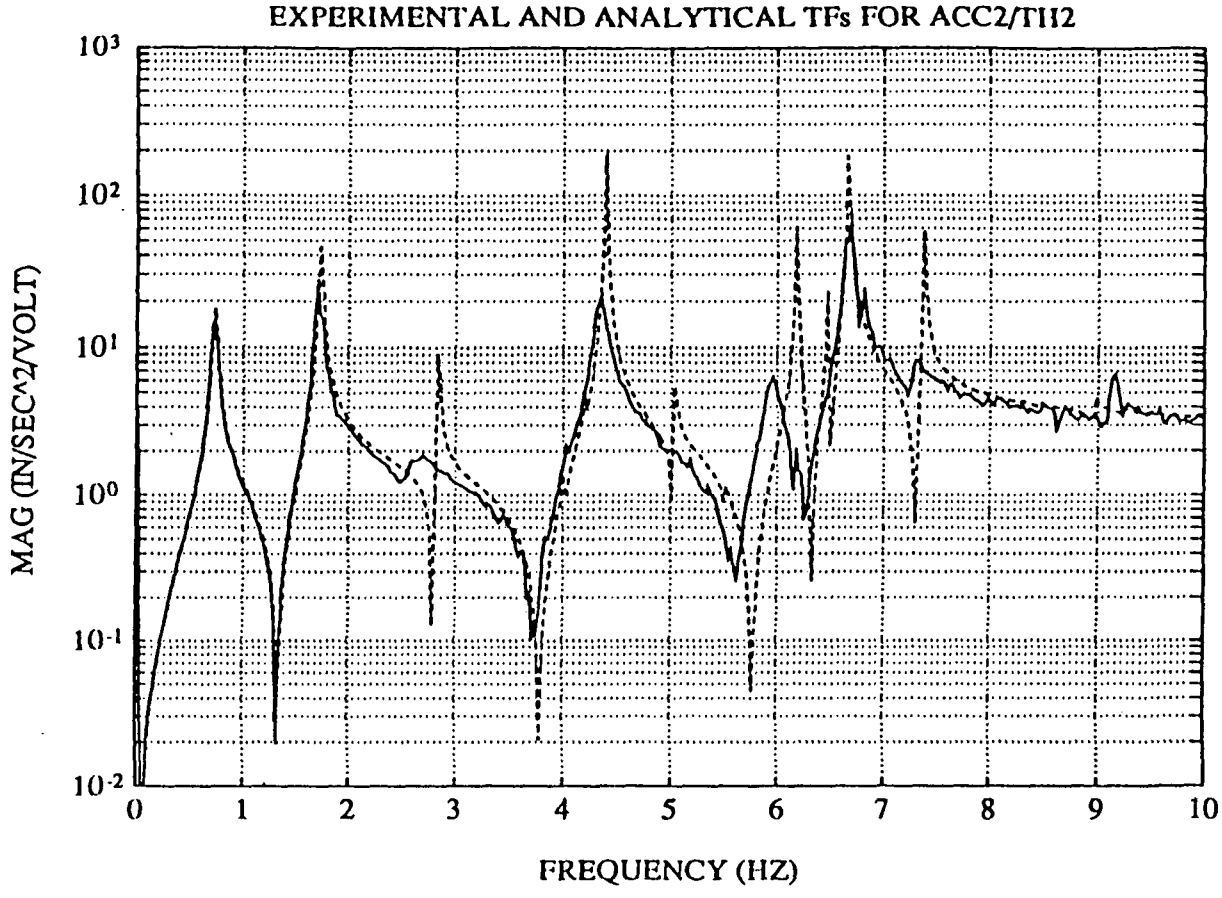
EXPERIMENTAL AND ANALYTICAL TFs FOR ACC2/TH2
MAG (IN/SEC^2/VOLT)
FREQUENCY (HZ)

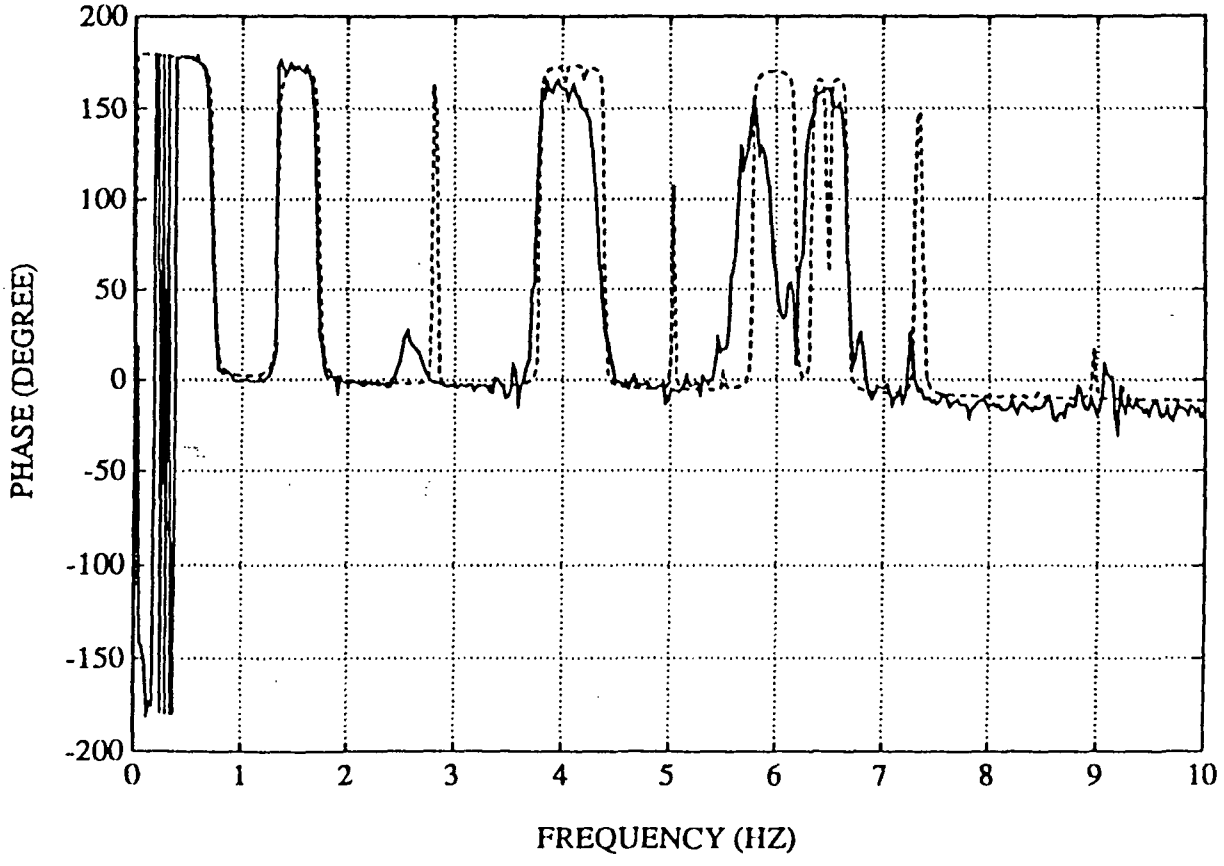
PHASE (DEGREE)
FREQUENCY (HZ)

Figure A1

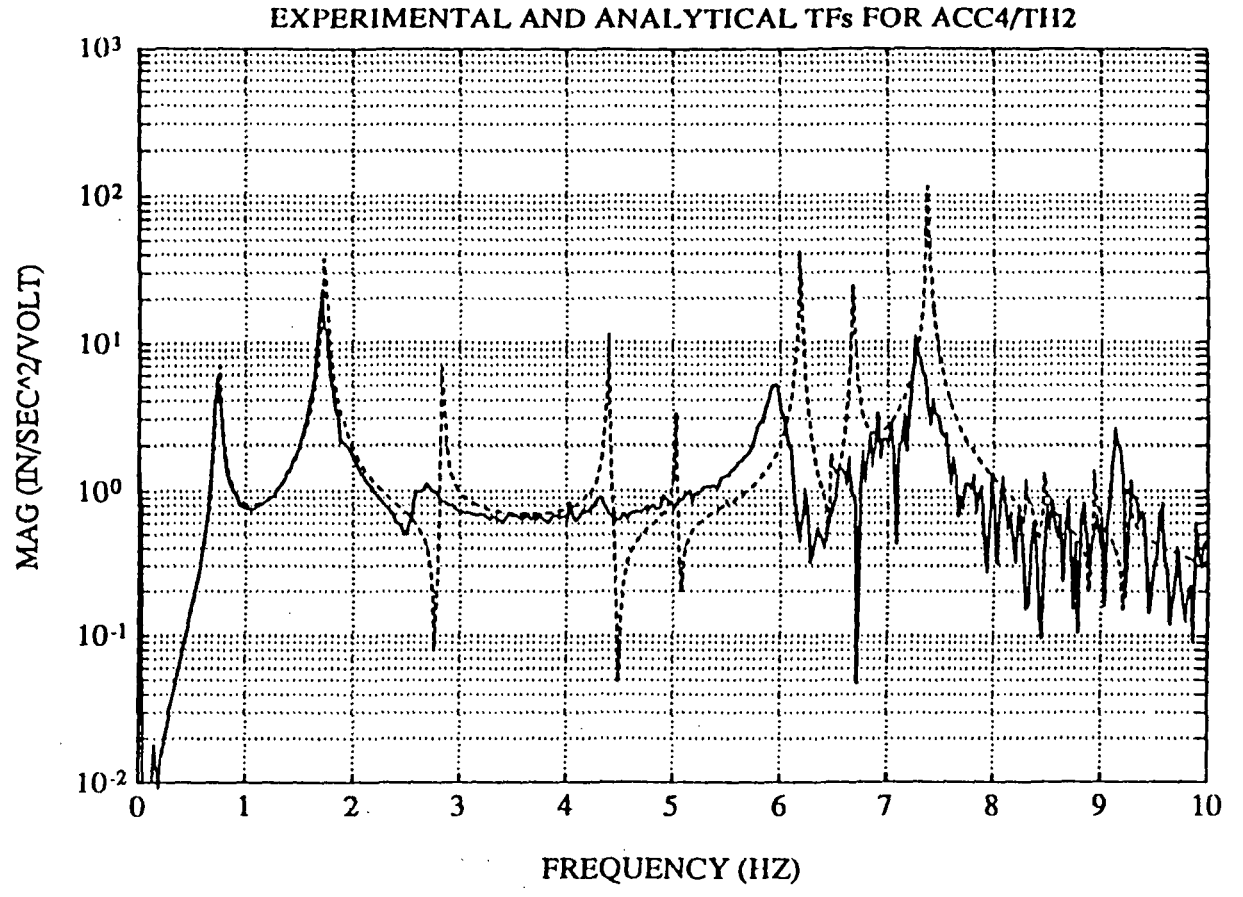
EXPERIMENTAL AND ANALYTICAL TFs FOR ACC4/TH2
MAG (IN/SEC^2/VOLT)
10^3
10^2
10^1
10^0
10^-1
10^-2
0
1
2
3
4
5
6
7
8
9
10
FREQUENCY (HZ)

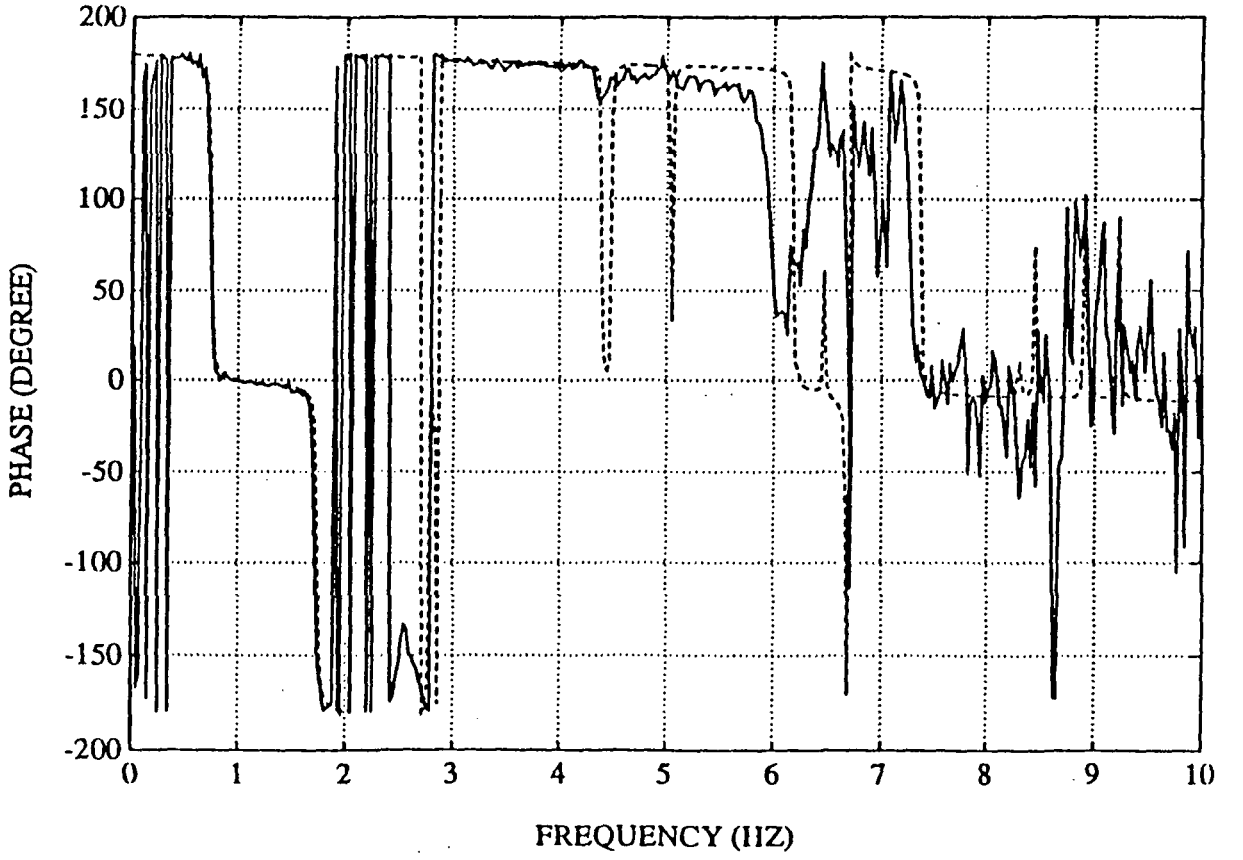
PHASE (DEGREE)
200
150
100
50
0
-50
-100
-150
-200
0
1
2
3
4
5
6
7
8
9
10
FREQUENCY (HZ)

Figure A2

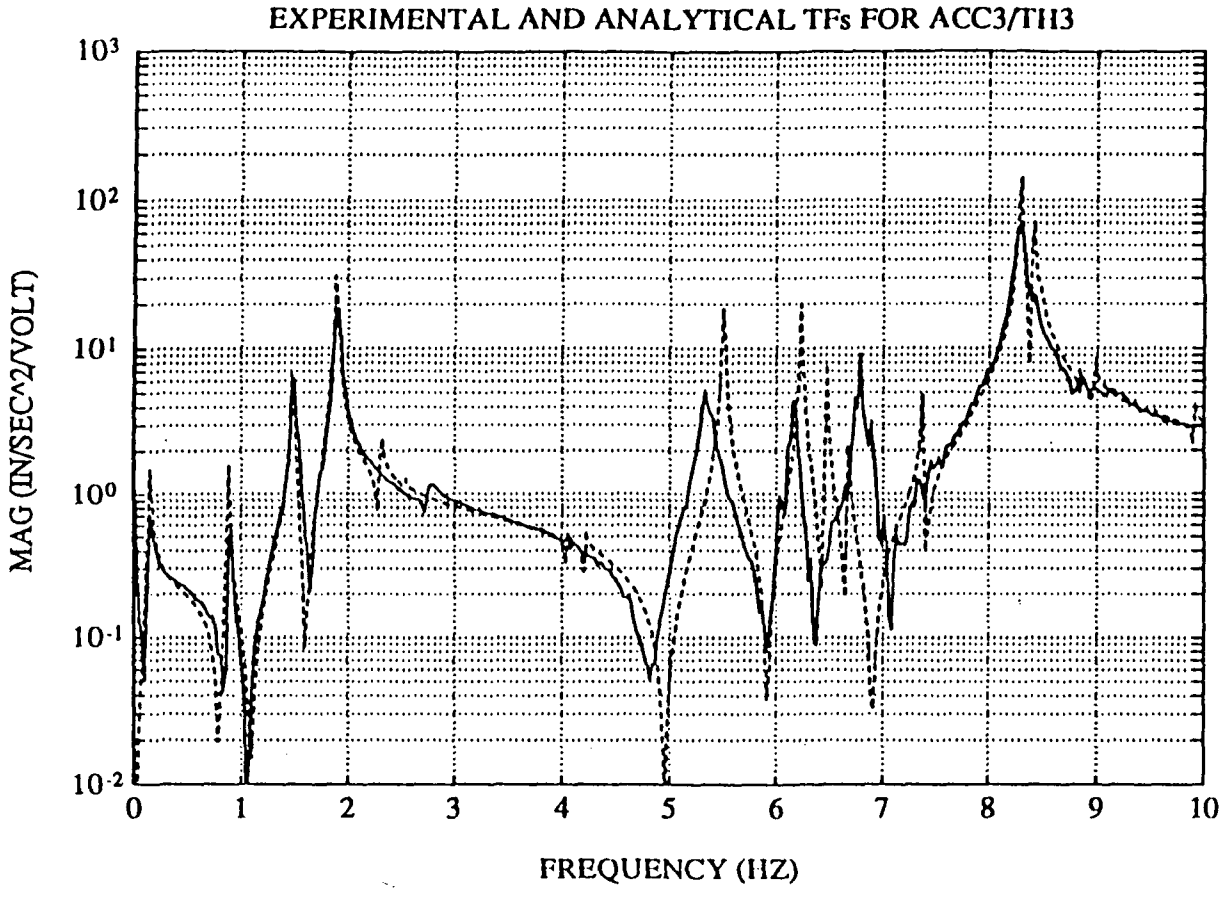
EXPERIMENTAL AND ANALYTICAL TFs FOR ACC3/TH3
MAG (IN/SEC^2/VOLT)
FREQUENCY (HZ)

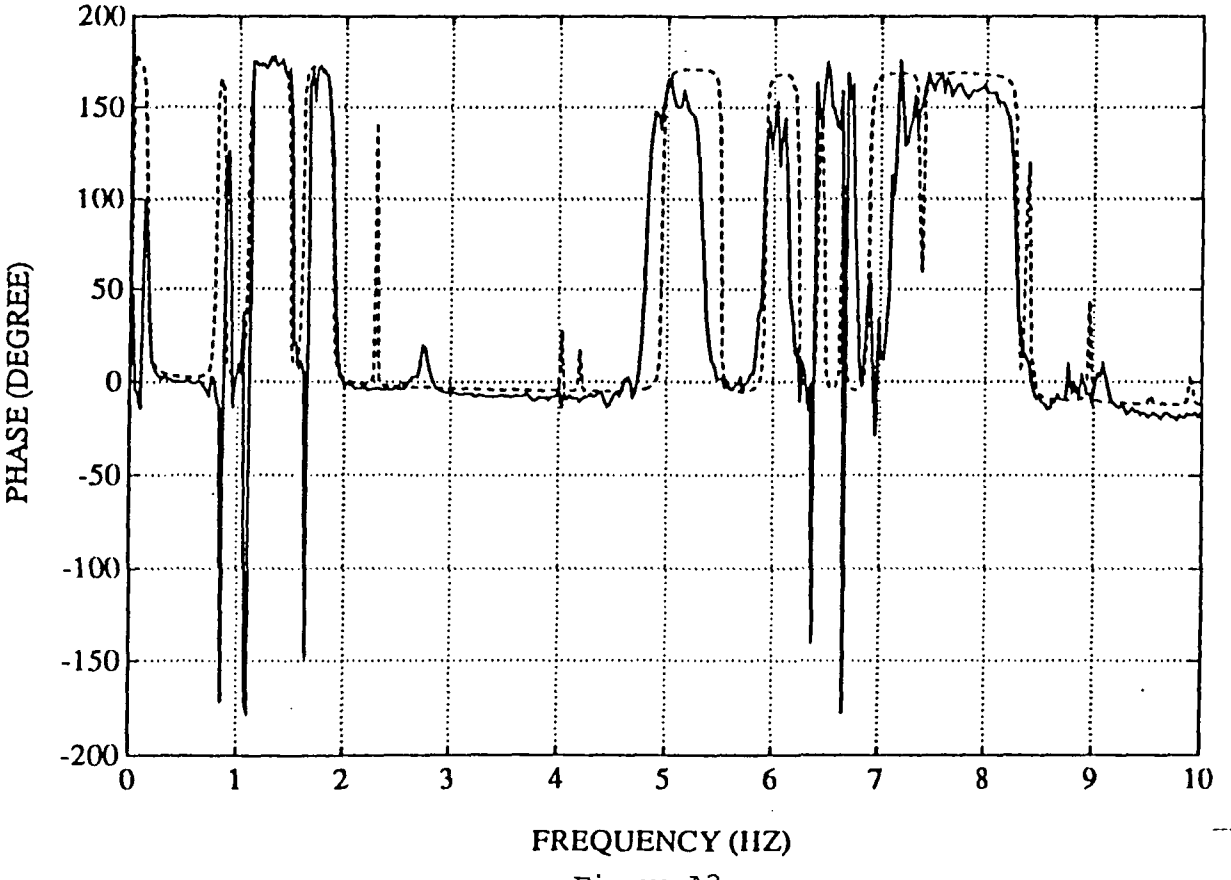
PHASE (DEGREE)
FREQUENCY (HZ)

Figure A3

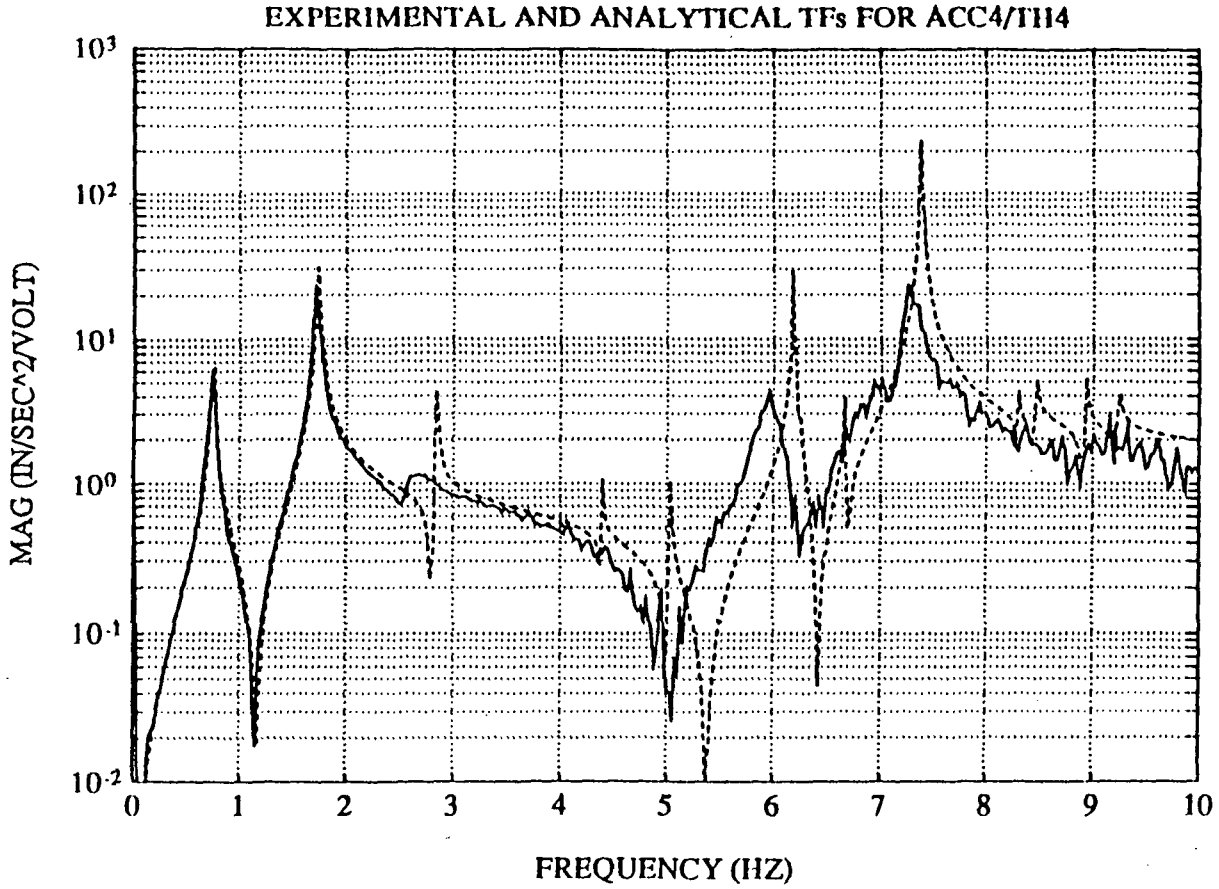
EXPERIMENTAL AND ANALYTICAL TFs FOR ACC4/TH4
MAG (IN/SEC^2/VOLT)
FREQUENCY (HZ)

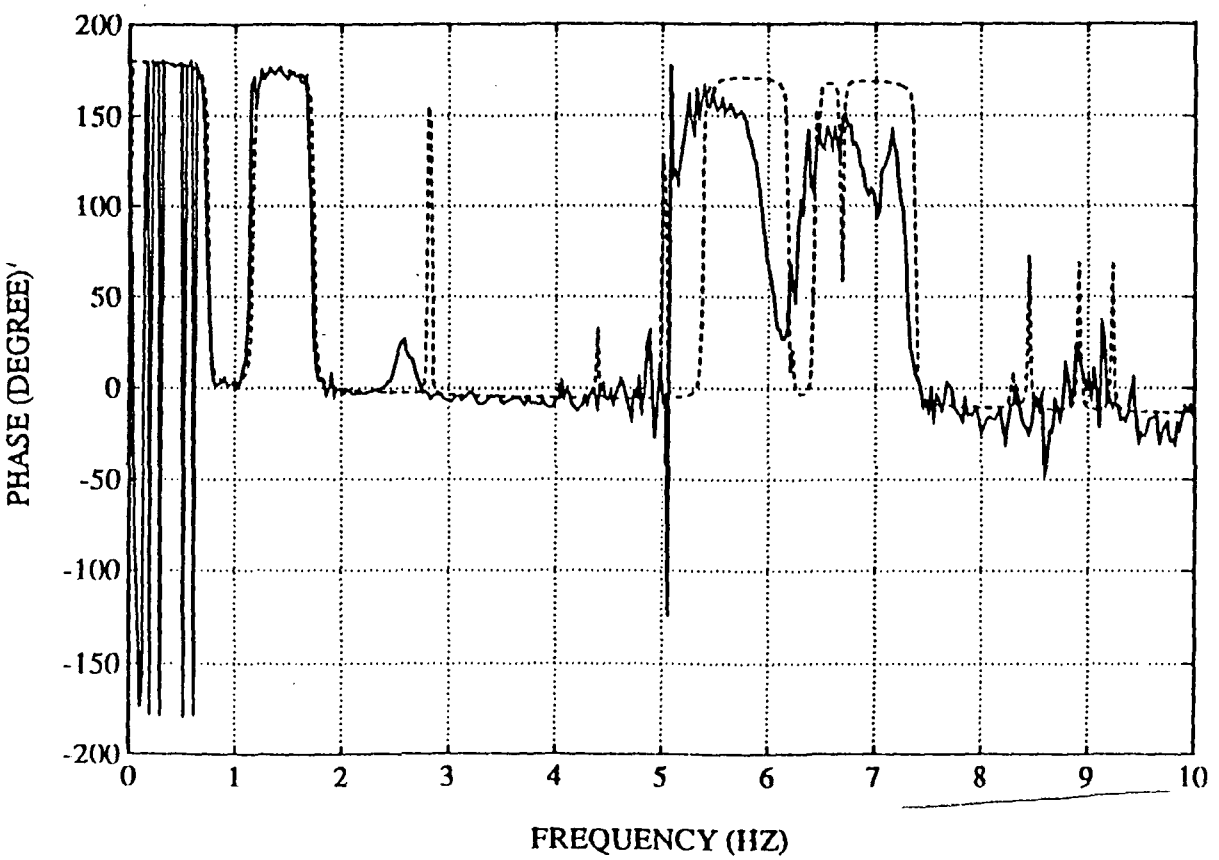
PHASE (DEGREE)
FREQUENCY (HZ)

Figure A4.

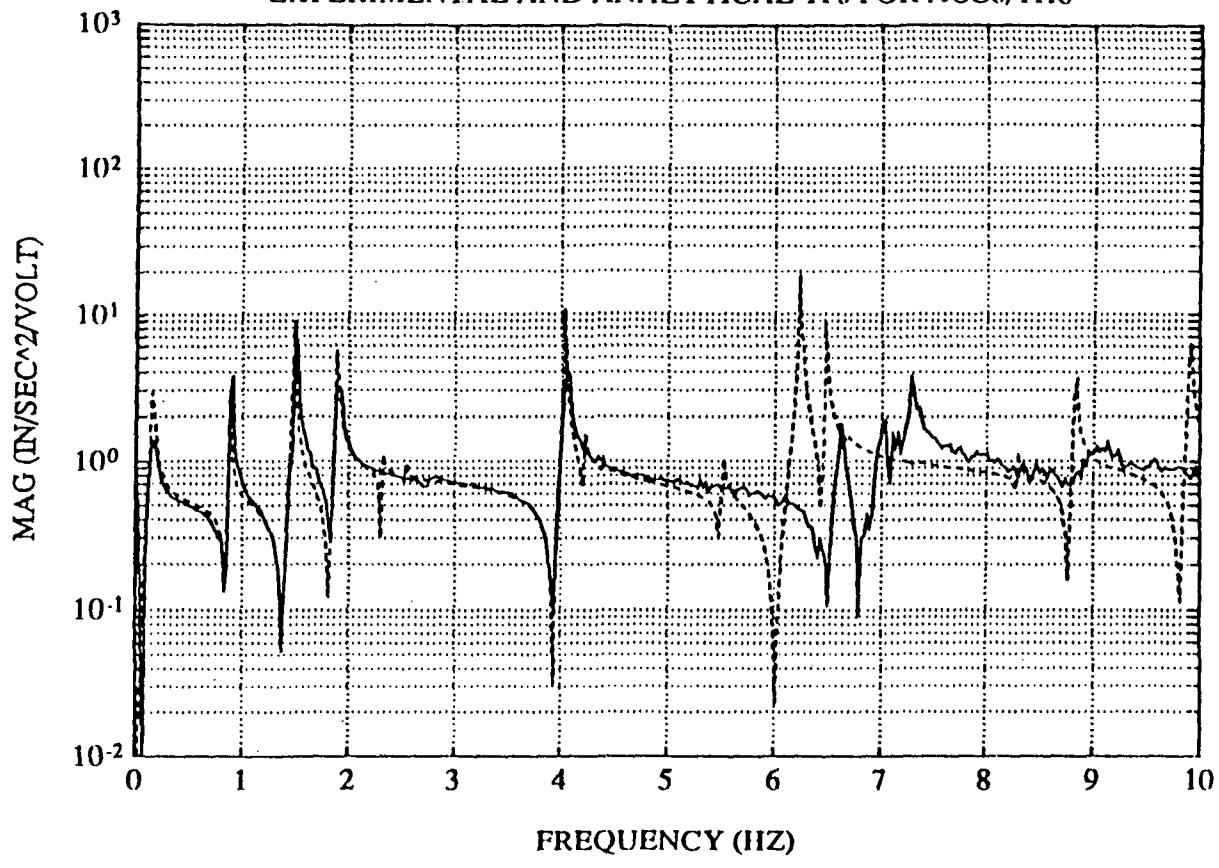
EXPERIMENTAL AND ANALYTICAL TFs FOR ACC6/TH6
MAG (IN/SEC^2/VOLT)
10³
10²
10¹
10⁰
10⁻¹
10⁻²
0
1
2
3
4
5
6
7
8
9
10
FREQUENCY (HZ)

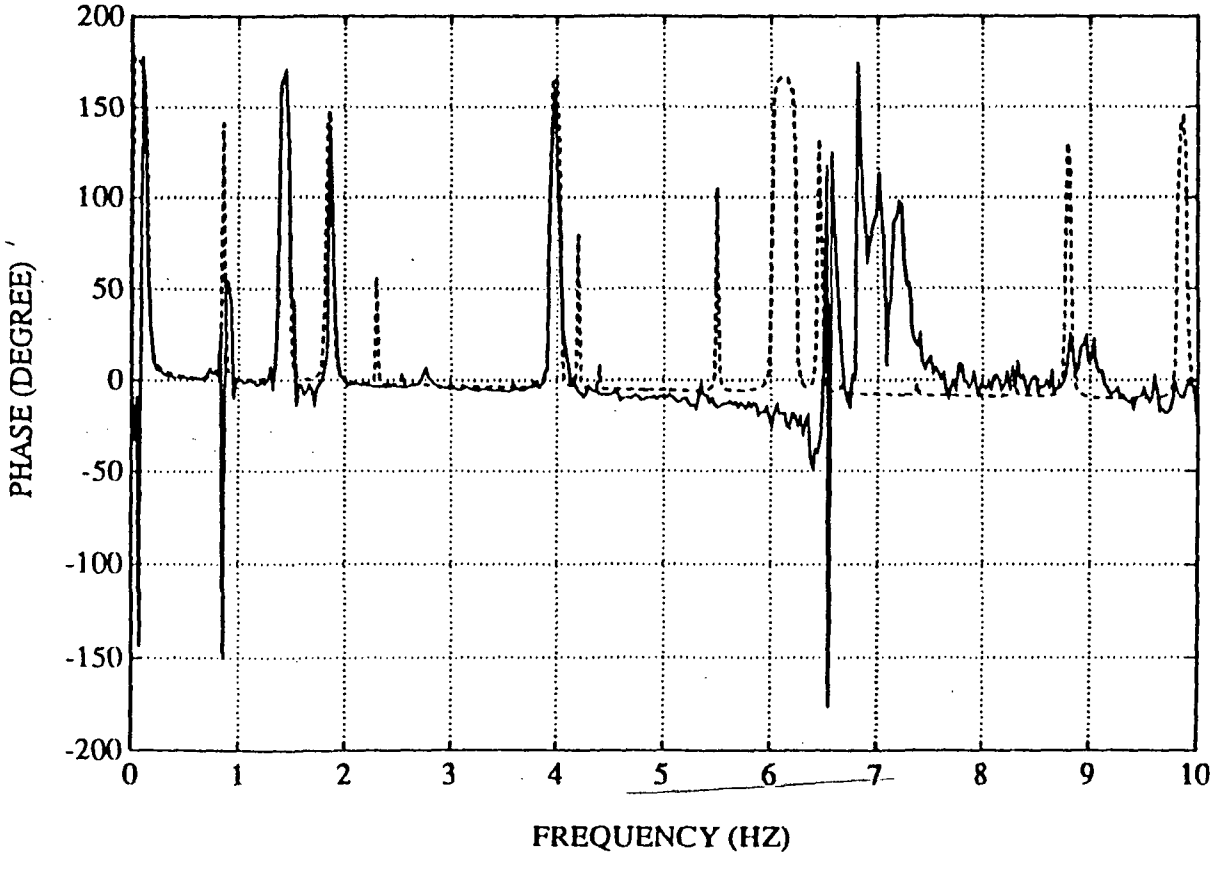
PHASE (DEGREE)
200
150
100
50
0
-50
-100
-150
-200
0
1
2
3
4
5
6
7
8
9
10
FREQUENCY (HZ)

Figure A5

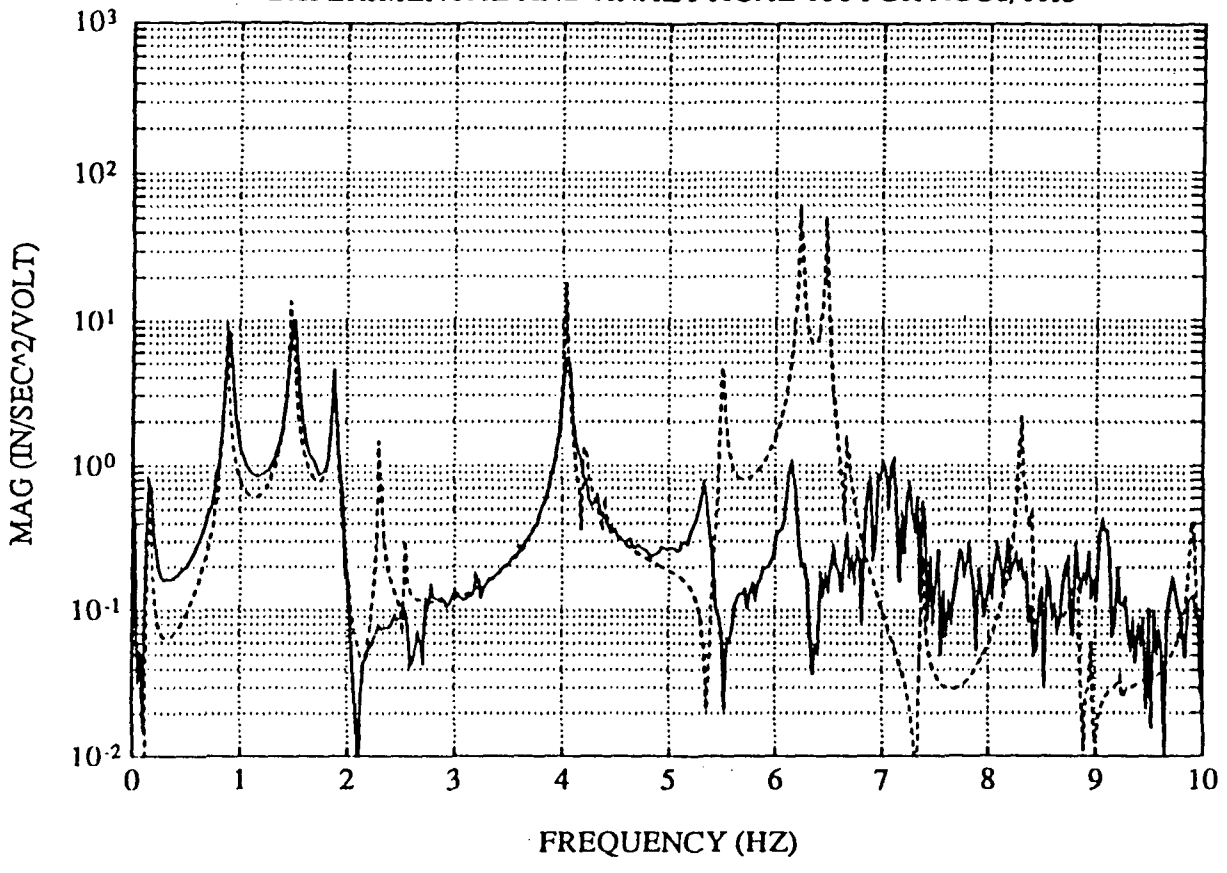
EXPERIMENTAL AND ANALYTICAL TFs FOR ACC6/TH8
MAG (IN/SEC^2/VOLT)
FREQUENCY (HZ)

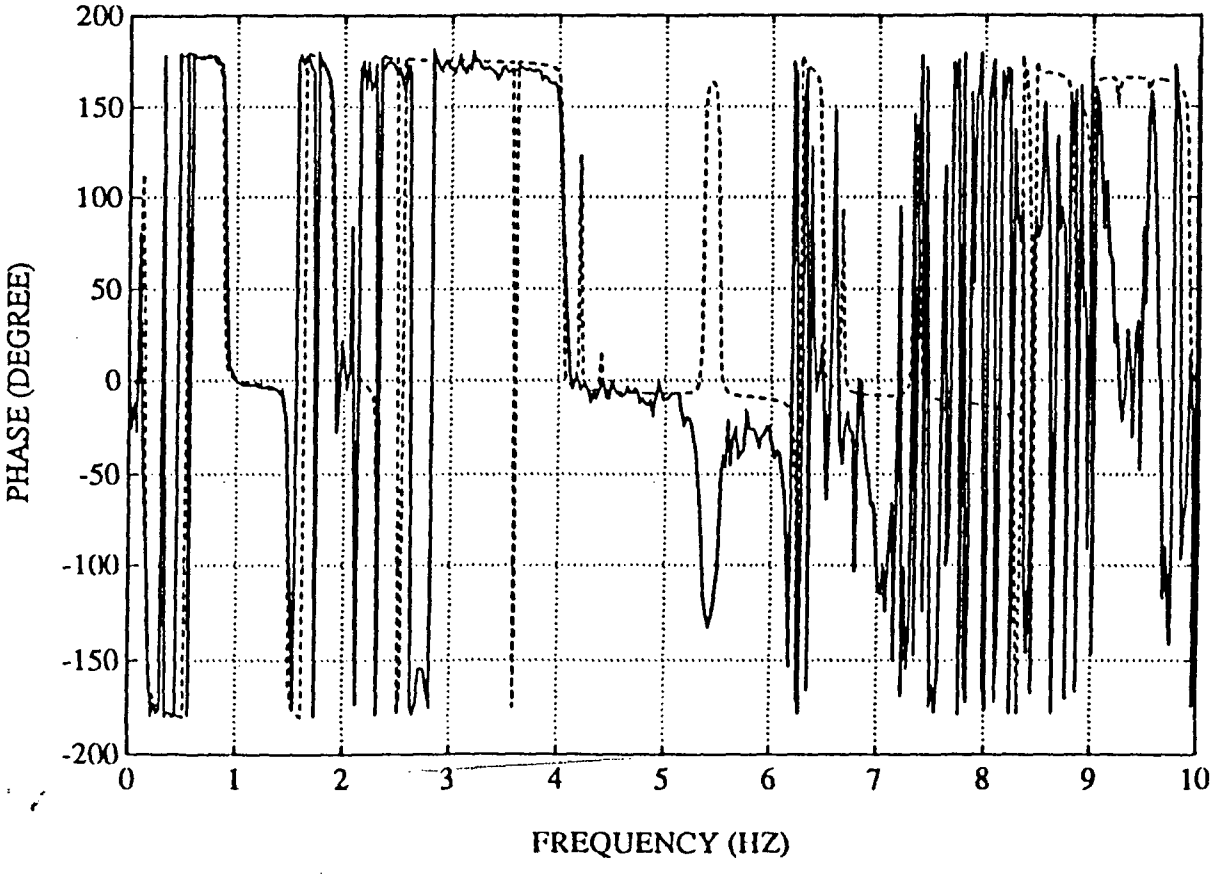
PHASE (DEGREE)
FREQUENCY (HZ)

Figure A6

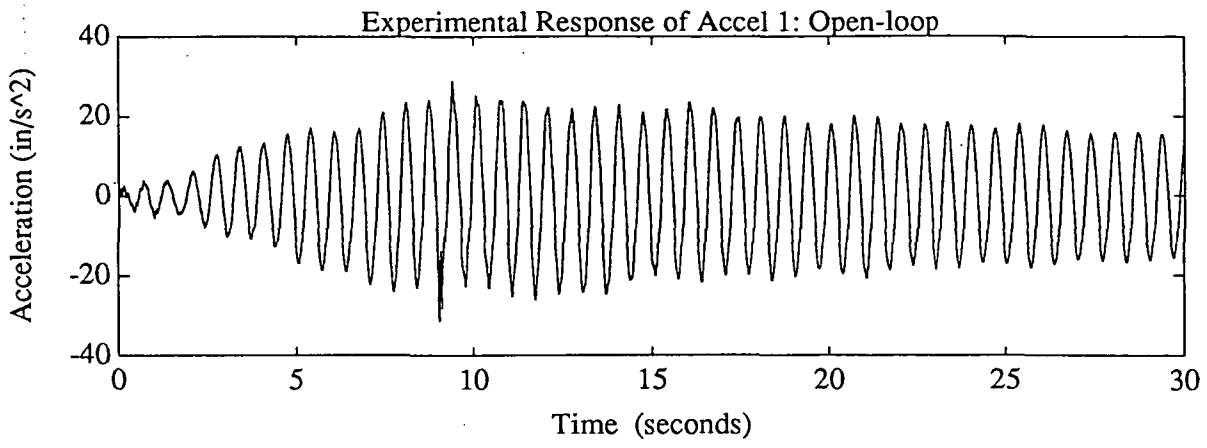
Experimental Response of Accel 1: Open-loop
Acceleration (in/s^2)
40
20
0
-20
-40
0
5
10
15
20
25
30
Time (seconds)

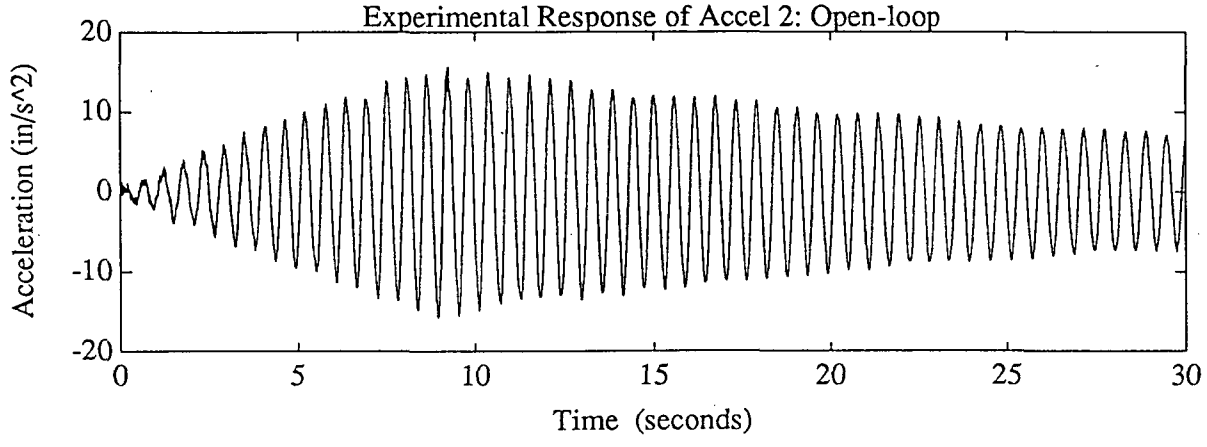
Experimental Response of Accel 2: Open-loop
Acceleration (in/s^2)
20
10
0
-10
-20
0
5
10
15
20
25
30
Time (seconds)

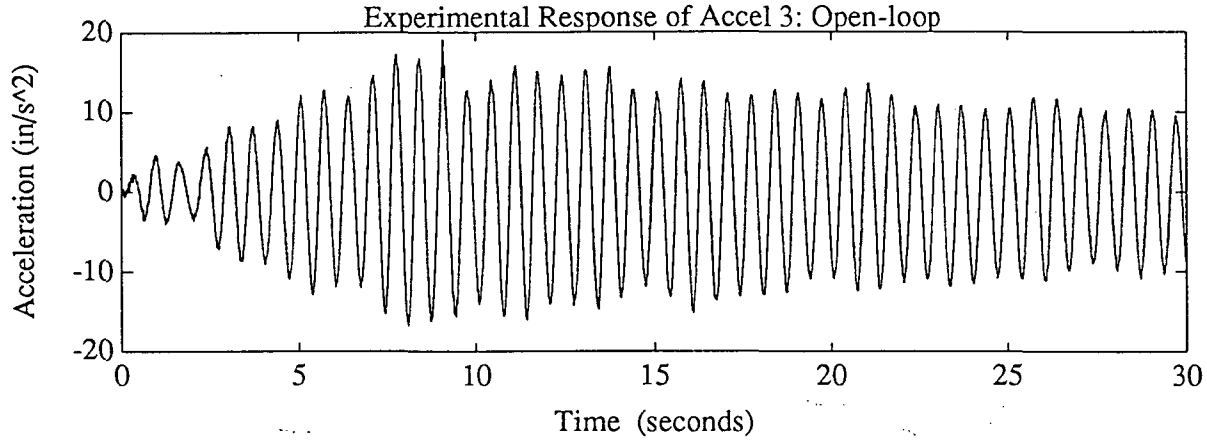
Experimental Response of Accel 3: Open-loop
Acceleration (in/s^2)
20
10
0
-10
-20
0
5
10
15
20
25
30
Time (seconds)

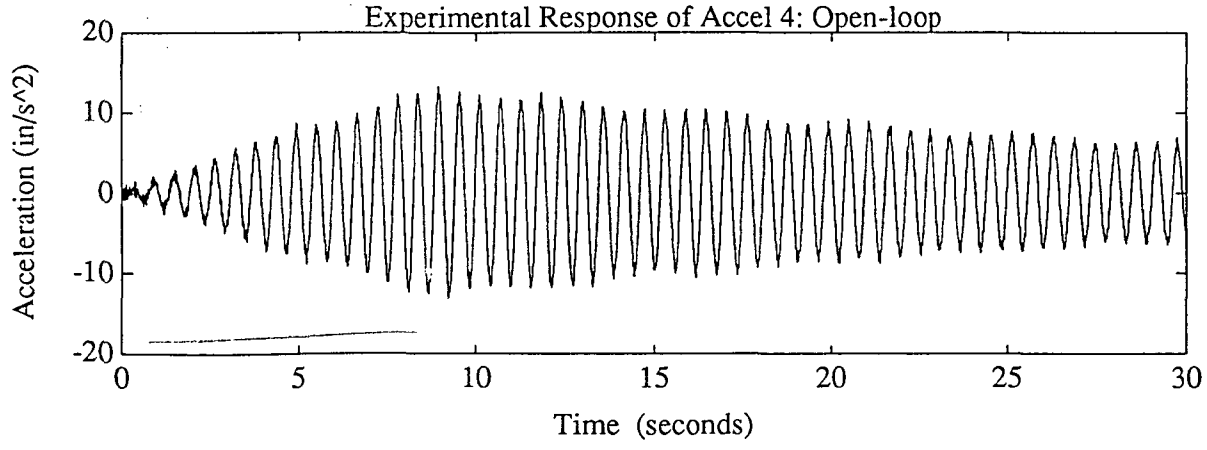
Experimental Response of Accel 4: Open-loop
Acceleration (in/s^2)
20
10
0
-10
-20
0
5
10
15
20
25
30
Time (seconds)

Figure A7

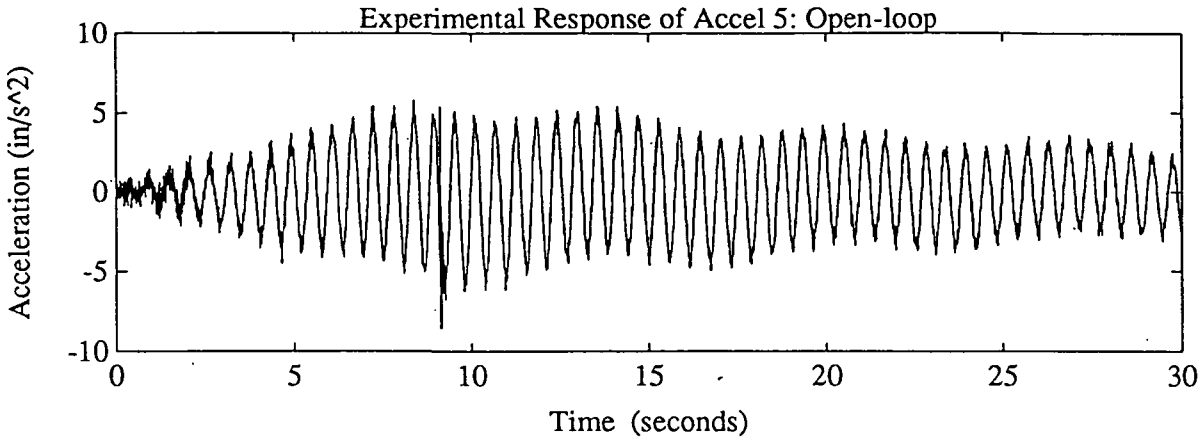
Experimental Response of Accel 5: Open-loop
Acceleration (in/s^2)
10
5
0
-5
-10
0
5
10
15
20
25
30
Time (seconds)

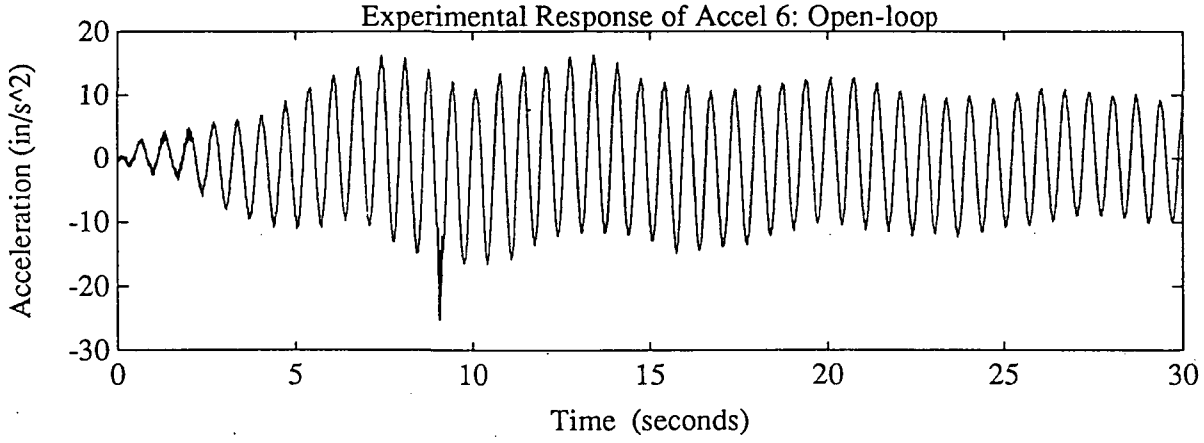
Experimental Response of Accel 6: Open-loop
Acceleration (in/s^2)
20
10
0
-10
-20
-30
0
5
10
15
20
25
30
Time (seconds)

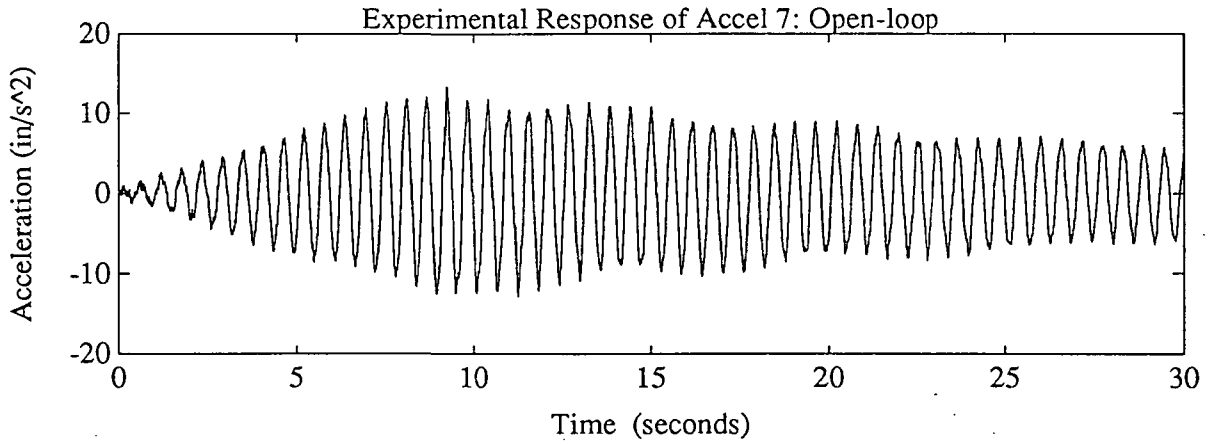
Experimental Response of Accel 7: Open-loop
Acceleration (in/s^2)
20
10
0
-10
-20
0
5
10
15
20
25
30
Time (seconds)

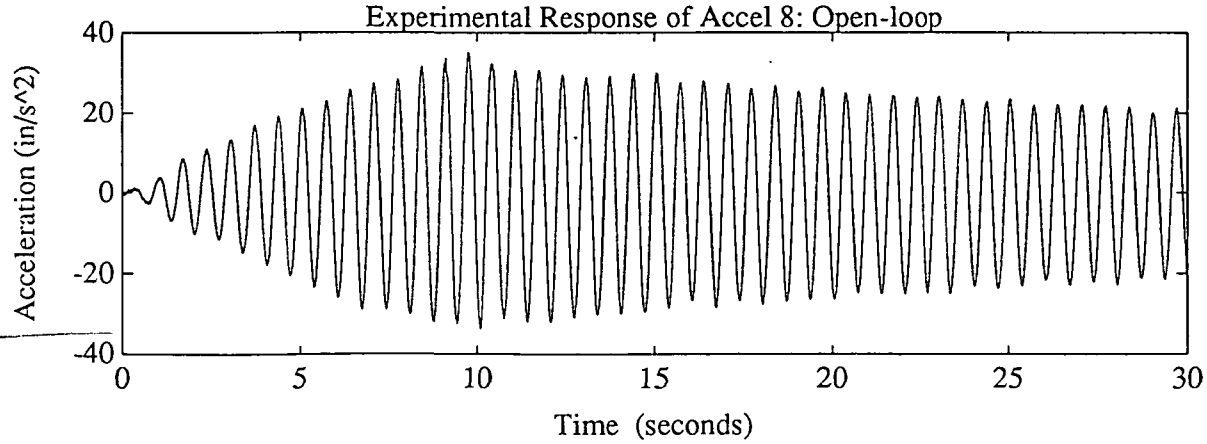
Experimental Response of Accel 8: Open-loop
Acceleration (in/s^2)
40
20
0
-20
-40
0
5
10
15
20
25
30
Time (seconds)

Figure A8

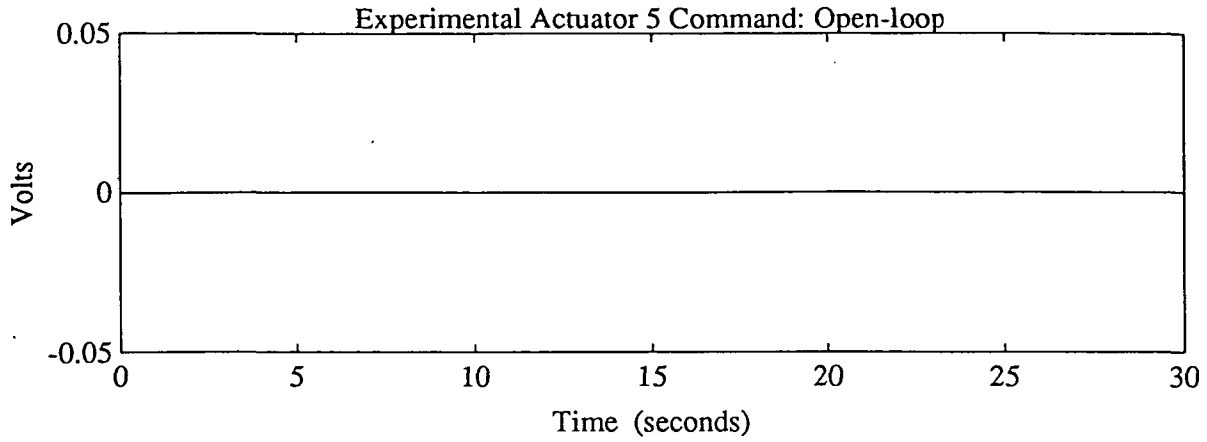
Experimental Actuator 5 Command: Open-loop
0.05
0
-0.05
Volts
0
5
10
15
20
25
30
Time (seconds)

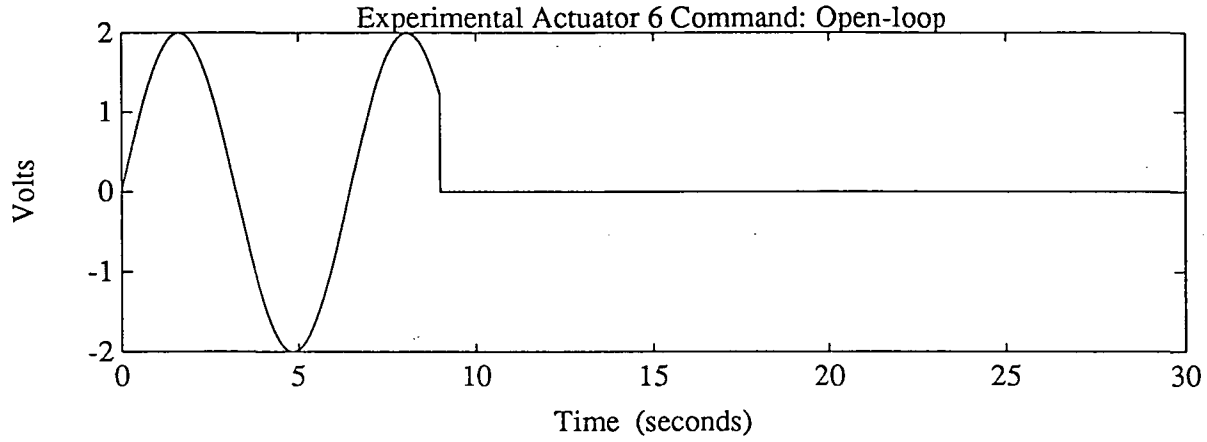
Experimental Actuator 6 Command: Open-loop
2
1
0
-1
-2
Volts
0
5
10
15
20
25
30
Time (seconds)

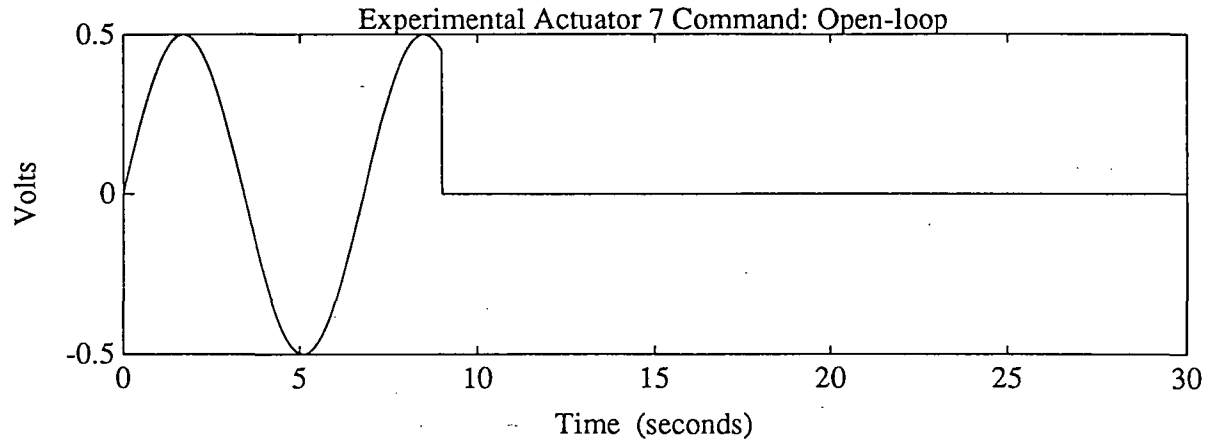
Experimental Actuator 7 Command: Open-loop
0.5
0
-0.5
Volts
0
5
10
15
20
25
30
Time (seconds)

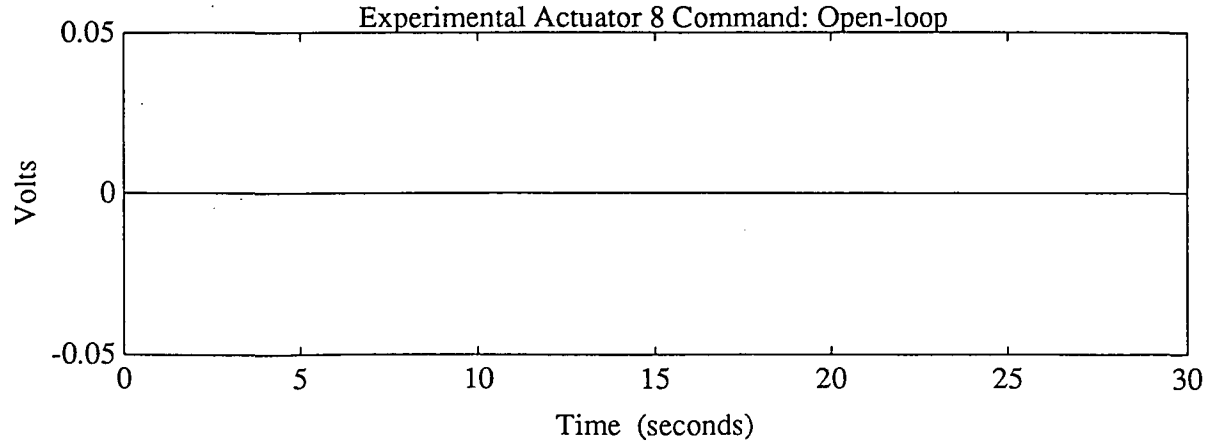
Experimental Actuator 8 Command: Open-loop
0.05
0
-0.05
Volts
0
5
10
15
20
25
30
Time (seconds)

Figure A9

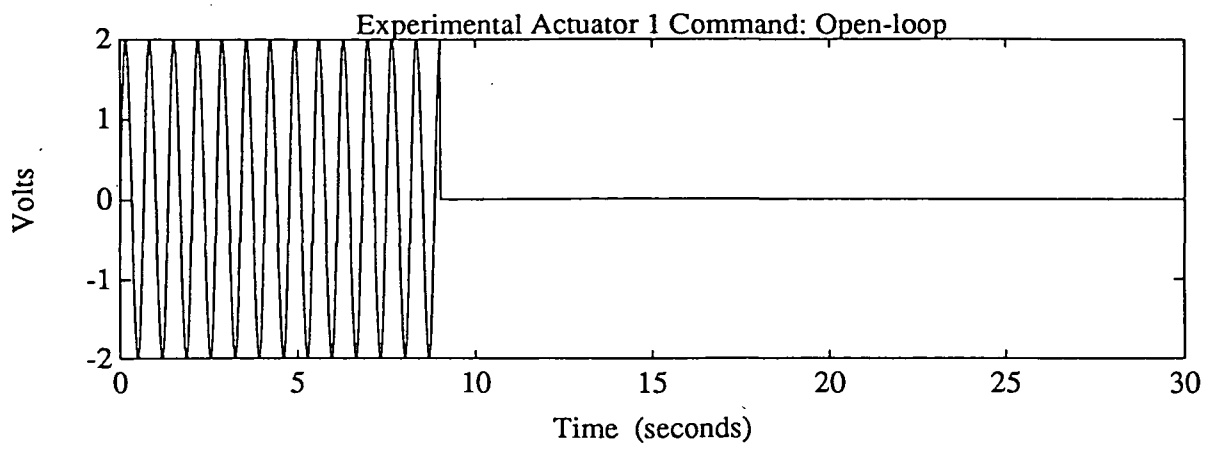
Experimental Actuator 1 Command: Open-loop
Volts
2
1
0
-1
-2
0
5
10
15
20
25
30
Time (seconds)

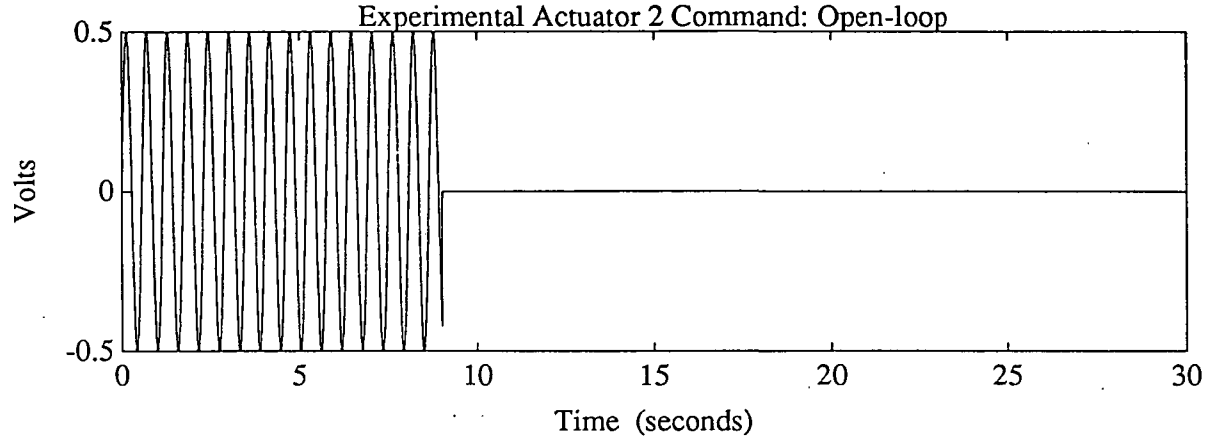
Experimental Actuator 2 Command: Open-loop
Volts
0.5
0
-0.5
0
5
10
15
20
25
30
Time (seconds)

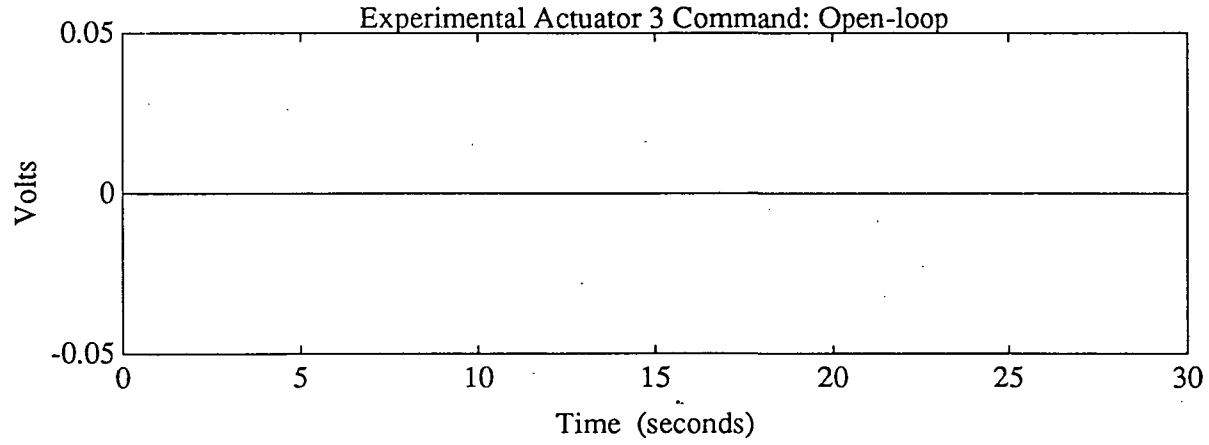
Experimental Actuator 3 Command: Open-loop
Volts
0.05
0
-0.05
0
5
10
15
20
25
30
Time (seconds)

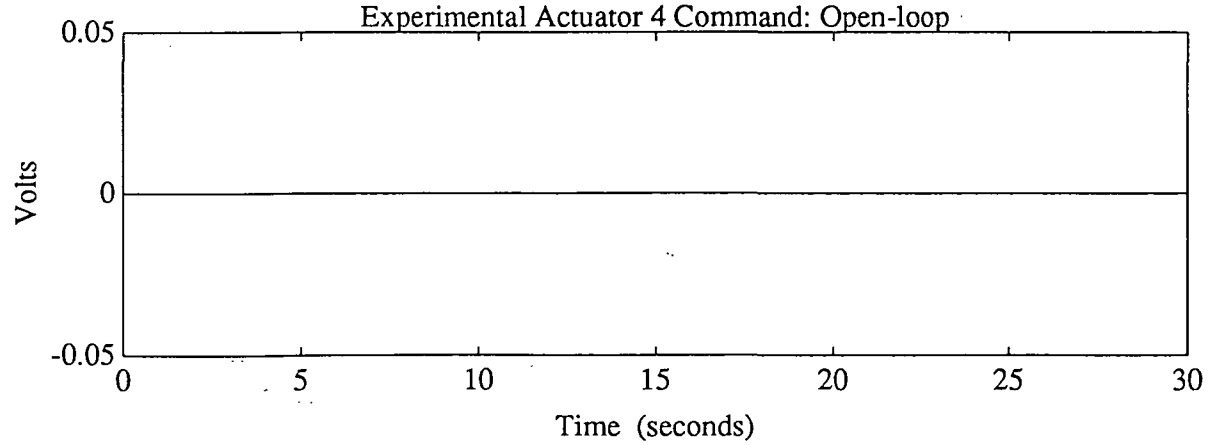
Experimental Actuator 4 Command: Open-loop
Volts
0.05
0
-0.05
0
5
10
15
20
25
30
Time (seconds)

Figure A10

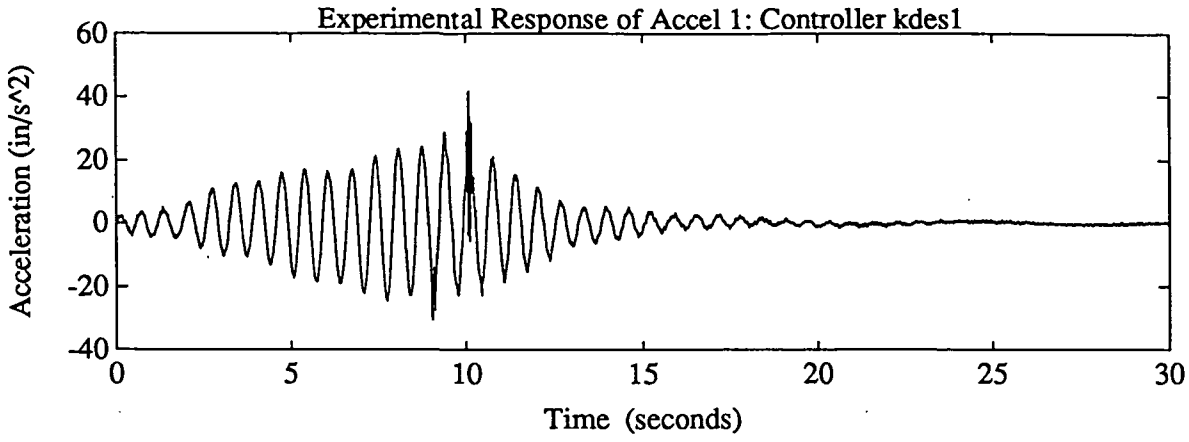
Experimental Response of Accel 1: Controller kdes1
Acceleration (in/s^2)
60
40
20
0
-20
-40
0
5
10
15
20
25
30
Time (seconds)

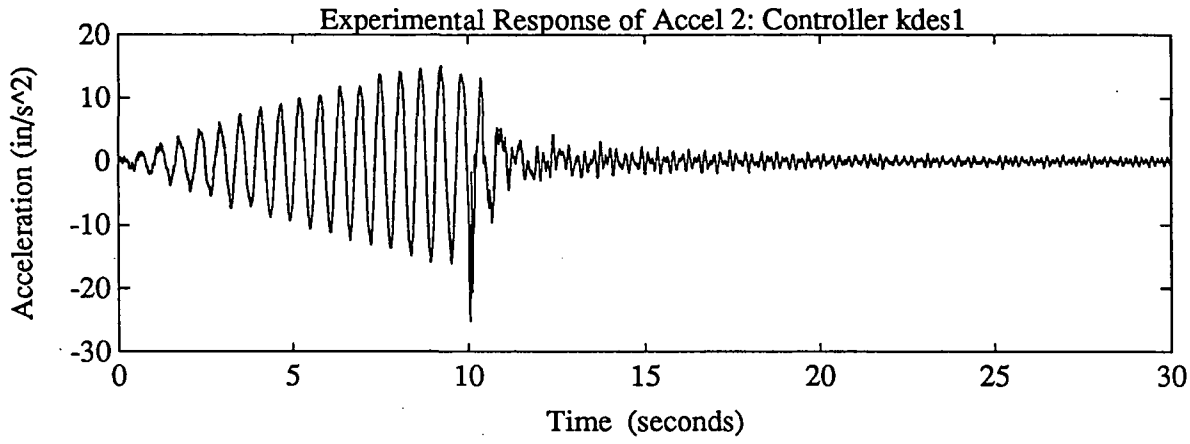
Experimental Response of Accel 2: Controller kdes1
Acceleration (in/s^2)
20
10
0
-10
-20
-30
0
5
10
15
20
25
30
Time (seconds)

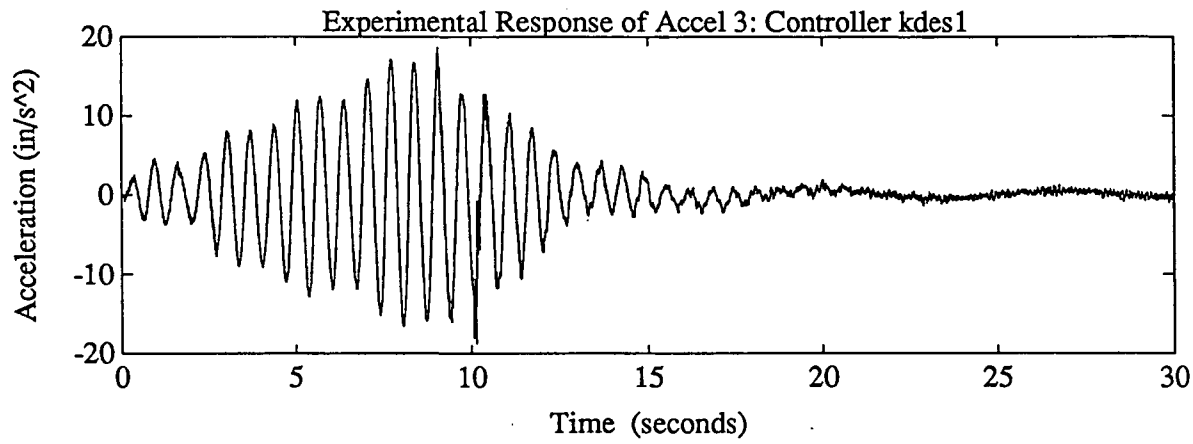
Experimental Response of Accel 3: Controller kdes1
Acceleration (in/s^2)
20
10
0
-10
-20
0
5
10
15
20
25
30
Time (seconds)

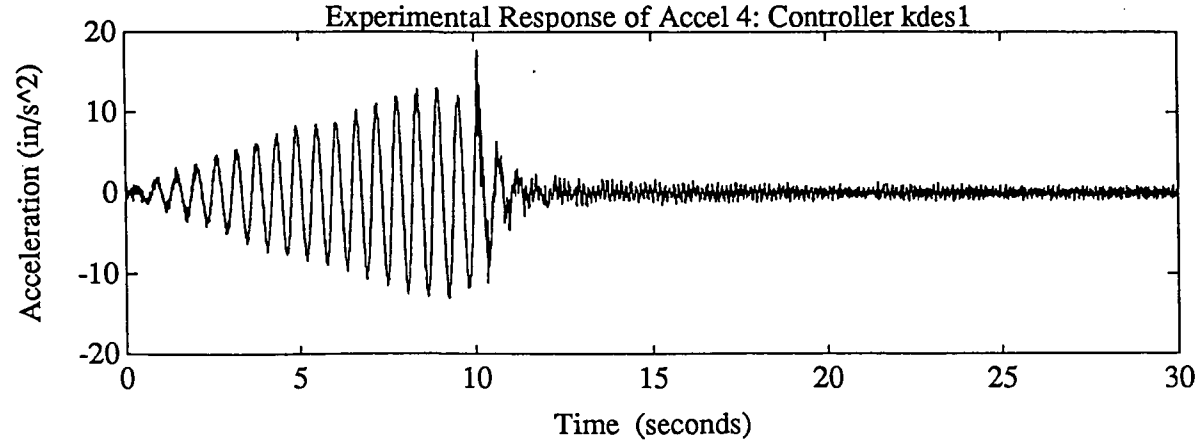
Experimental Response of Accel 4: Controller kdes1
Acceleration (in/s^2)
20
10
0
-10
-20
0
5
10
15
20
25
30
Time (seconds)

Figure All

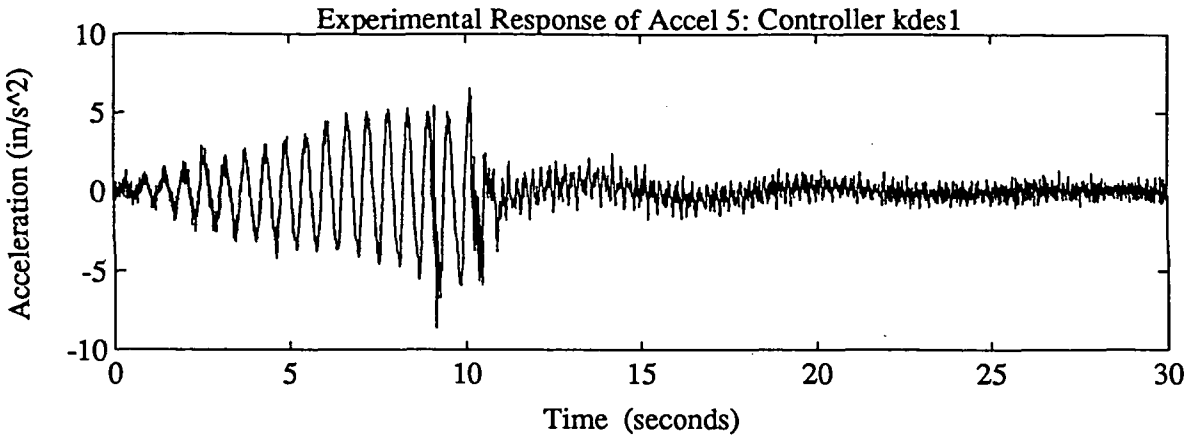
Experimental Response of Accel 5: Controller kdes1
Acceleration (in/s^2)
10
5
0
-5
-10
0
5
10
15
20
25
30
Time (seconds)

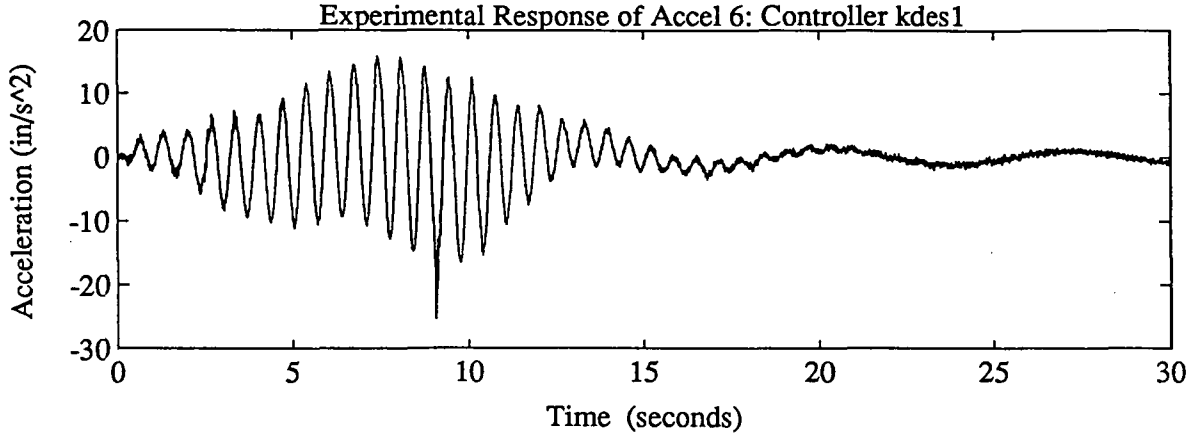
Experimental Response of Accel 6: Controller kdes1
Acceleration (in/s^2)
20
10
0
-10
-20
-30
0
5
10
15
20
25
30
Time (seconds)

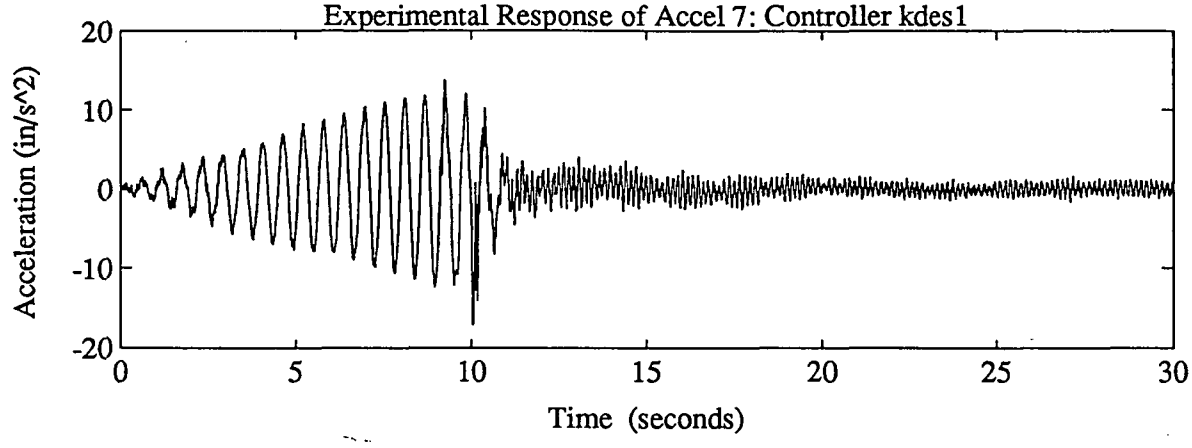
Experimental Response of Accel 7: Controller kdes1
Acceleration (in/s^2)
20
10
0
-10
-20
0
5
10
15
20
25
30
Time (seconds)

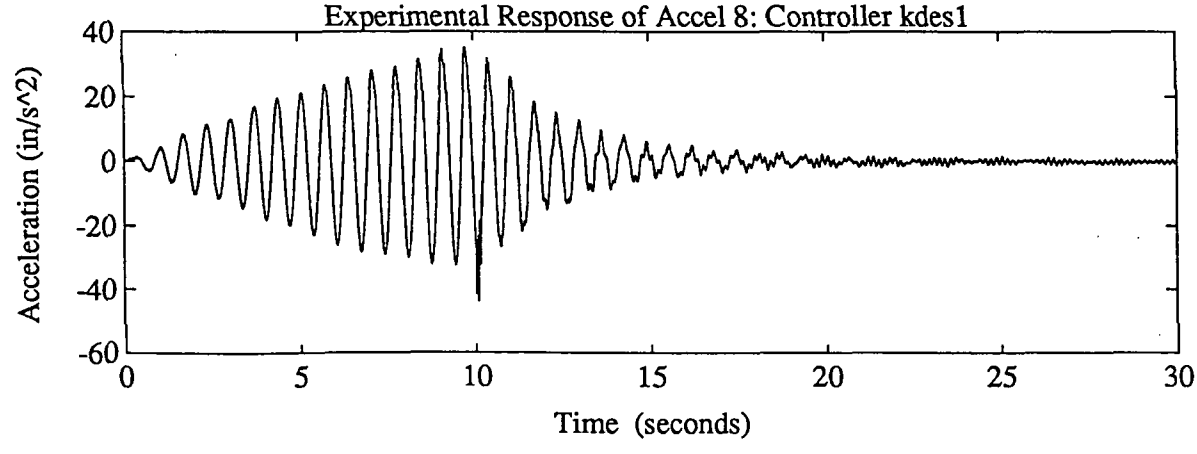
Experimental Response of Accel 8: Controller kdes1
Acceleration (in/s^2)
40
20
0
-20
-40
-60
0
5
10
15
20
25
30
Time (seconds)

Figure A12

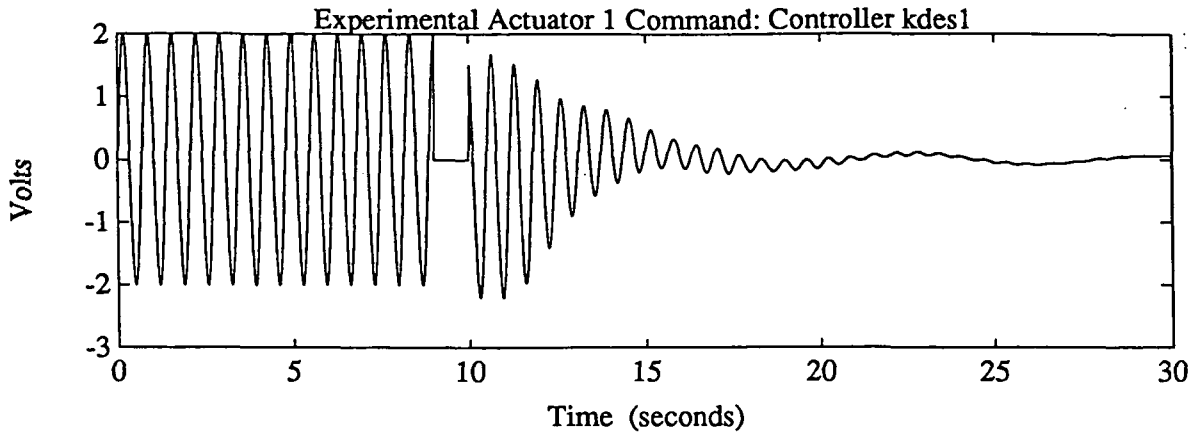
Experimental Actuator 1 Command: Controller kdes1
Volts
2
1
0
-1
-2
-3
0
5
10
15
20
25
30
Time (seconds)

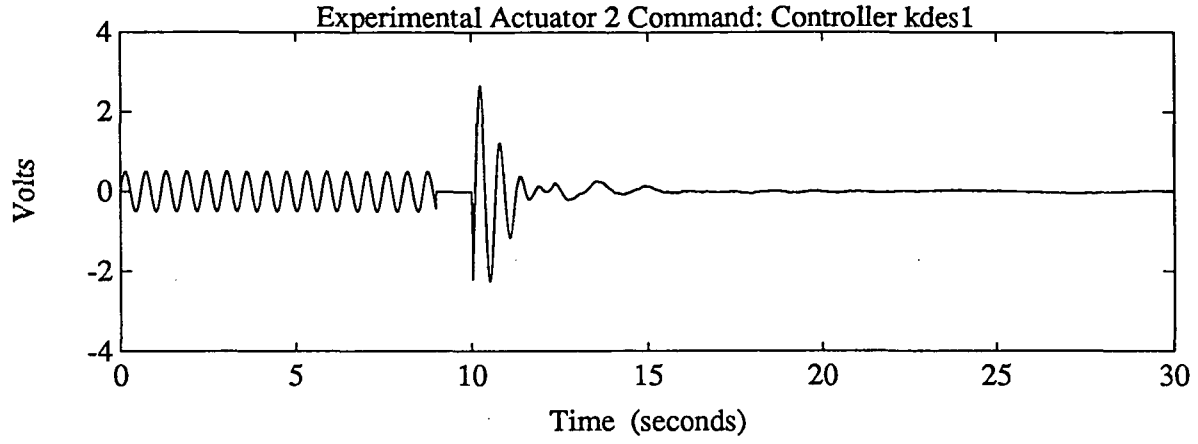
Experimental Actuator 2 Command: Controller kdes1
Volts
4
2
0
-2
-4
0
5
10
15
20
25
30
Time (seconds)

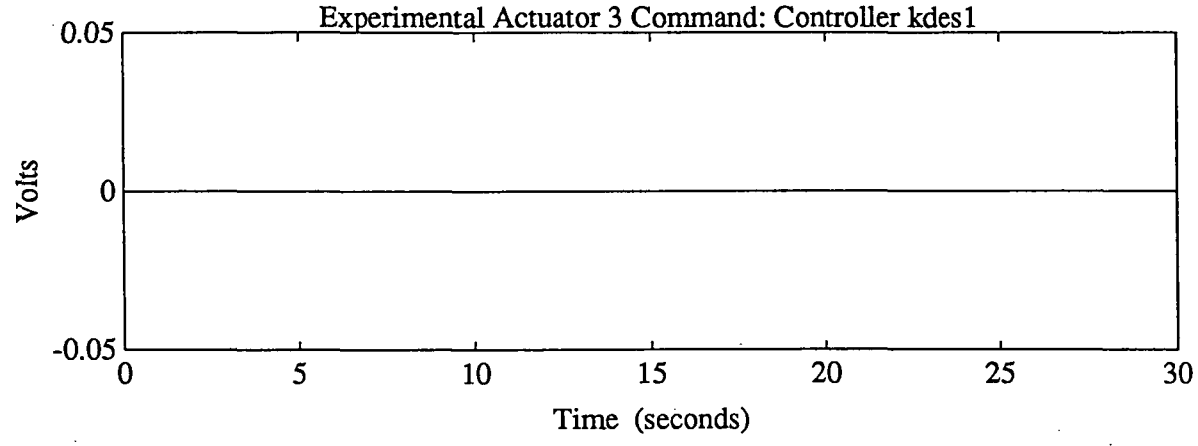
Experimental Actuator 3 Command: Controller kdes1
Volts
0.05
0
-0.05
0
5
10
15
20
25
30
Time (seconds)

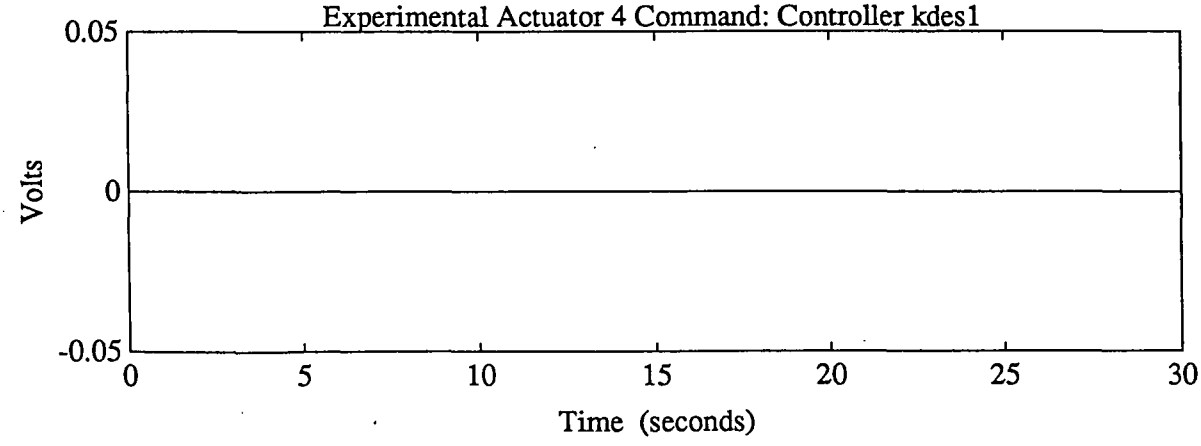
Experimental Actuator 4 Command: Controller kdes1
Volts
0.05
0
-0.05
0
5
10
15
20
25
30
Time (seconds)

Figure A13

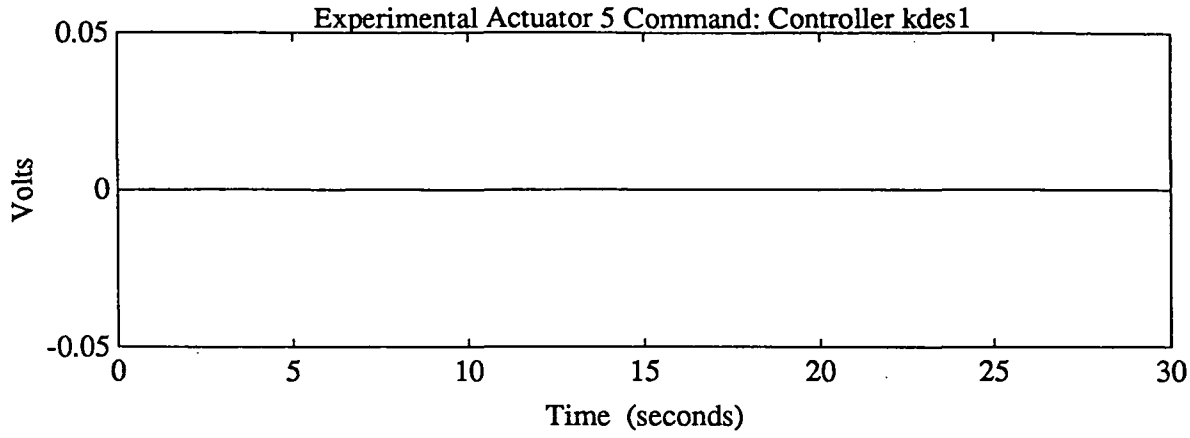
Experimental Actuator 5 Command: Controller kdes1
0.05
0
-0.05
Volts
0
5
10
15
20
25
30
Time (seconds)

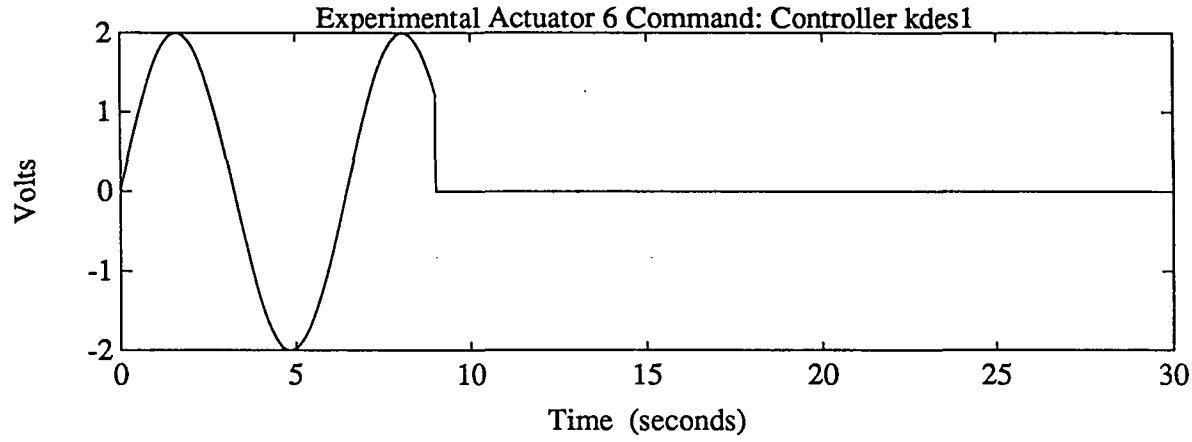
Experimental Actuator 6 Command: Controller kdes1
2
1
0
-1
-2
Volts
0
5
10
15
20
25
30
Time (seconds)

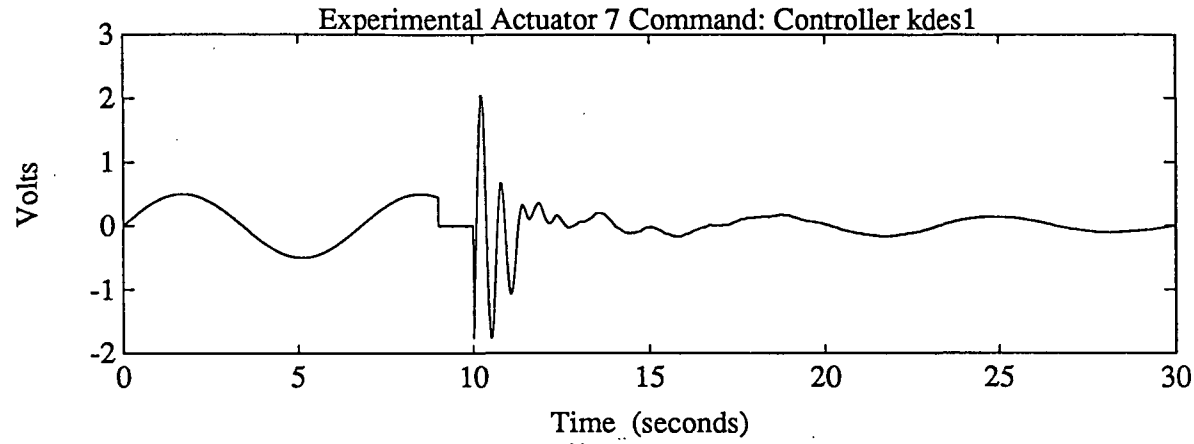
Experimental Actuator 7 Command: Controller kdes1
3
2
1
0
-1
-2
Volts
0
5
10
15
20
25
30
Time (seconds)

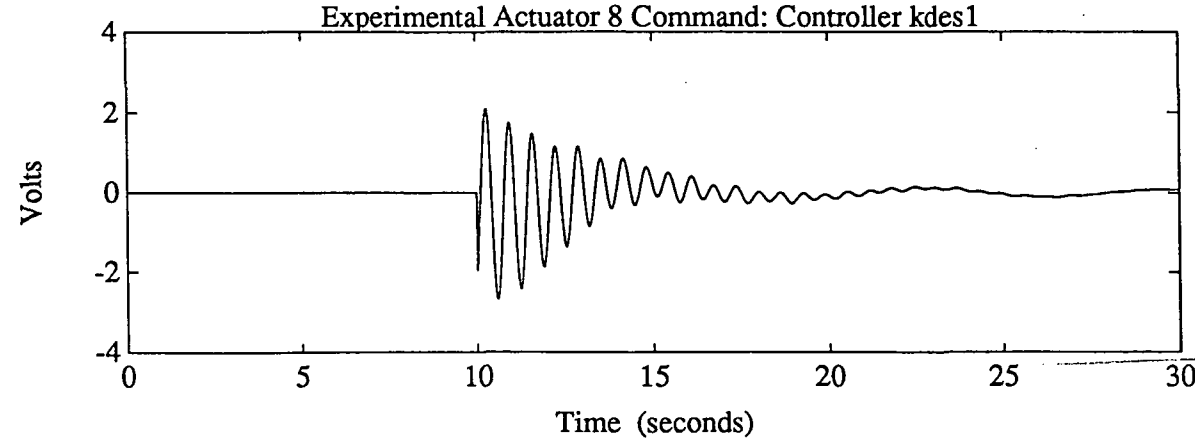
Experimental Actuator 8 Command: Controller kdes1
4
2
0
-2
-4
Volts
0
5
10
15
20
25
30
Time (seconds)

Figure A14

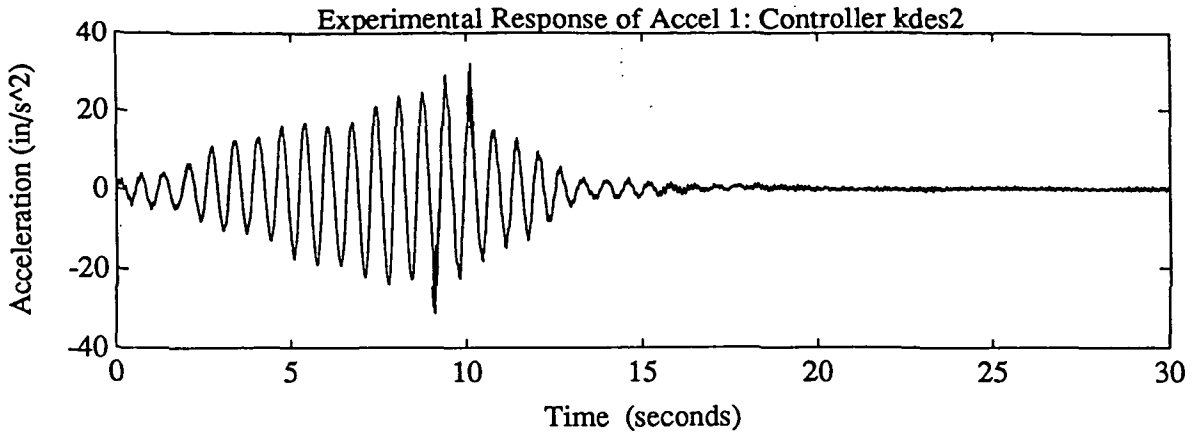
Experimental Response of Accel 1: Controller kdes2
Acceleration (in/s^2)
40
20
0
-20
-40
0
5
10
15
20
25
30
Time (seconds)

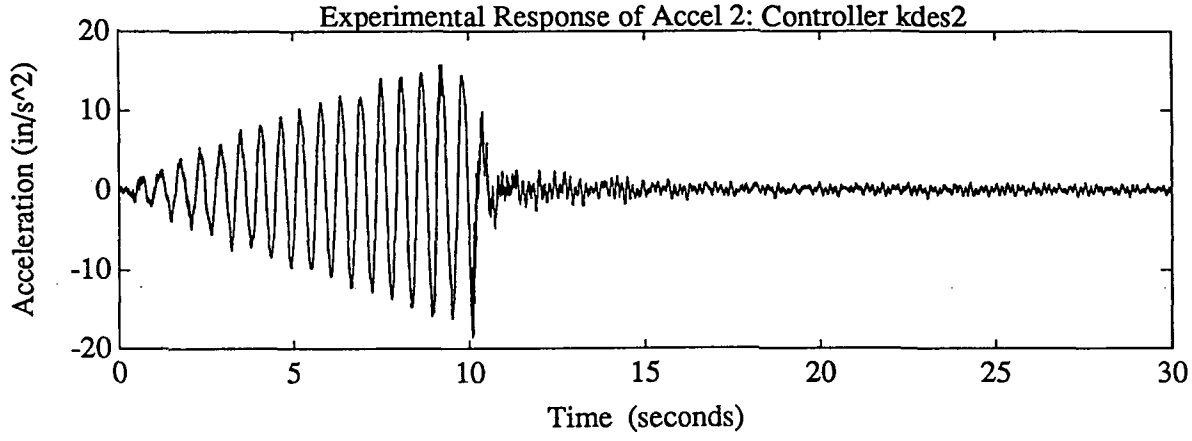
Experimental Response of Accel 2: Controller kdes2
Acceleration (in/s^2)
20
10
0
-10
-20
0
5
10
15
20
25
30
Time (seconds)

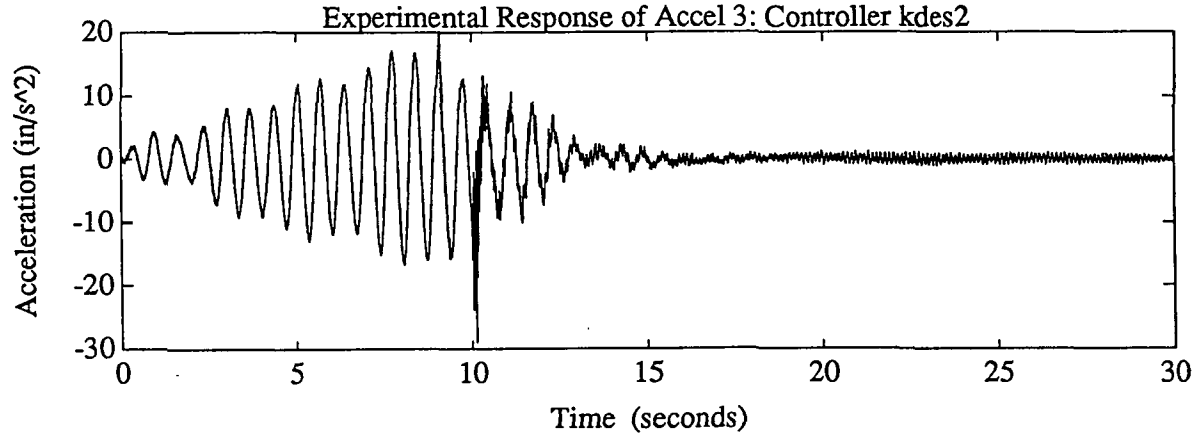
Experimental Response of Accel 3: Controller kdes2
Acceleration (in/s^2)
20
10
0
-10
-20
-30
0
5
10
15
20
25
30
Time (seconds)

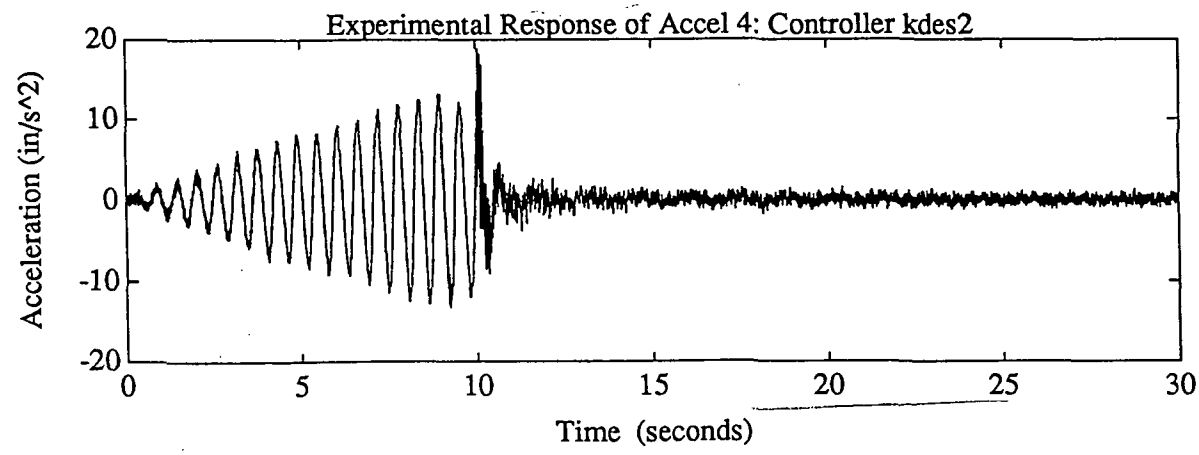
Experimental Response of Accel 4: Controller kdes2
Acceleration (in/s^2)
20
10
0
-10
-20
0
5
10
15
20
25
30
Time (seconds)

Figure A15

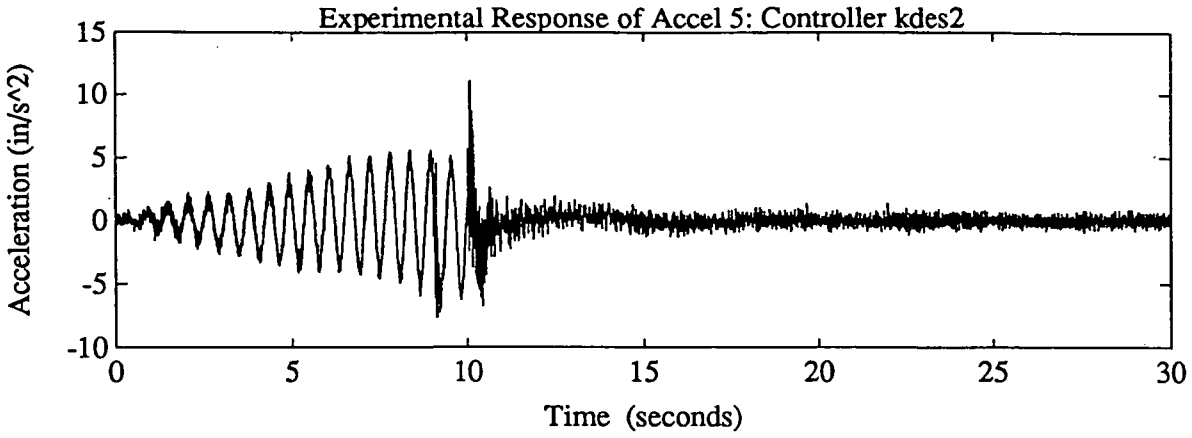
Experimental Response of Accel 5: Controller kdes2
Acceleration (in/s^2)
15
10
5
0
-5
-10
0
5
10
15
20
25
30
Time (seconds)

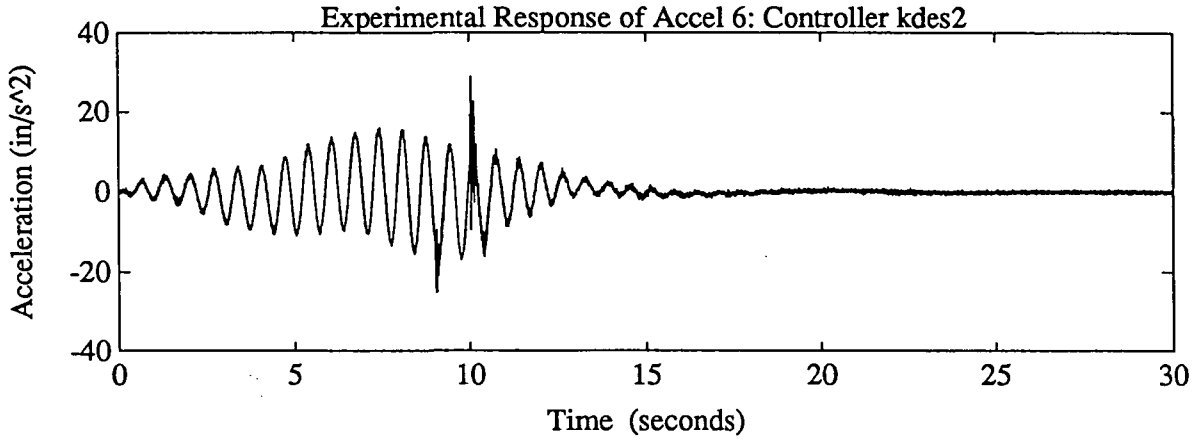
Experimental Response of Accel 6: Controller kdes2
Acceleration (in/s^2)
40
20
0
-20
-40
0
5
10
15
20
25
30
Time (seconds)

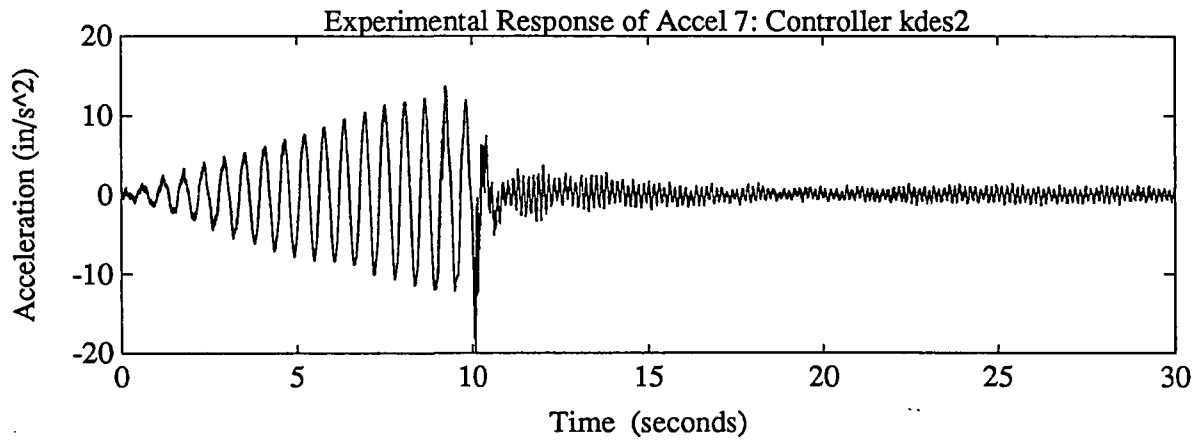
Experimental Response of Accel 7: Controller kdes2
Acceleration (in/s^2)
20
10
0
-10
-20
0
5
10
15
20
25
30
Time (seconds)

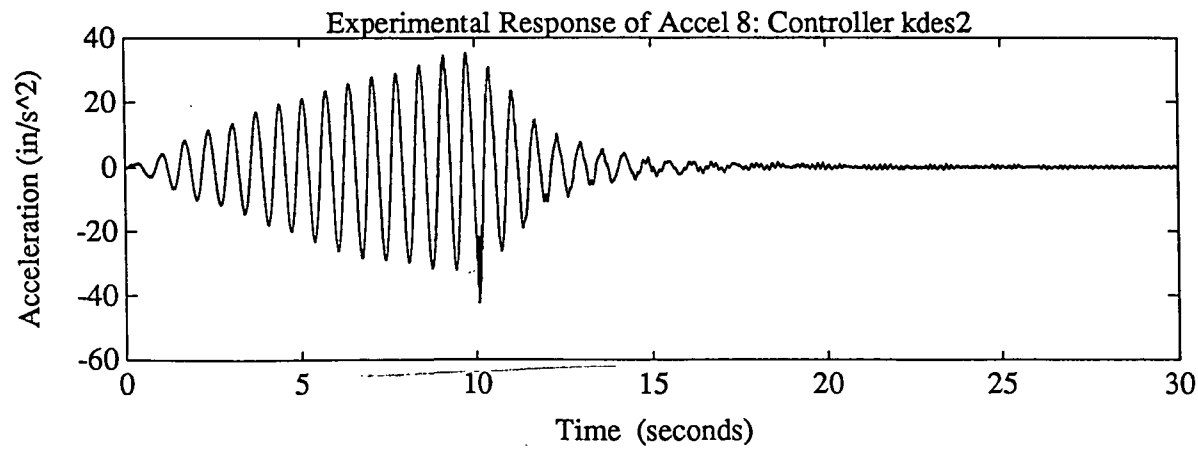
Experimental Response of Accel 8: Controller kdes2
Acceleration (in/s^2)
40
20
0
-20
-40
-60
0
5
10
15
20
25
30
Time (seconds)

Figure A16

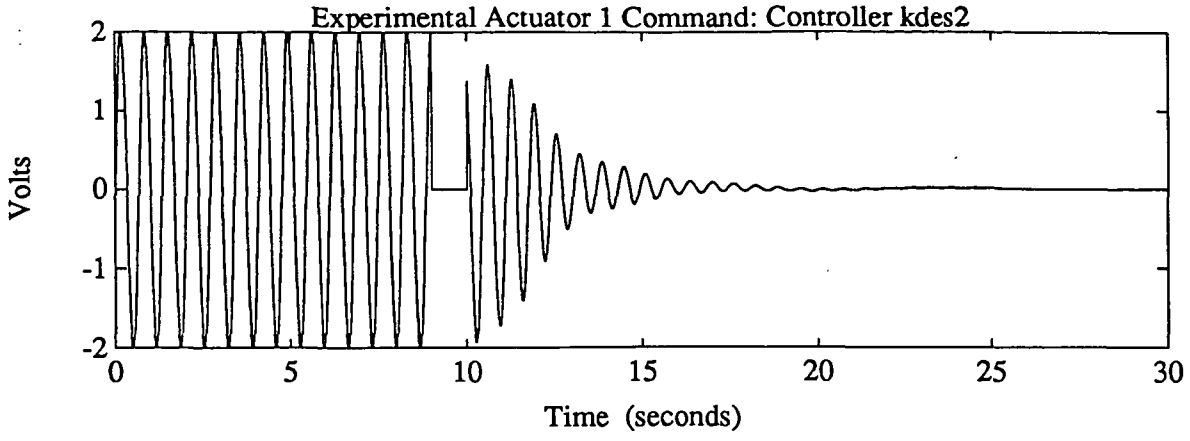
Experimental Actuator 1 Command: Controller kdes2
Volts
Time (seconds)

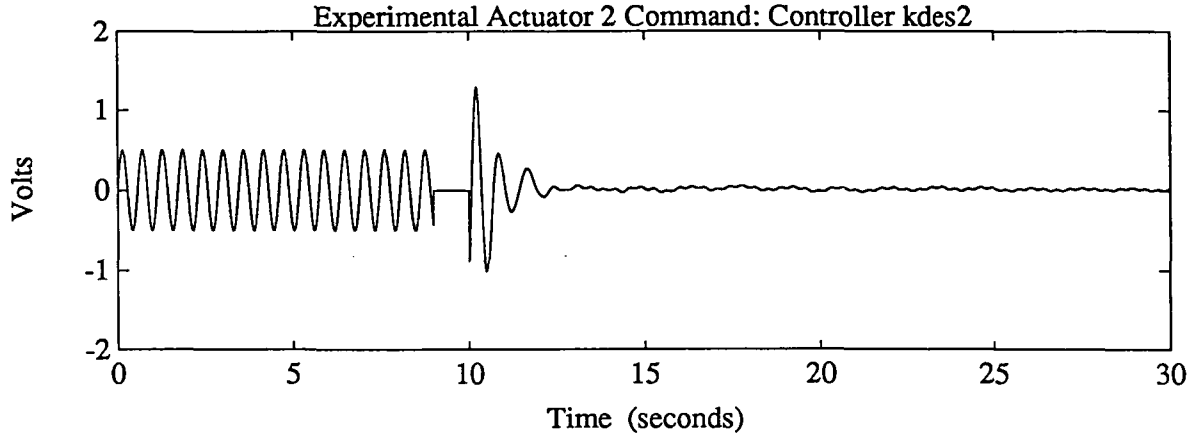
Experimental Actuator 2 Command: Controller kdes2
Volts
Time (seconds)

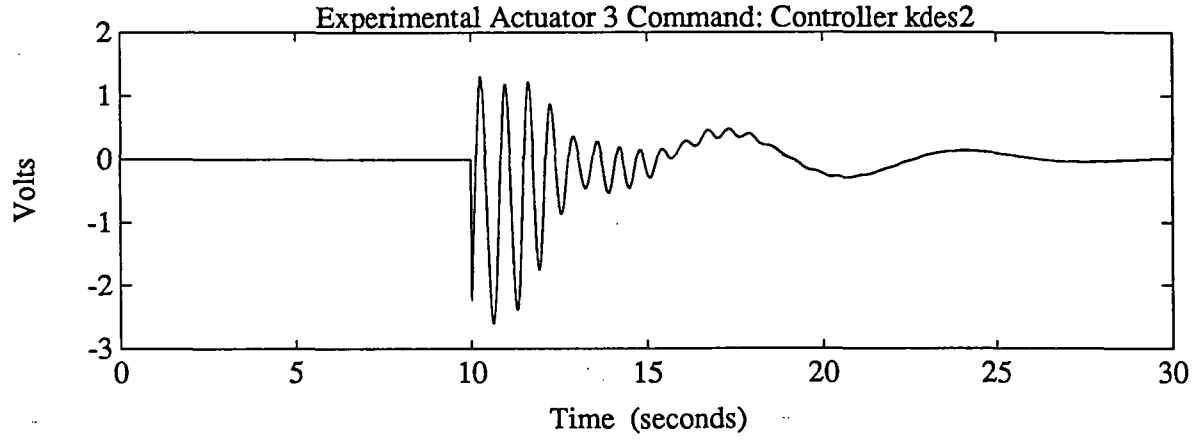
Experimental Actuator 3 Command: Controller kdes2
Volts
Time (seconds)

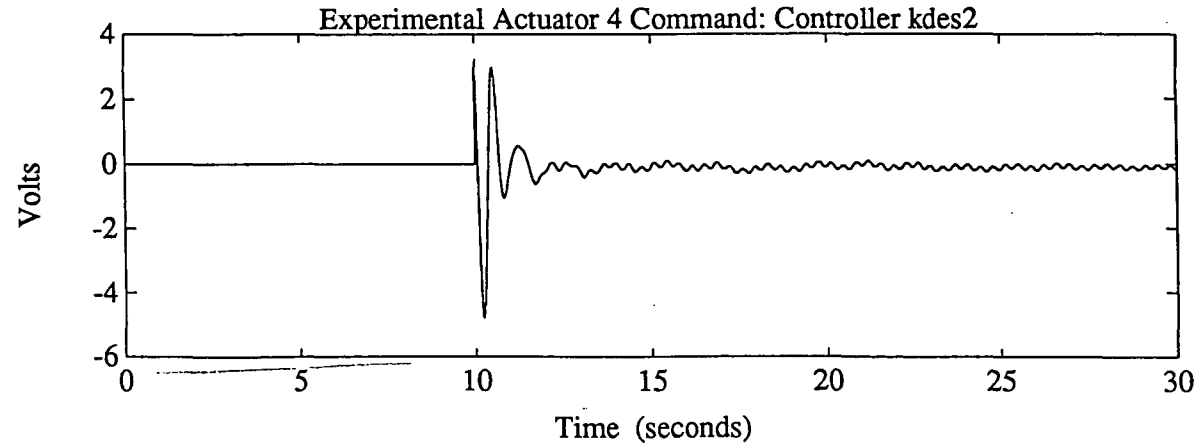
Experimental Actuator 4 Command: Controller kdes2
Volts
Time (seconds)

Figure A17

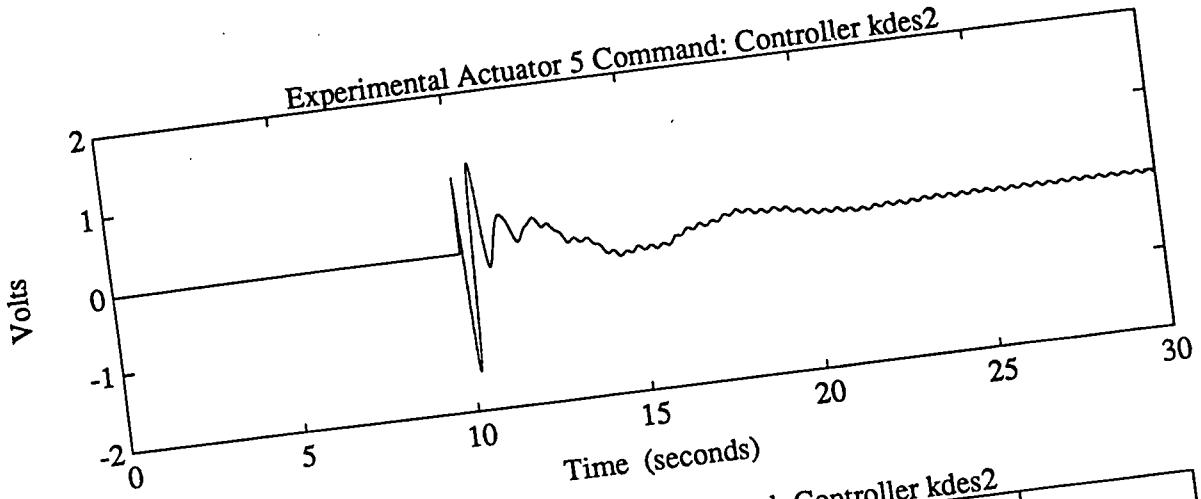

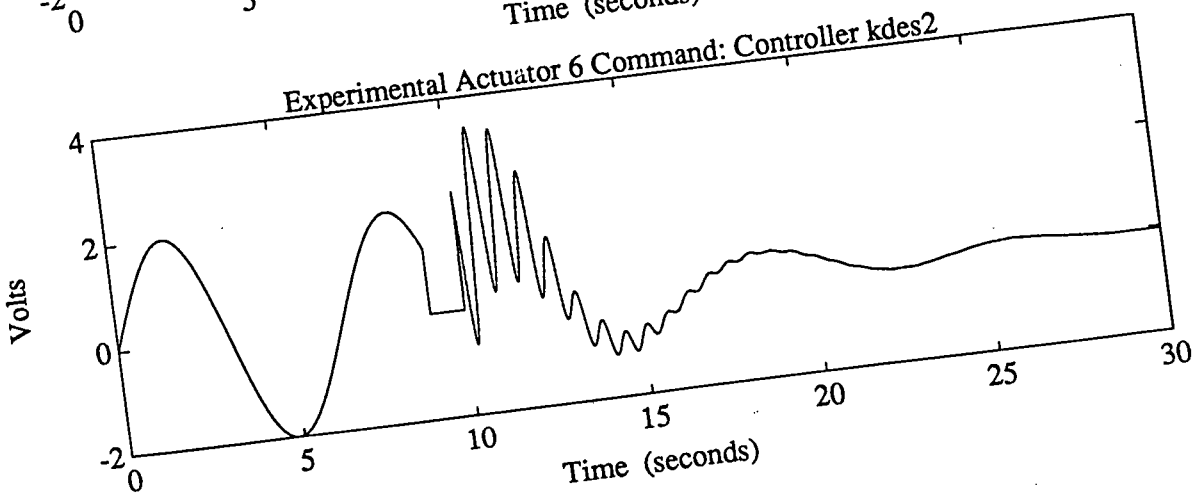

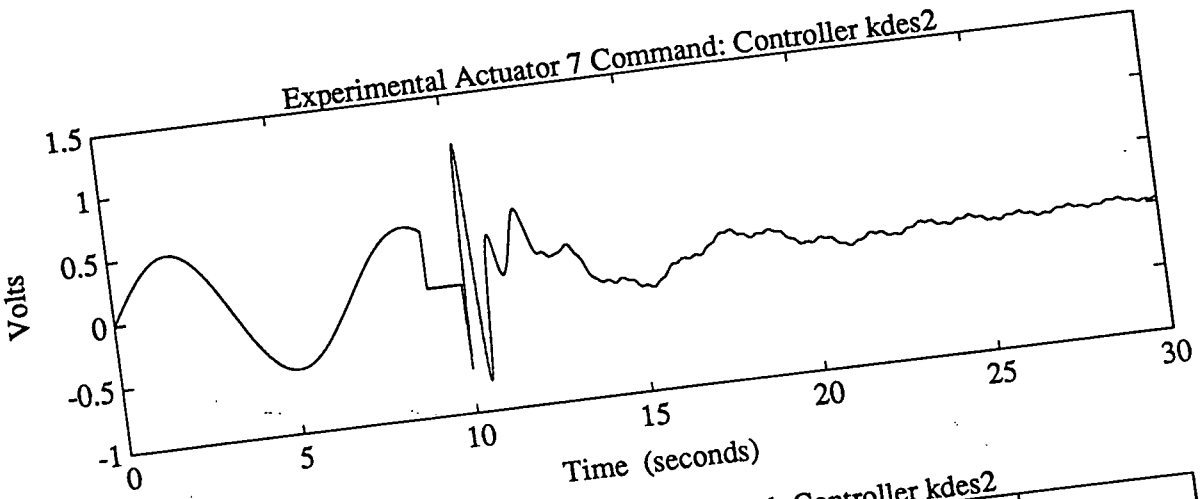

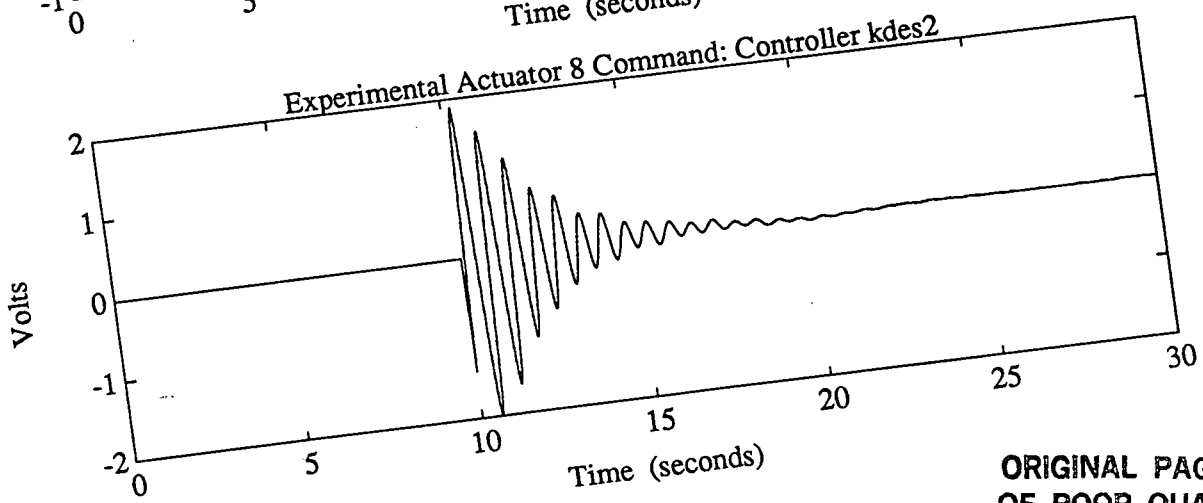

ORIGINAL PAGE IS
OF POOR QUALITY

Figure A18

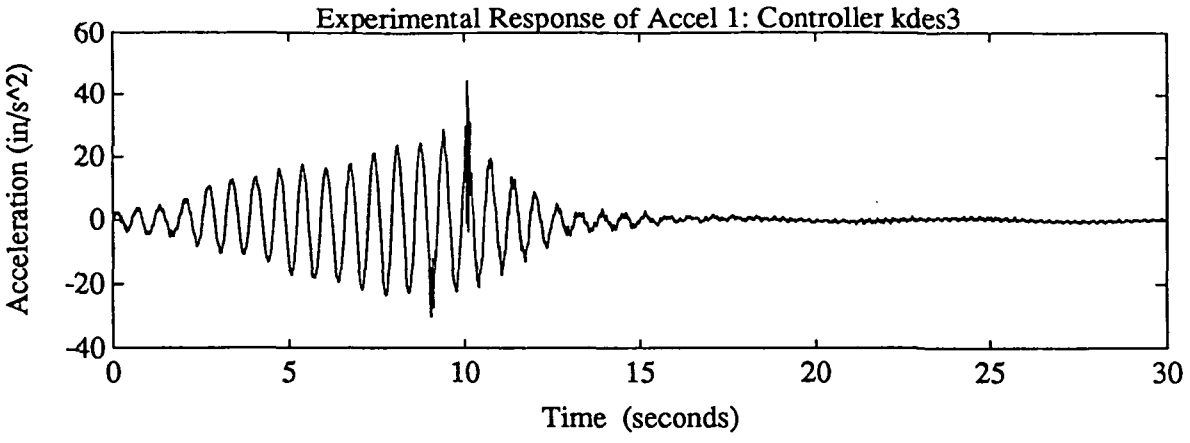
Experimental Response of Accel 1: Controller kdes3
Acceleration (in/s^2)
60
40
20
0
-20
-40
0
5
10
15
20
25
30
Time (seconds)

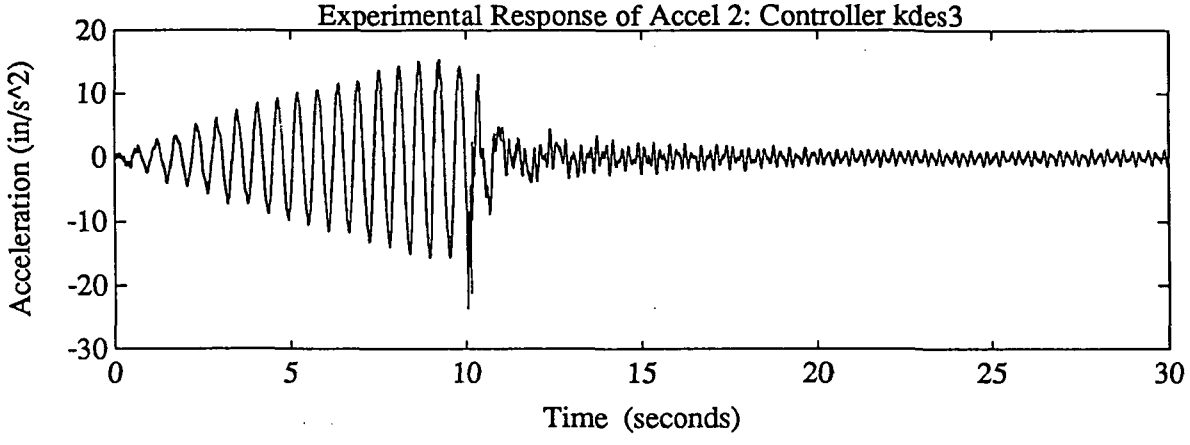
Experimental Response of Accel 2: Controller kdes3
Acceleration (in/s^2)
20
10
0
-10
-20
-30
0
5
10
15
20
25
30
Time (seconds)

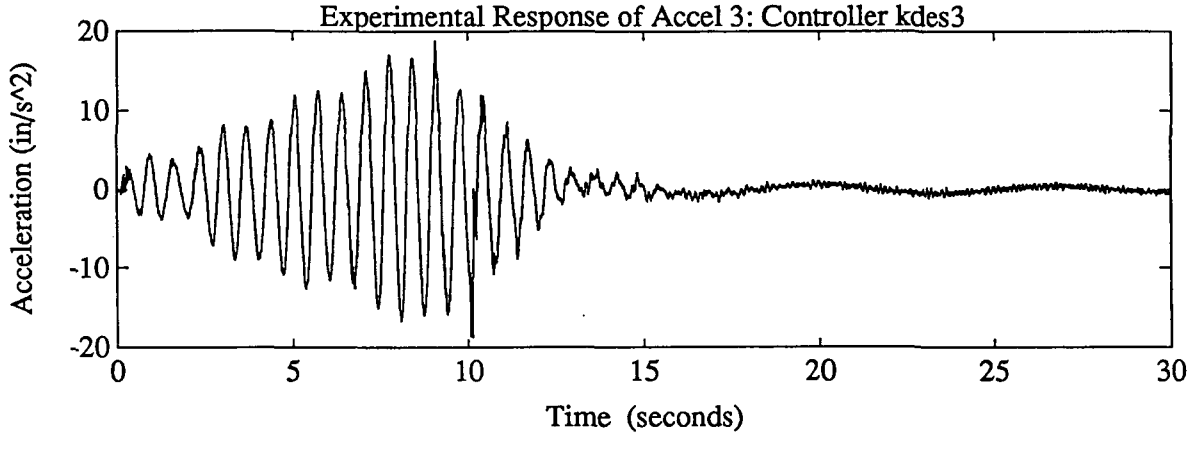
Experimental Response of Accel 3: Controller kdes3
Acceleration (in/s^2)
20
10
0
-10
-20
0
5
10
15
20
25
30
Time (seconds)

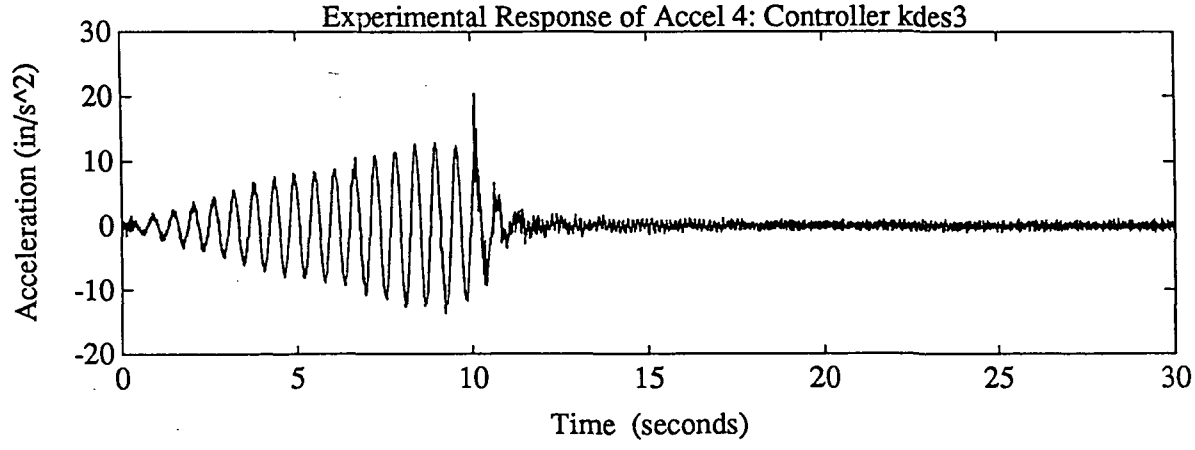
Experimental Response of Accel 4: Controller kdes3
Acceleration (in/s^2)
30
20
10
0
-10
-20
0
5
10
15
20
25
30
Time (seconds)

Figure A19

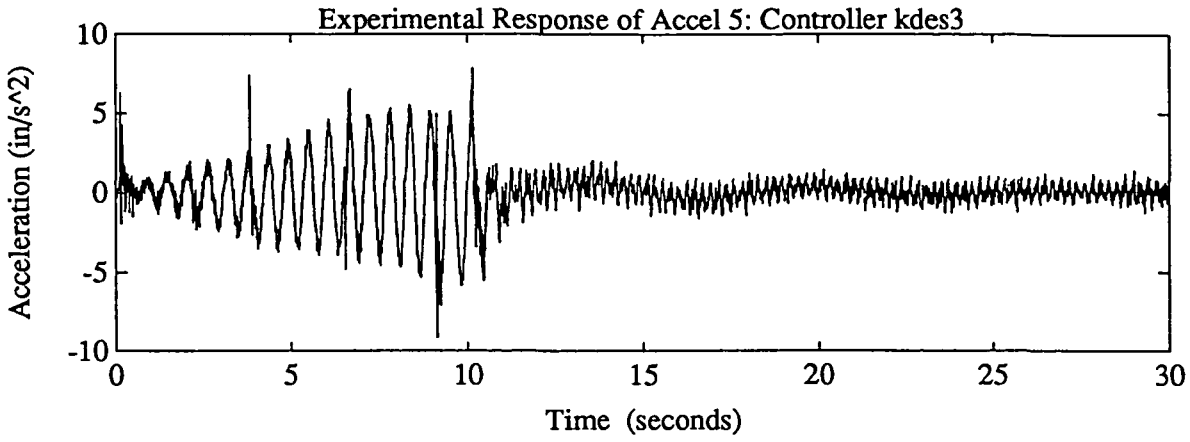
Experimental Response of Accel 5: Controller kdes3
Acceleration (in/s^2)
10
5
0
-5
-10
0
5
10
15
20
25
30
Time (seconds)

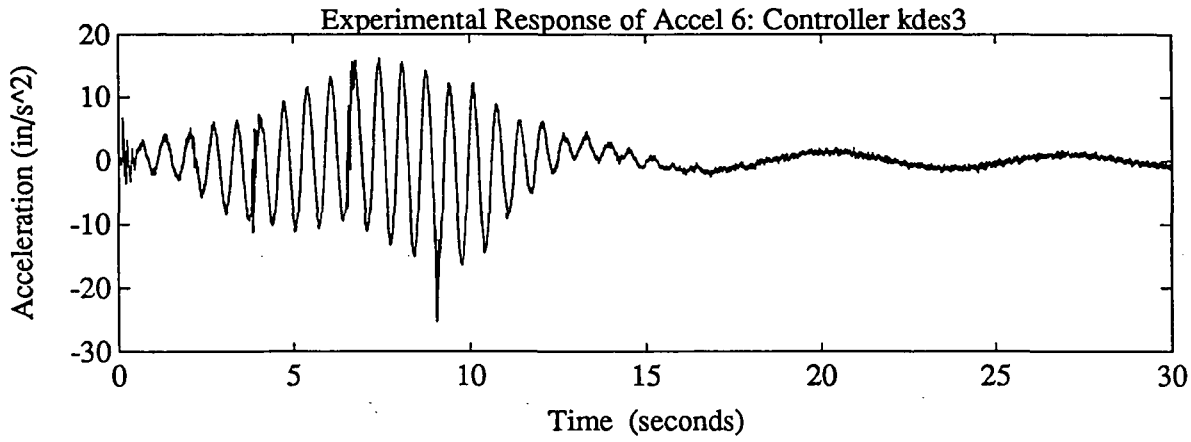
Experimental Response of Accel 6: Controller kdes3
Acceleration (in/s^2)
20
10
0
-10
-20
-30
0
5
10
15
20
25
30
Time (seconds)

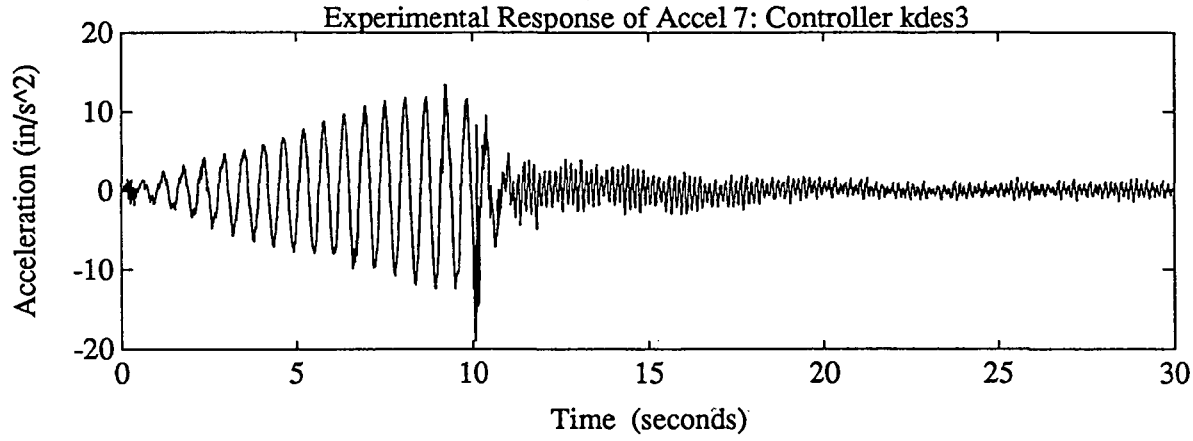
Experimental Response of Accel 7: Controller kdes3
Acceleration (in/s^2)
20
10
0
-10
-20
0
5
10
15
20
25
30
Time (seconds)

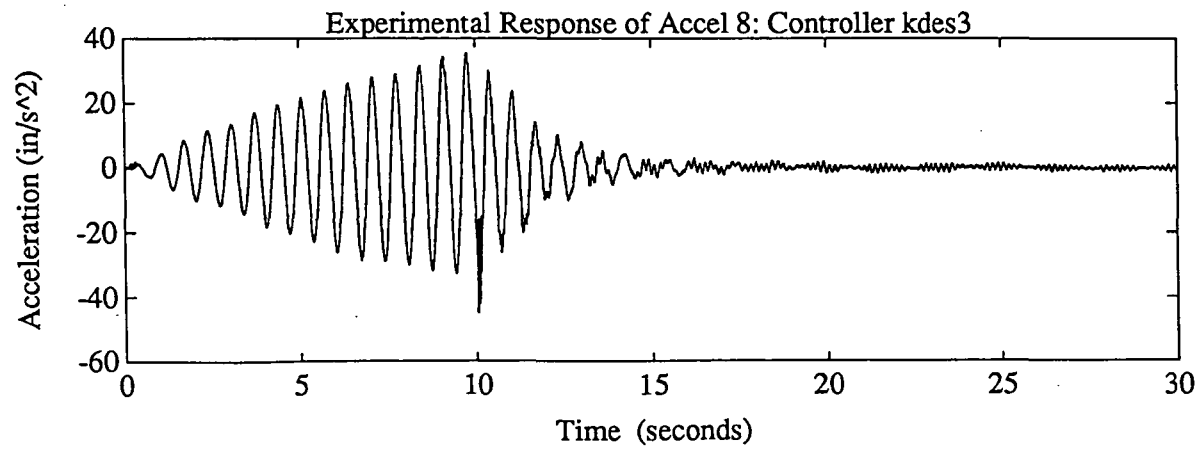
Experimental Response of Accel 8: Controller kdes3
Acceleration (in/s^2)
40
20
0
-20
-40
-60
0
5
10
15
20
25
30
Time (seconds)

Figure A20

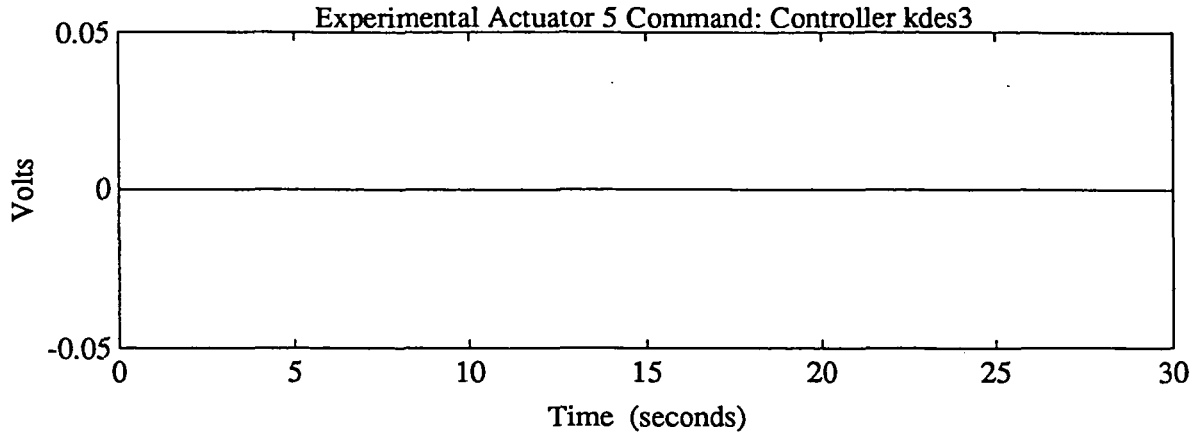
Experimental Actuator 5 Command: Controller kdes3
0.05
0
-0.05
Volts
0
5
10
15
20
25
30
Time (seconds)

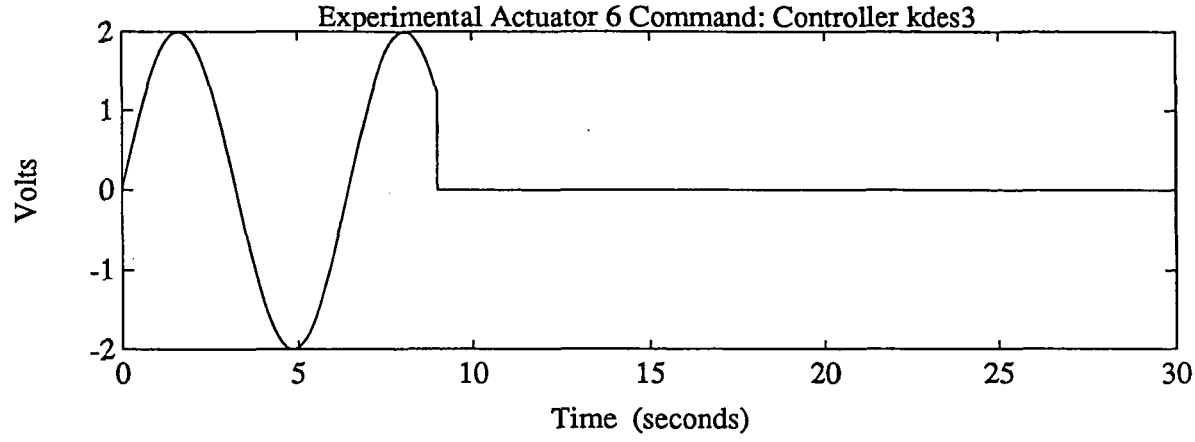
Experimental Actuator 6 Command: Controller kdes3
2
1
0
-1
-2
Volts
0
5
10
15
20
25
30
Time (seconds)

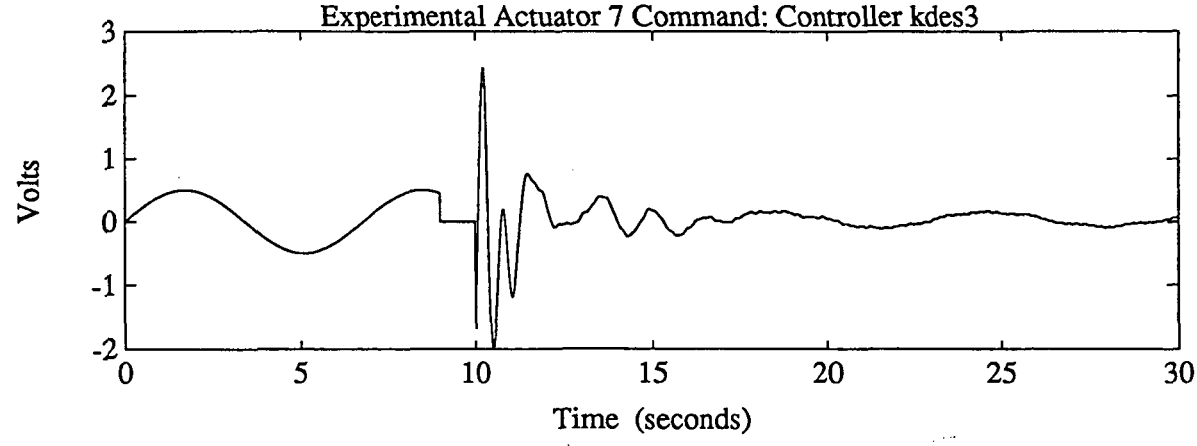
Experimental Actuator 7 Command: Controller kdes3
3
2
1
0
-1
-2
Volts
0
5
10
15
20
25
30
Time (seconds)

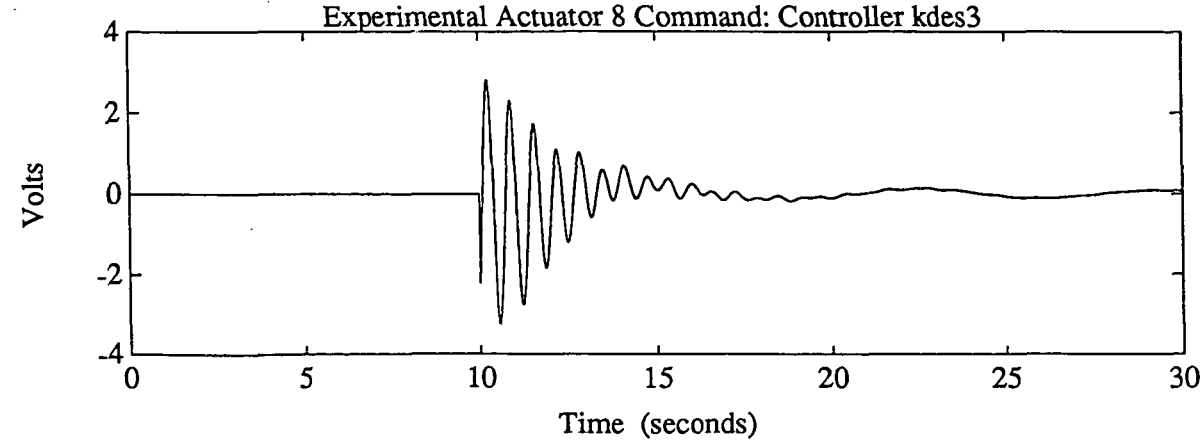
Experimental Actuator 8 Command: Controller kdes3
4
2
0
-2
-4
Volts
0
5
10
15
20
25
30
Time (seconds)

Figure A21

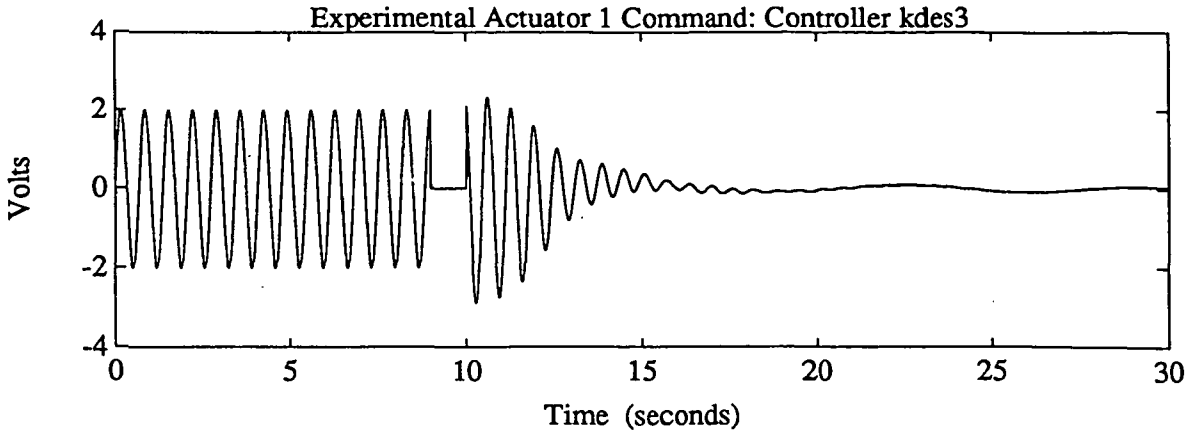
Experimental Actuator 1 Command: Controller kdes3
Volts
Time (seconds)

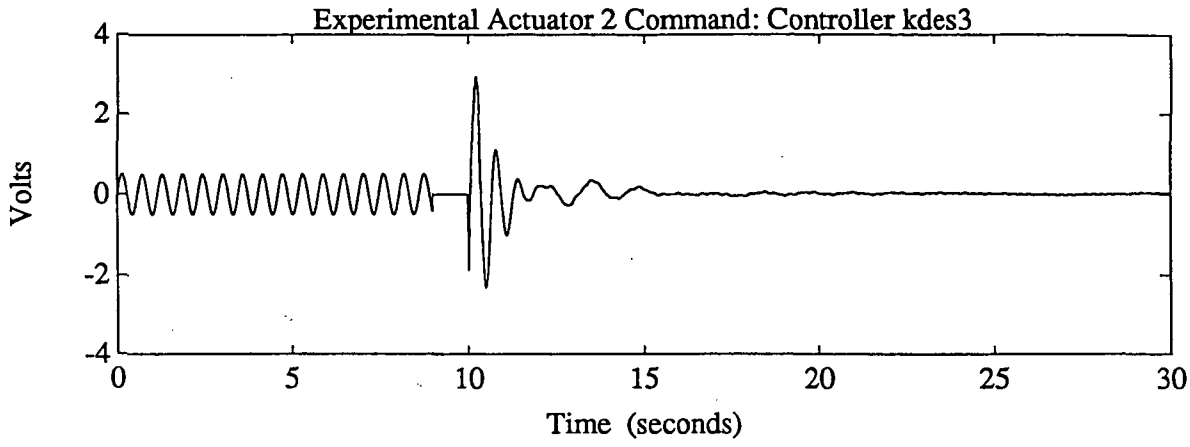
Experimental Actuator 2 Command: Controller kdes3
Volts
Time (seconds)

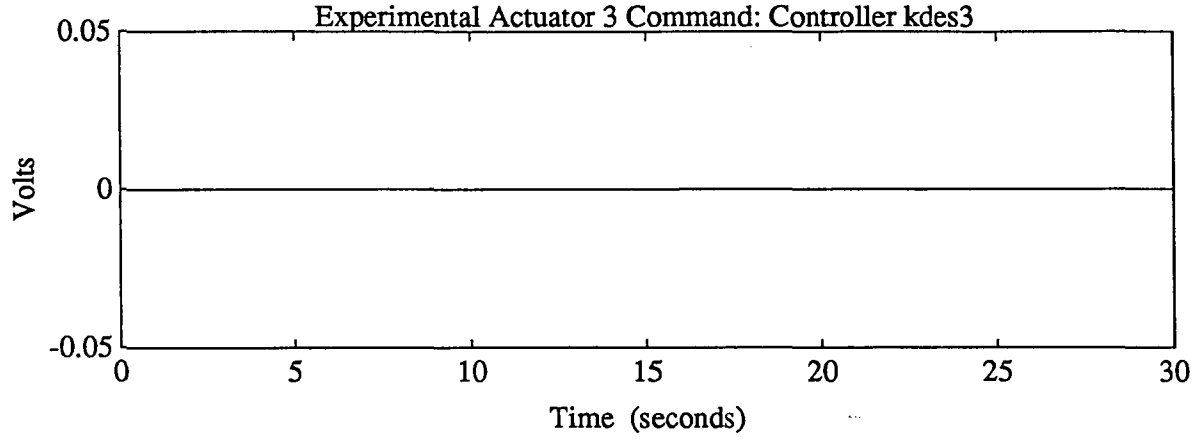
Experimental Actuator 3 Command: Controller kdes3
Volts
Time (seconds)

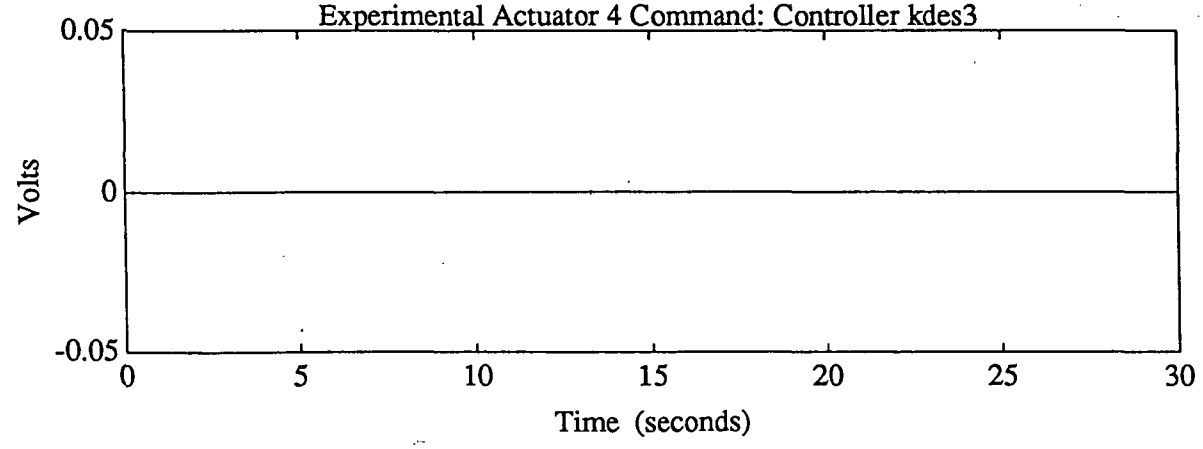
Experimental Actuator 4 Command: Controller kdes3
Volts
Time (seconds)

Figure A22

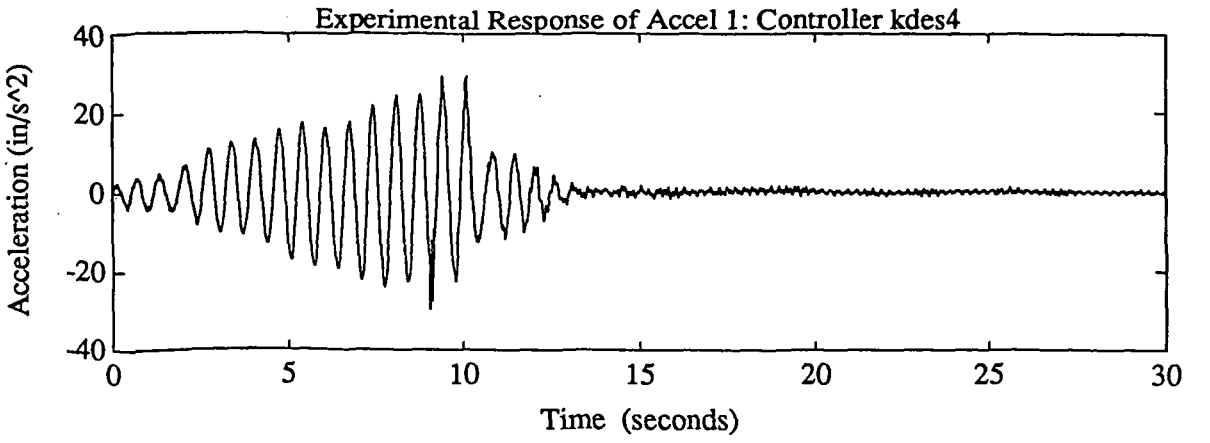
Experimental Response of Accel 1: Controller kdes4
Acceleration (in/s^2)
40
20
0
-20
-40
0
5
10
15
20
25
30
Time (seconds)

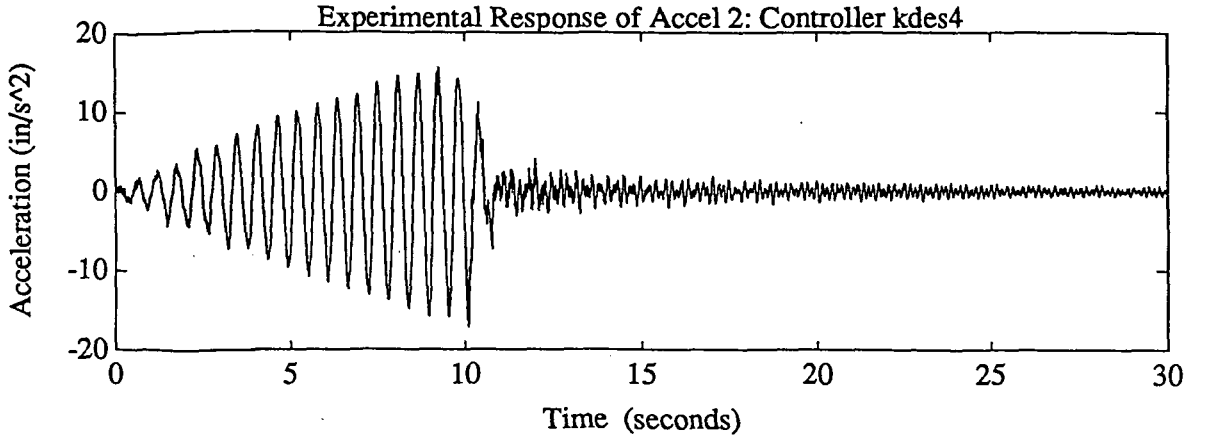
Experimental Response of Accel 2: Controller kdes4
Acceleration (in/s^2)
20
10
0
-10
-20
0
5
10
15
20
25
30
Time (seconds)

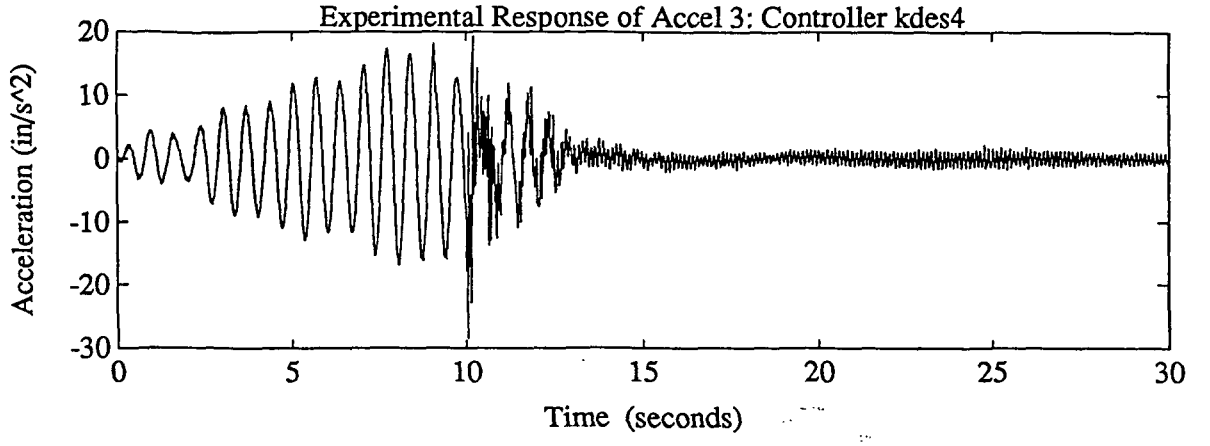
Experimental Response of Accel 3: Controller kdes4
Acceleration (in/s^2)
20
10
0
-10
-20
-30
0
5
10
15
20
25
30
Time (seconds)

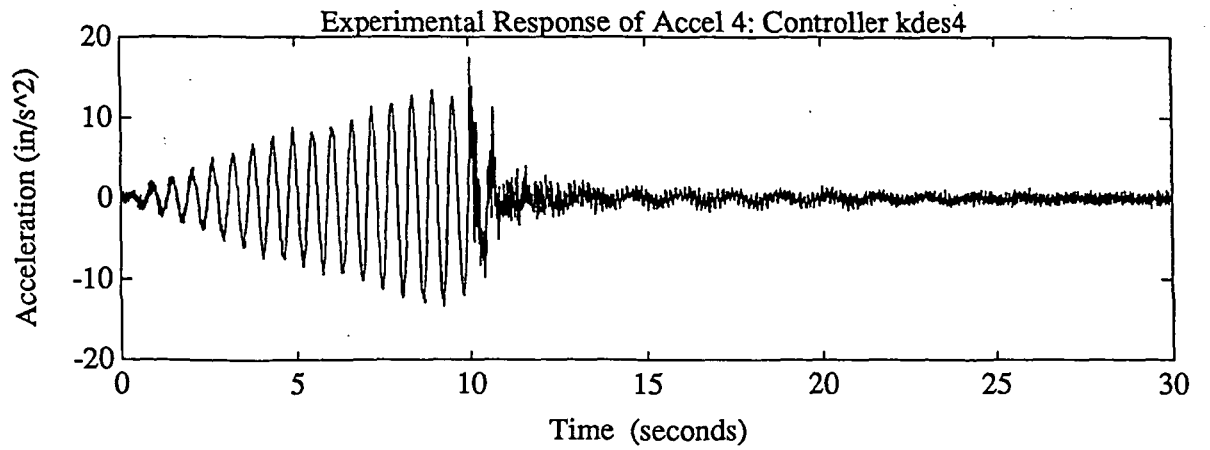
Experimental Response of Accel 4: Controller kdes4
Acceleration (in/s^2)
20
10
0
-10
-20
0
5
10
15
20
25
30
Time (seconds)

Figure A23

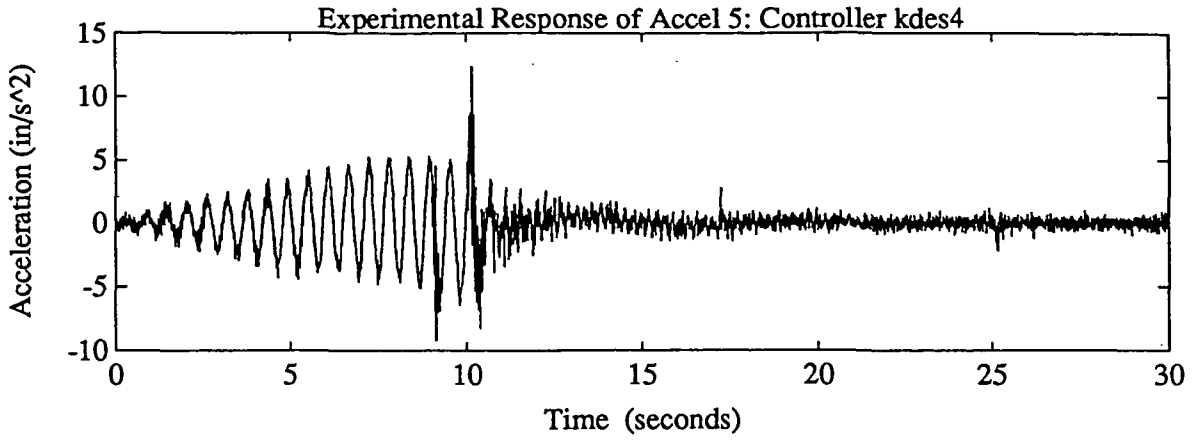
Experimental Response of Accel 5: Controller kdes4
Acceleration (in/s^2)
Time (seconds)

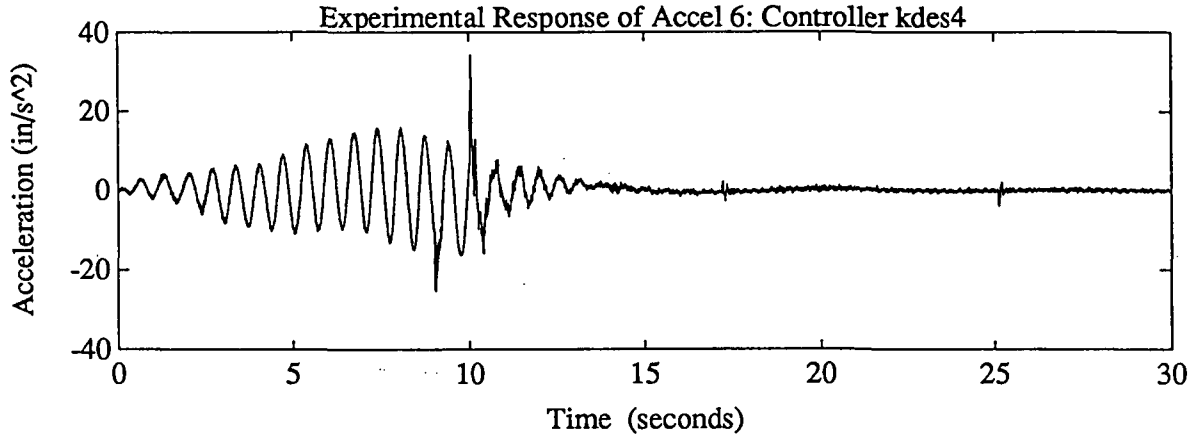
Experimental Response of Accel 6: Controller kdes4
Acceleration (in/s^2)
Time (seconds)

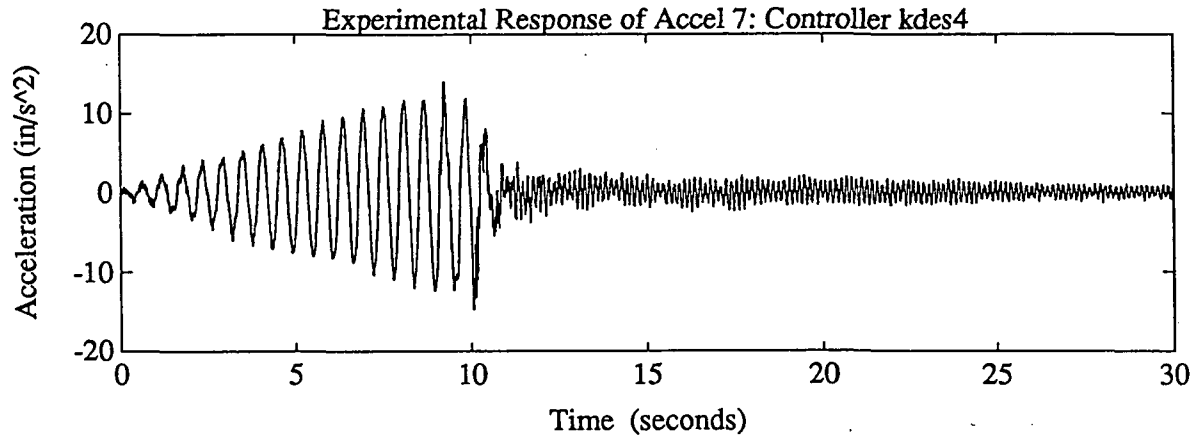
Experimental Response of Accel 7: Controller kdes4
Acceleration (in/s^2)
Time (seconds)

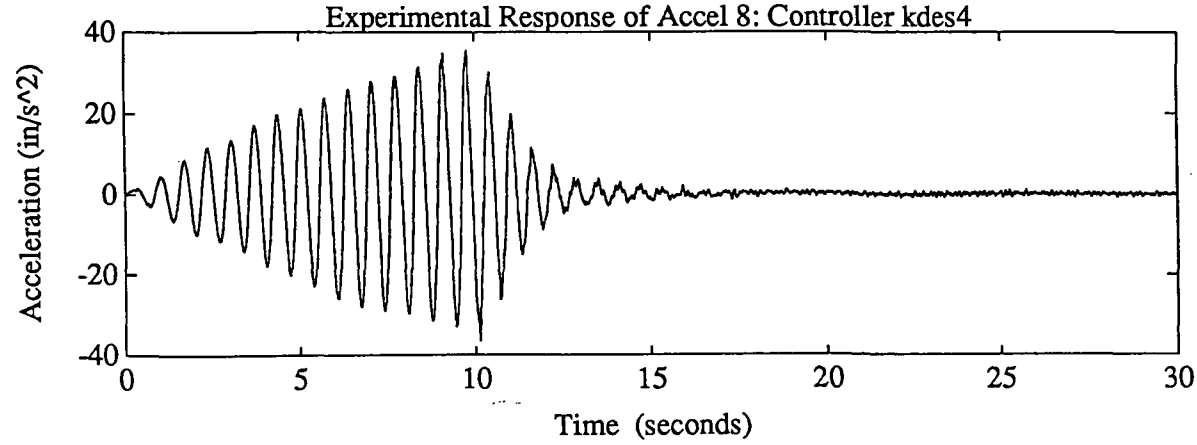
Experimental Response of Accel 8: Controller kdes4
Acceleration (in/s^2)
Time (seconds)

Figure A24

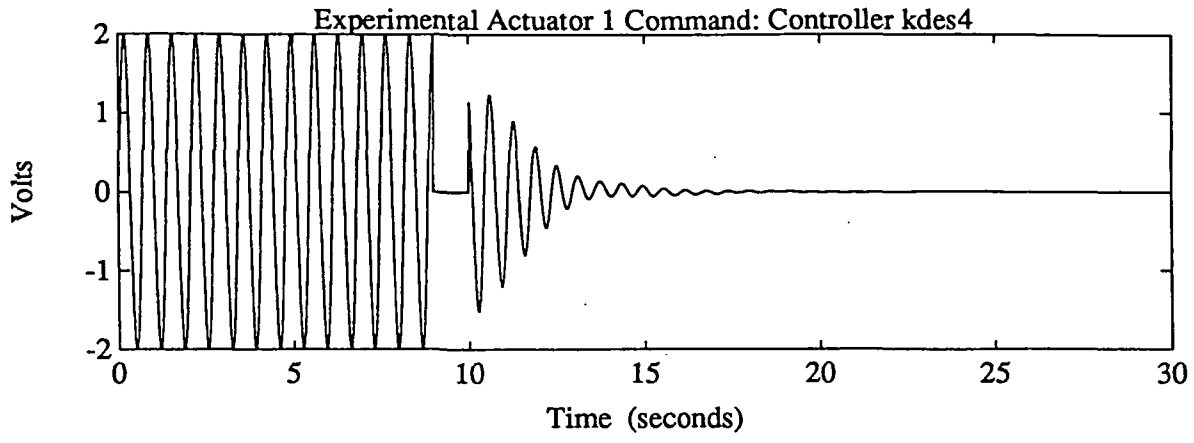
Experimental Actuator 1 Command: Controller kdes4
Volts
Time (seconds)

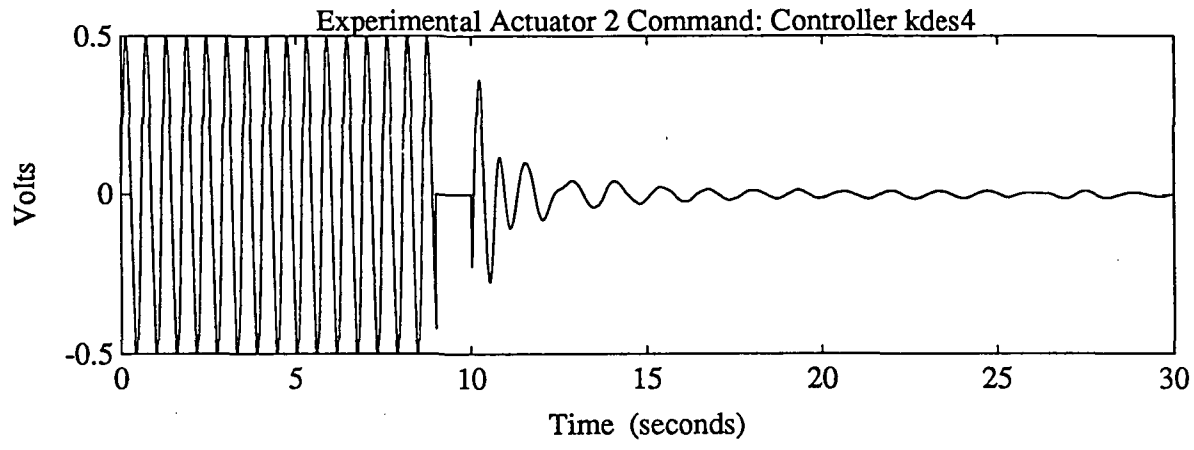
Experimental Actuator 2 Command: Controller kdes4
Volts
Time (seconds)

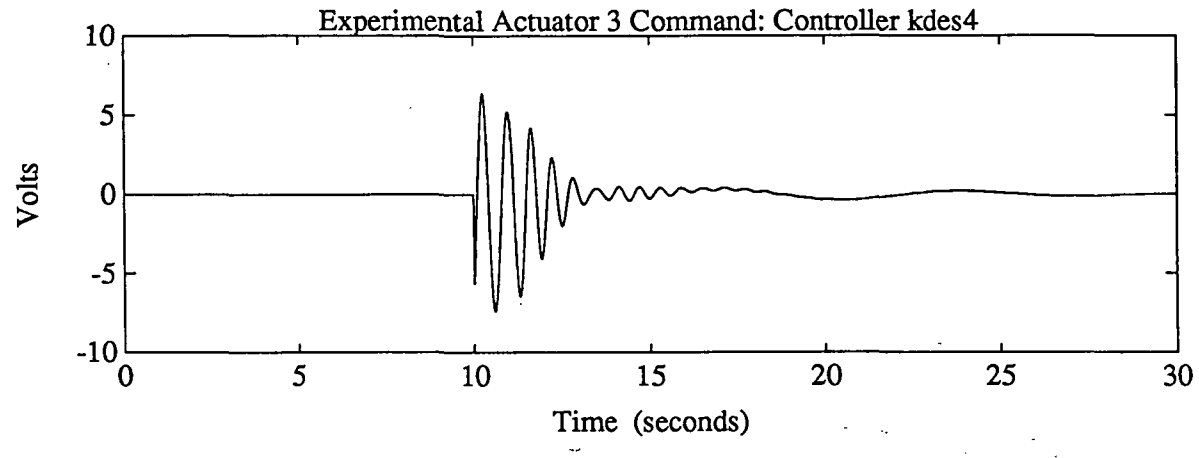
Experimental Actuator 3 Command: Controller kdes4
Volts
Time (seconds)

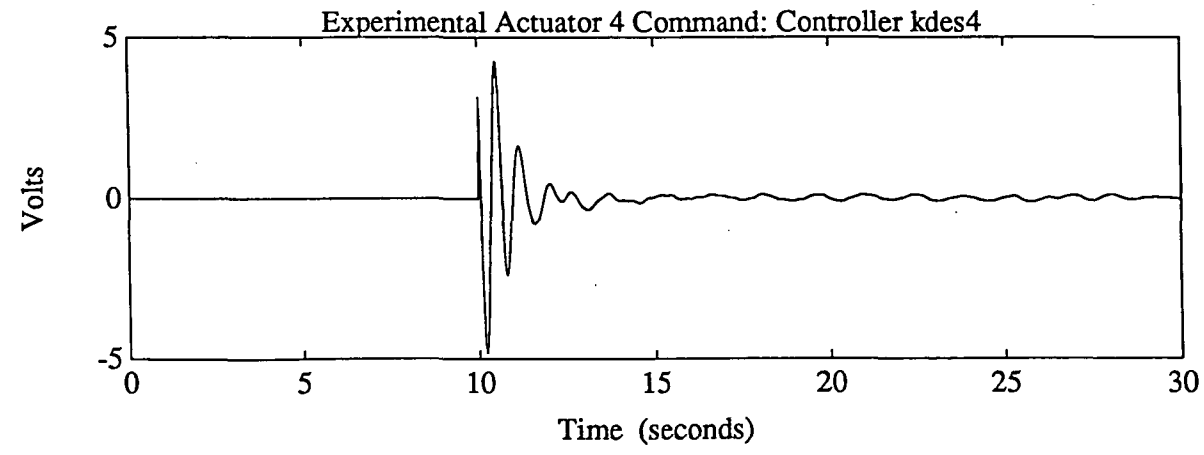
Experimental Actuator 4 Command: Controller kdes4
Volts
Time (seconds)

Figure A25

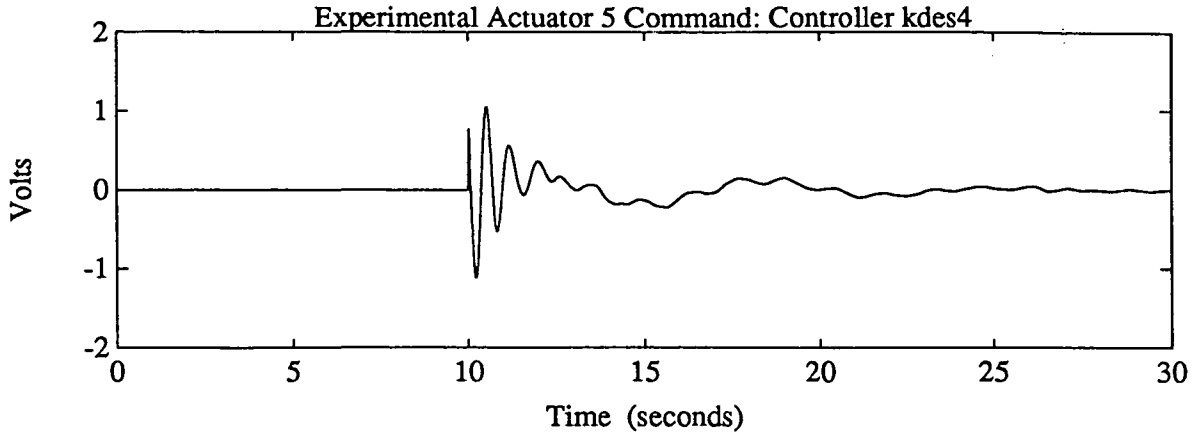
Experimental Actuator 5 Command: Controller kdes4
Volts
Time (seconds)

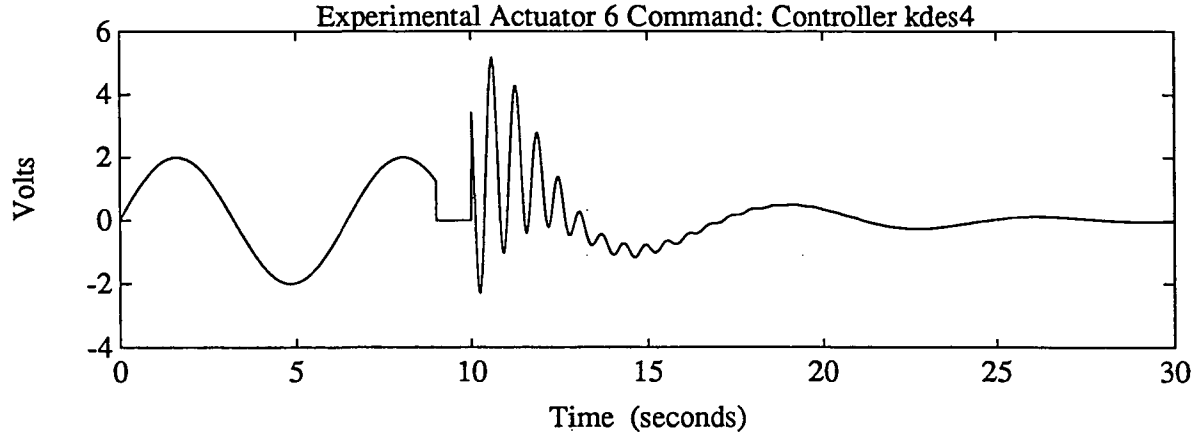
Experimental Actuator 6 Command: Controller kdes4
Volts
Time (seconds)

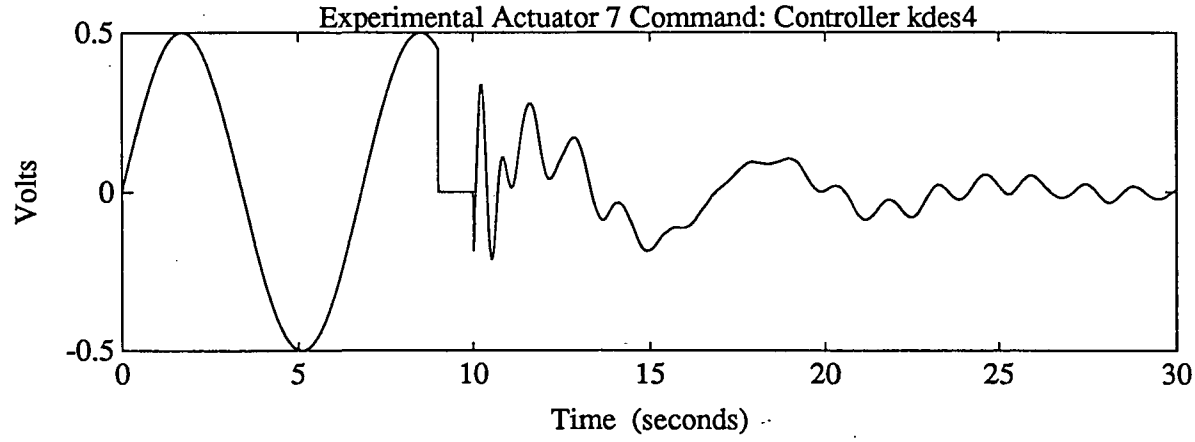
Experimental Actuator 7 Command: Controller kdes4
Volts
Time (seconds)

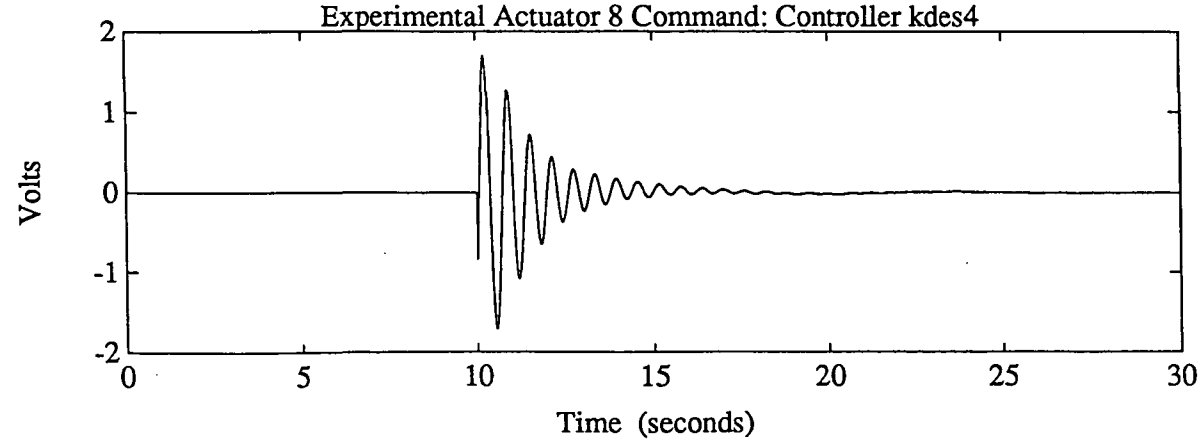
Experimental Actuator 8 Command: Controller kdes4
Volts
Time (seconds)

Figure A26

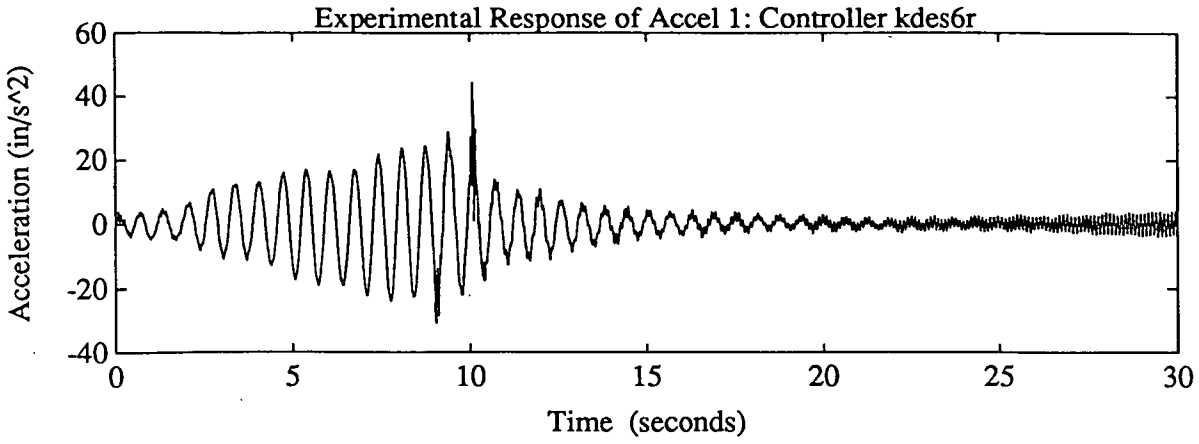
Experimental Response of Accel 1: Controller kdes6r
Acceleration (in/s^2)
60
40
20
0
-20
-40
0
5
10
15
20
25
30
Time (seconds)

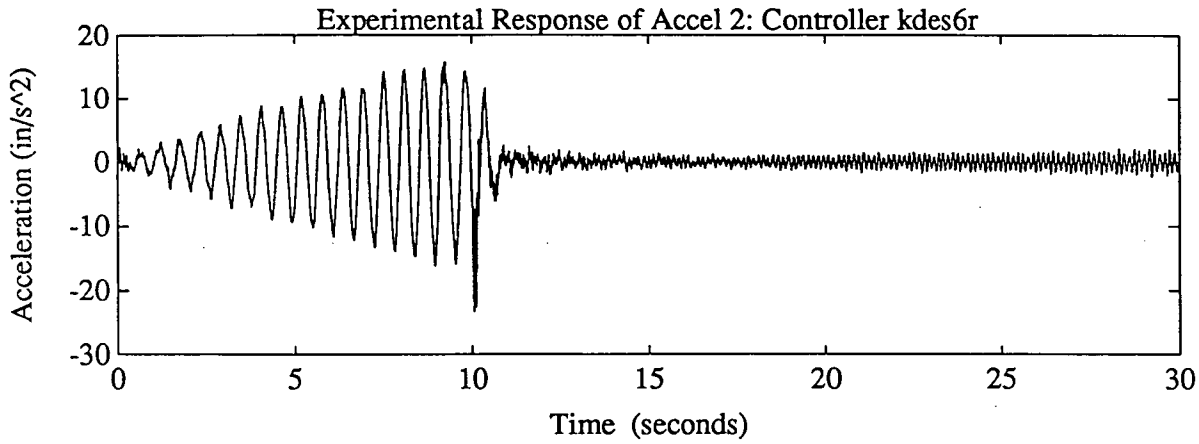
Experimental Response of Accel 2: Controller kdes6r
Acceleration (in/s^2)
20
10
0
-10
-20
-30
0
5
10
15
20
25
30
Time (seconds)

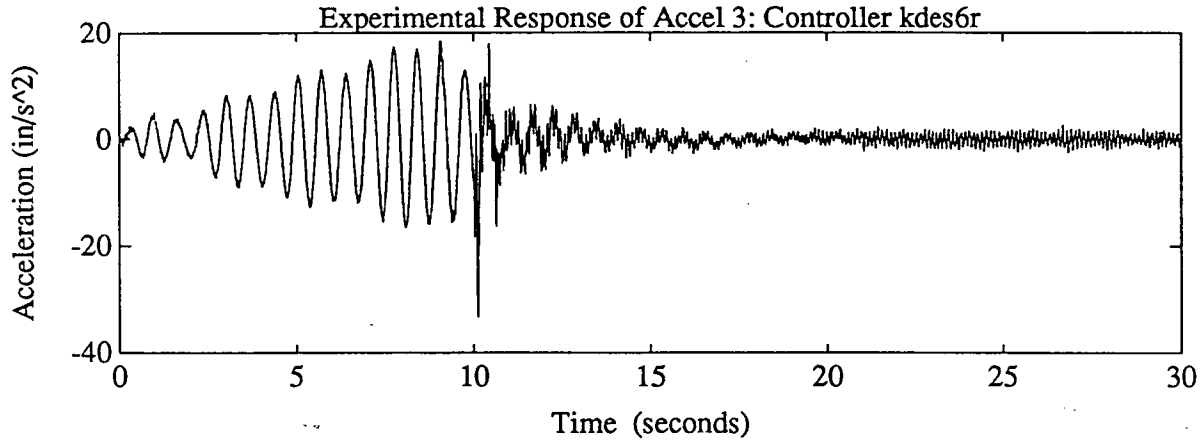
Experimental Response of Accel 3: Controller kdes6r
Acceleration (in/s^2)
20
0
-20
-40
0
5
10
15
20
25
30
Time (seconds)

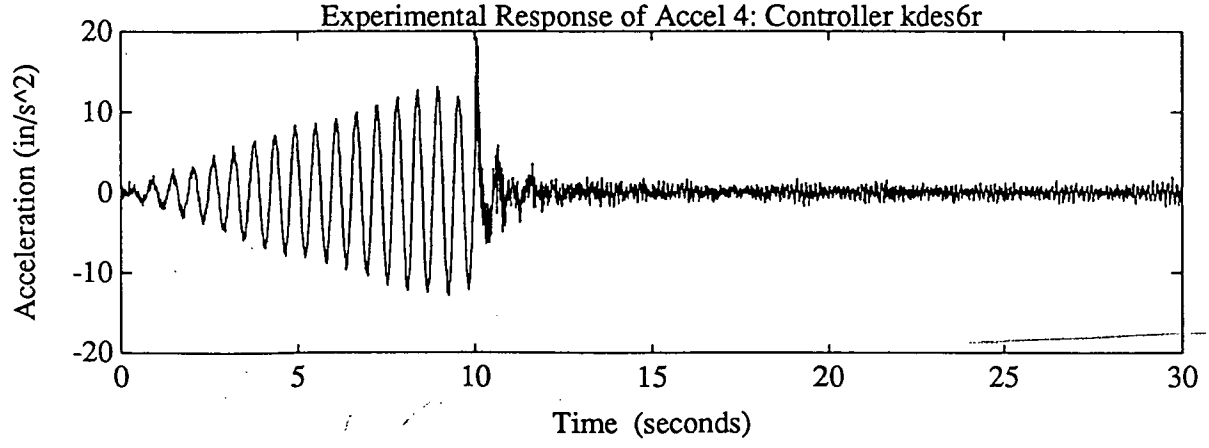
Experimental Response of Accel 4: Controller kdes6r
Acceleration (in/s^2)
20
10
0
-10
-20
0
5
10
15
20
25
30
Time (seconds)

Figure A27

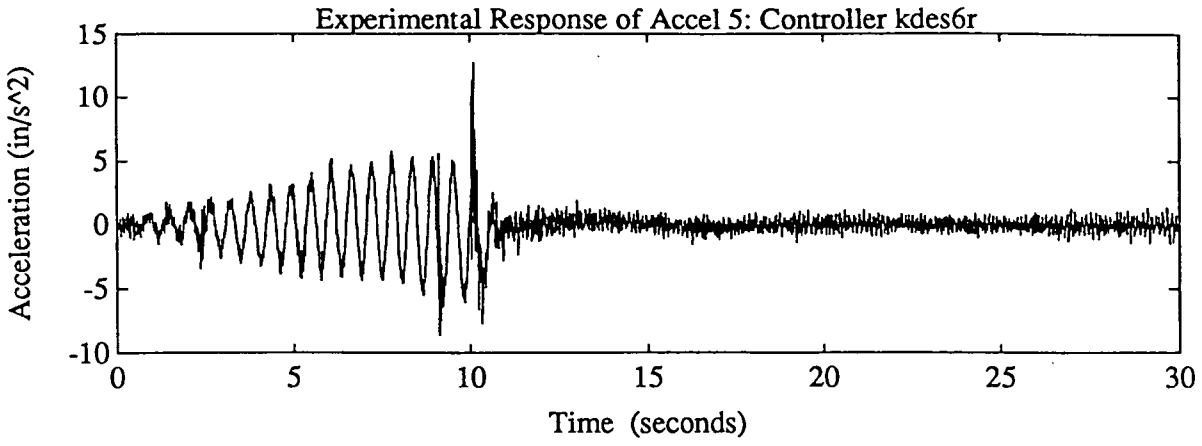
Experimental Response of Accel 5: Controller kdes6r
Acceleration (in/s^2)
Time (seconds)

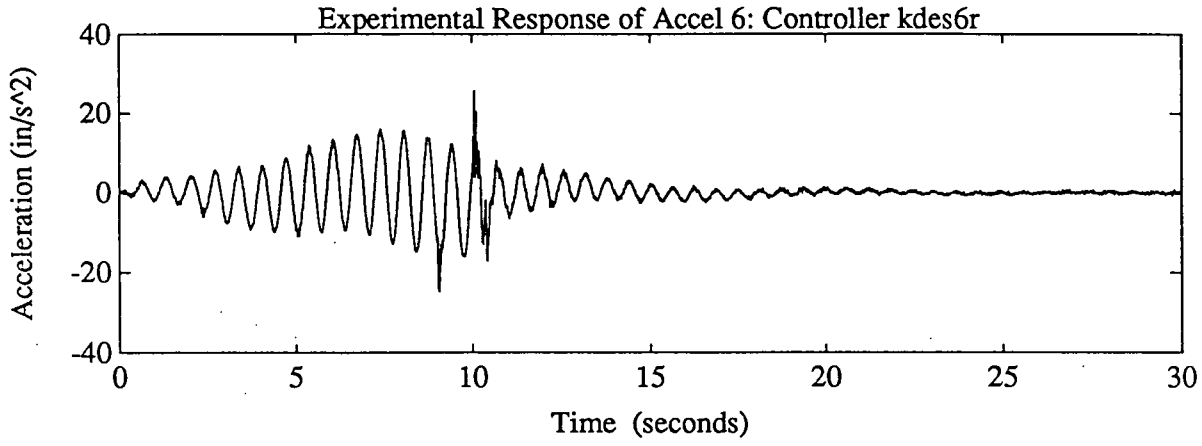
Experimental Response of Accel 6: Controller kdes6r
Acceleration (in/s^2)
Time (seconds)

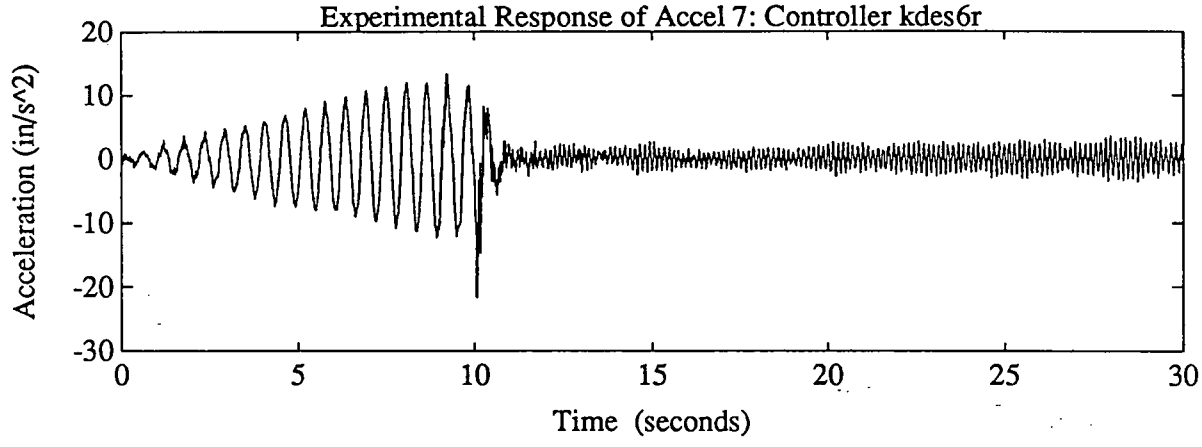
Experimental Response of Accel 7: Controller kdes6r
Acceleration (in/s^2)
Time (seconds)

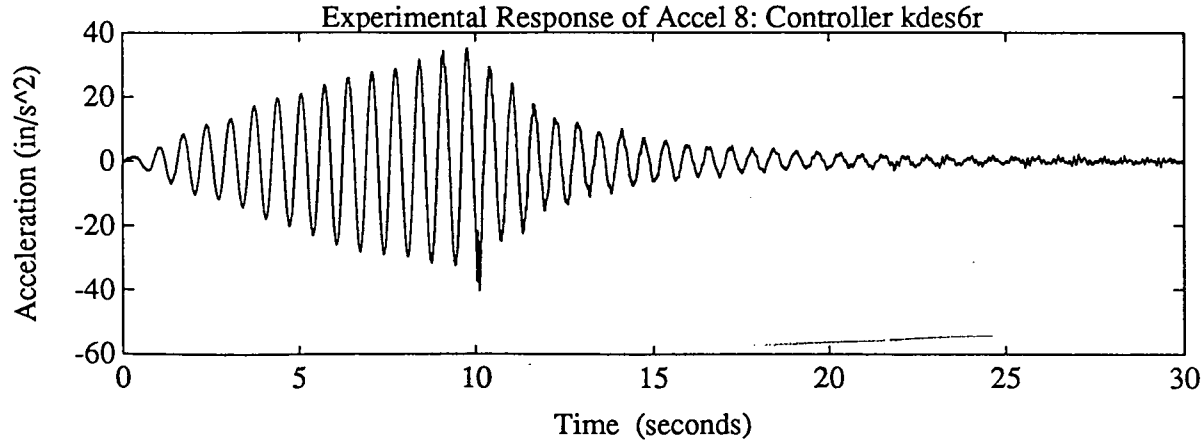
Experimental Response of Accel 8: Controller kdes6r
Acceleration (in/s^2)
Time (seconds)

Figure A28

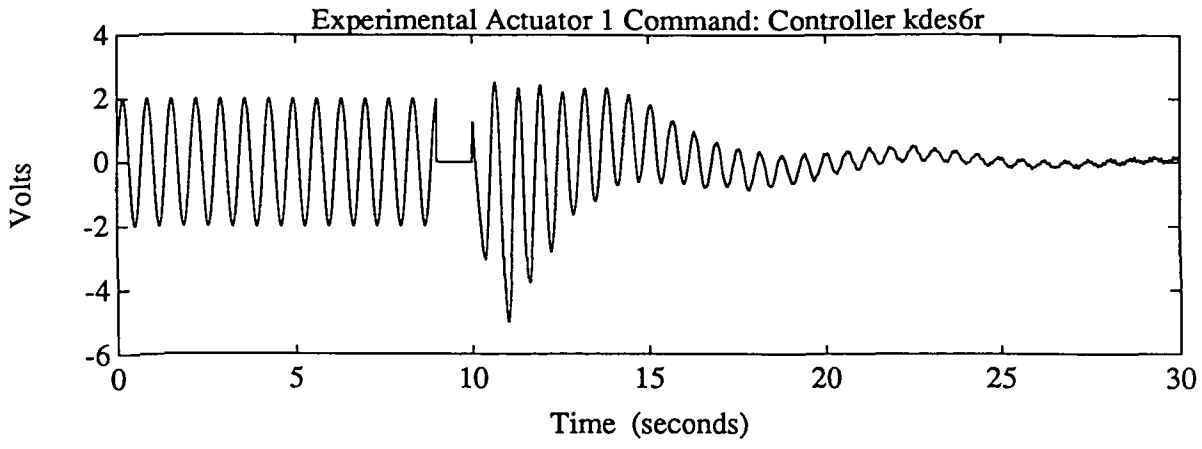
Experimental Actuator 1 Command: Controller kdes6r
Volts
Time (seconds)

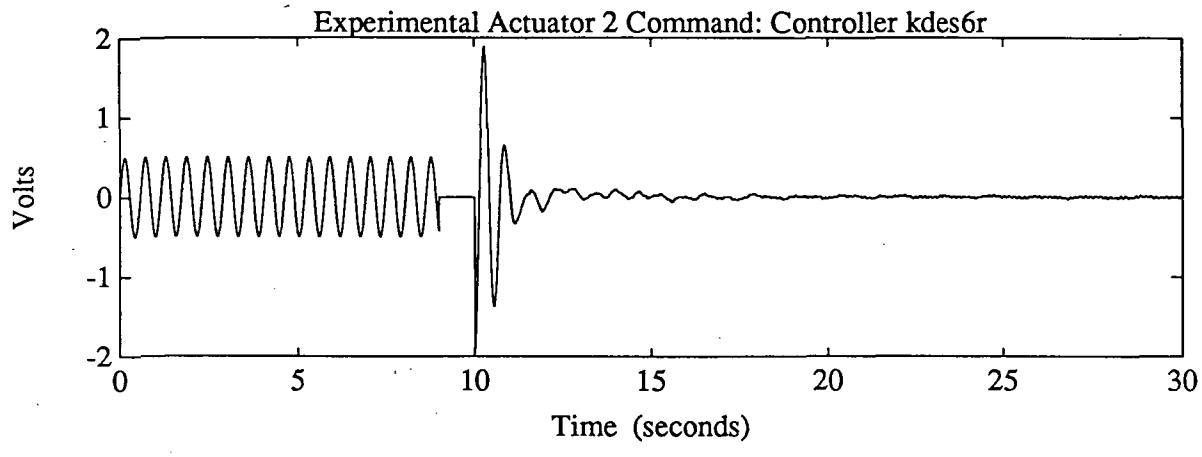
Experimental Actuator 2 Command: Controller kdes6r
Volts
Time (seconds)

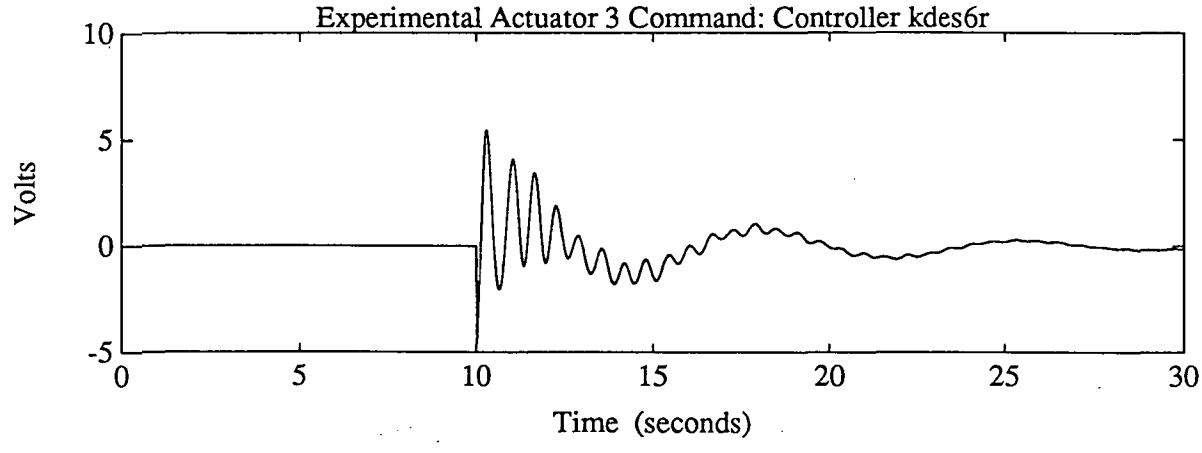
Experimental Actuator 3 Command: Controller kdes6r
Volts
Time (seconds)

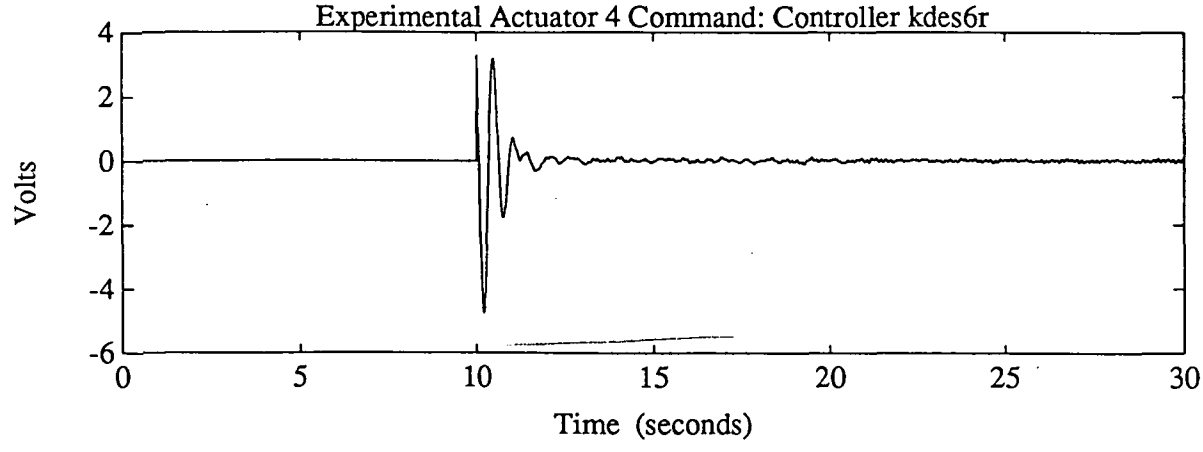
Experimental Actuator 4 Command: Controller kdes6r
Volts
Time (seconds)

Figure A29

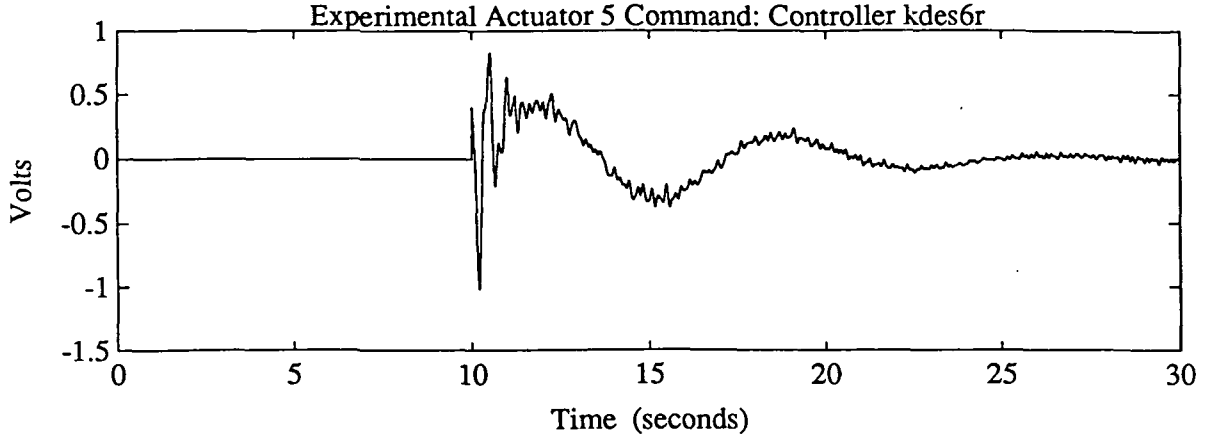
Experimental Actuator 5 Command: Controller kdes6r
Volts
Time (seconds)

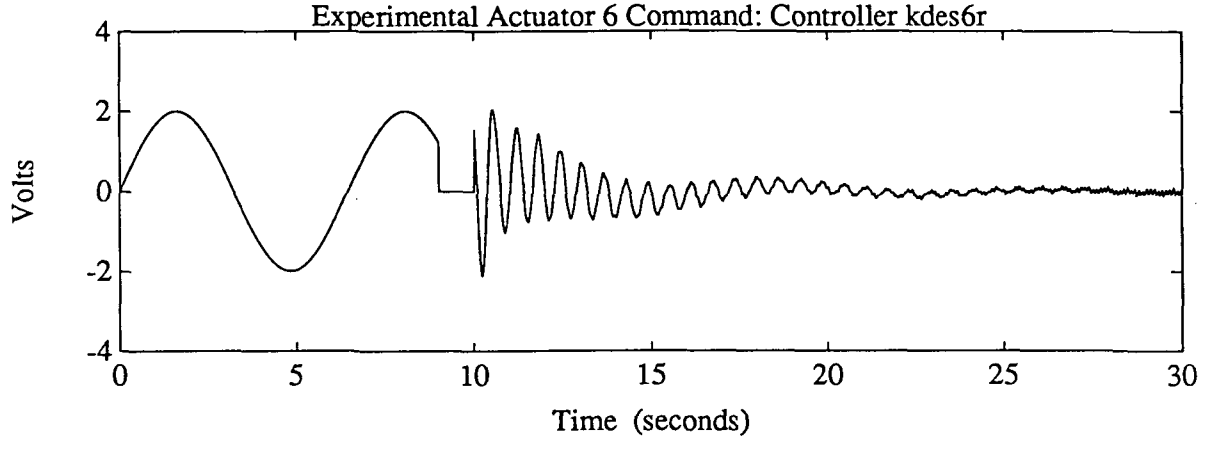
Experimental Actuator 6 Command: Controller kdes6r
Volts
Time (seconds)

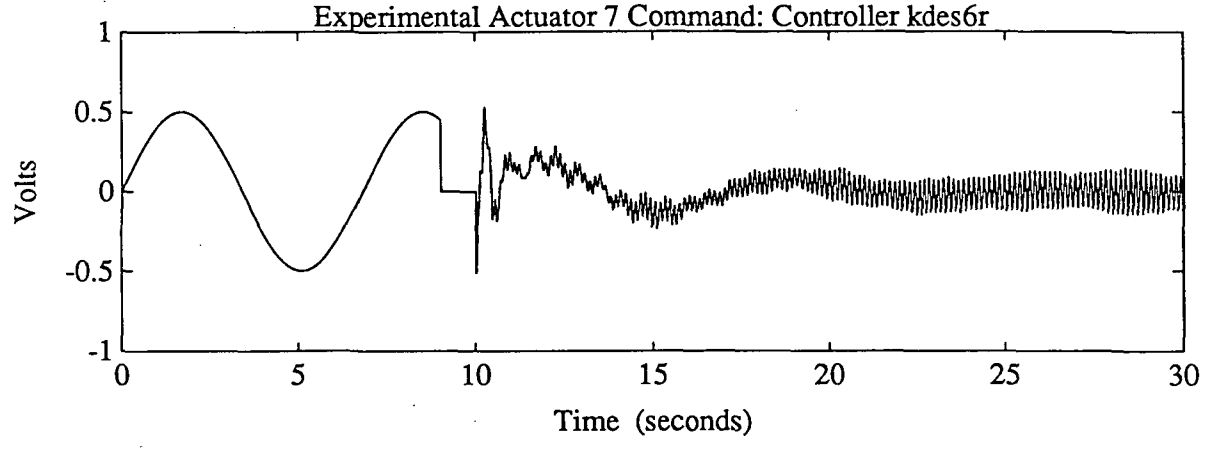
Experimental Actuator 7 Command: Controller kdes6r
Volts
Time (seconds)

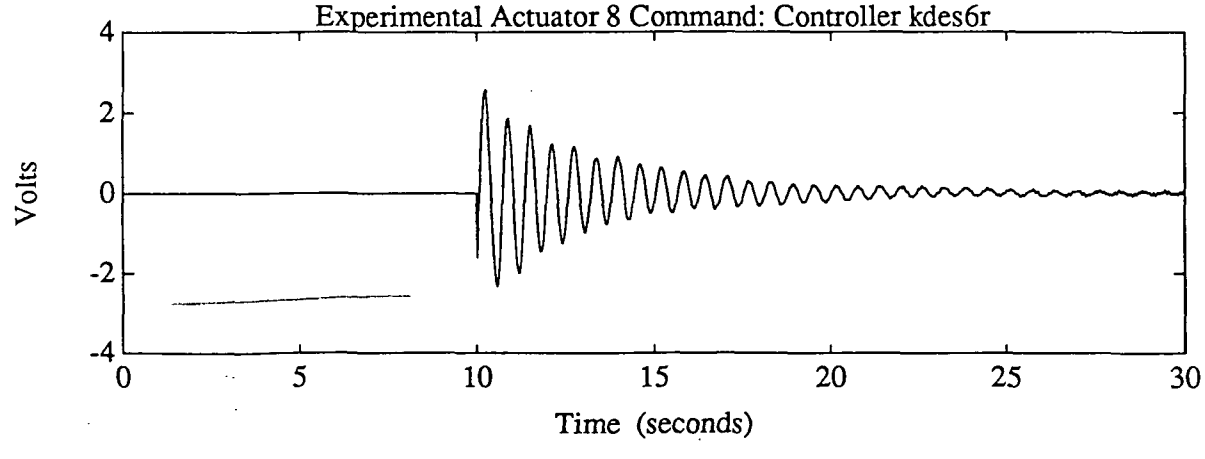
Experimental Actuator 8 Command: Controller kdes6r
Volts
Time (seconds)

Figure A30

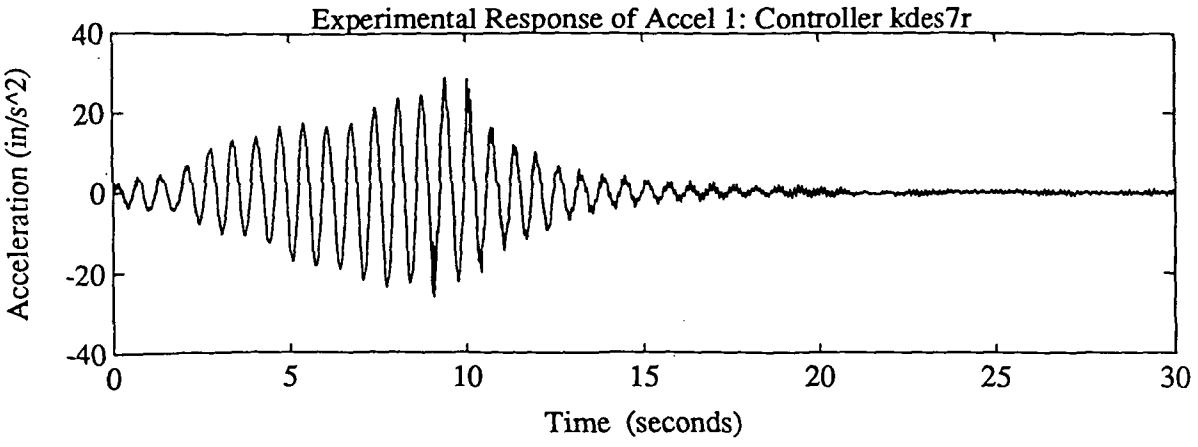
Experimental Response of Accel 1: Controller kdes7r
Acceleration (in/s^2)
40
20
0
-20
-40
0
5
10
15
20
25
30
Time (seconds)

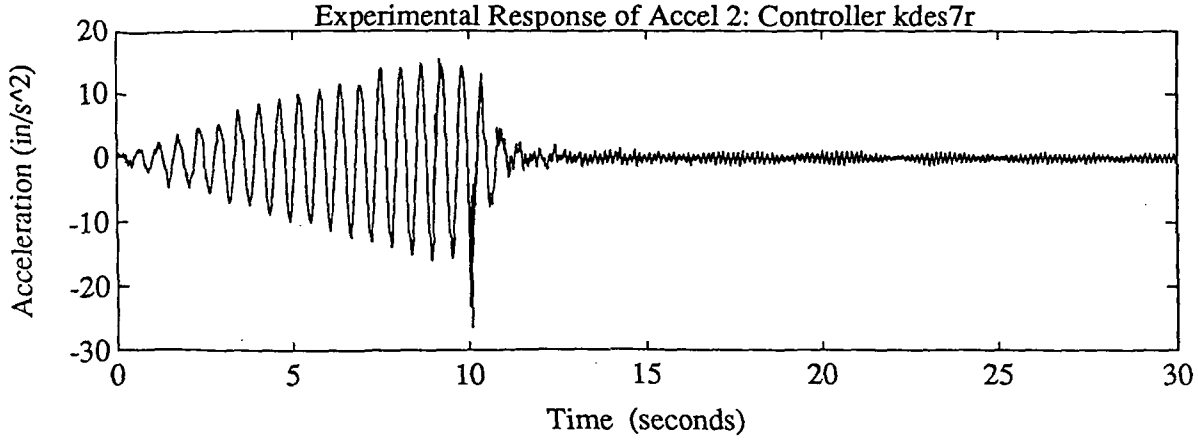
Experimental Response of Accel 2: Controller kdes7r
Acceleration (in/s^2)
20
10
0
-10
-20
-30
0
5
10
15
20
25
30
Time (seconds)

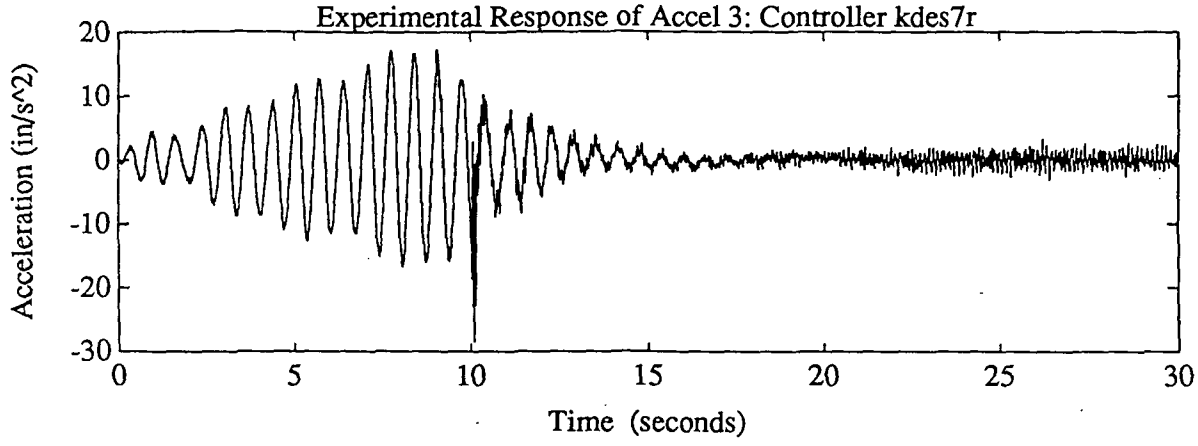
Experimental Response of Accel 3: Controller kdes7r
Acceleration (in/s^2)
20
10
0
-10
-20
-30
0
5
10
15
20
25
30
Time (seconds)

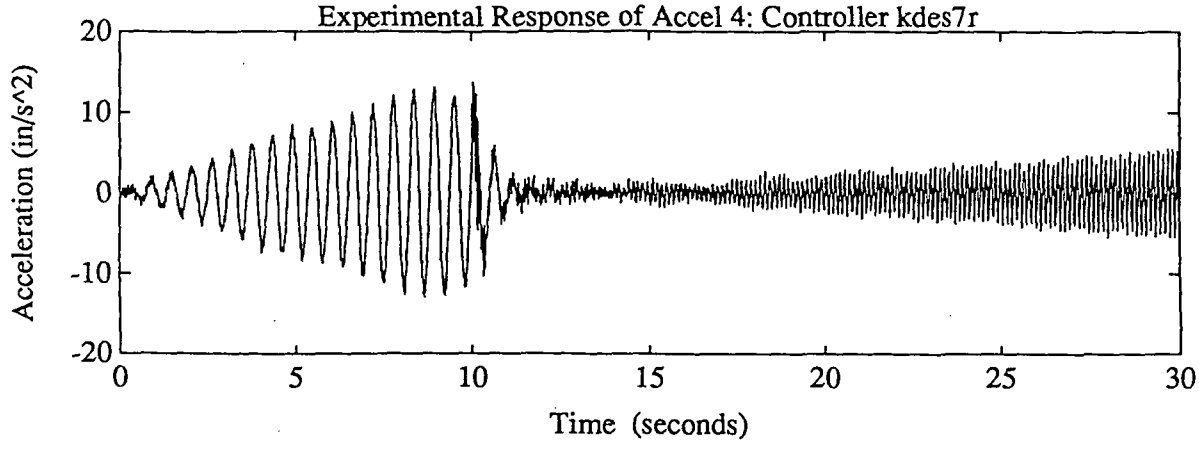
Experimental Response of Accel 4: Controller kdes7r
Acceleration (in/s^2)
20
10
0
-10
-20
0
5
10
15
20
25
30
Time (seconds)

Figure A31

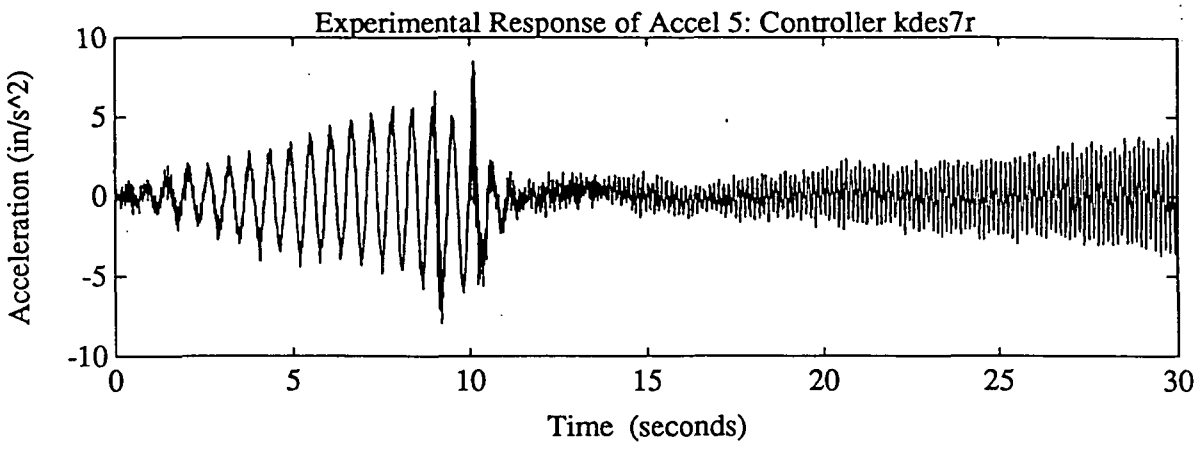
Experimental Response of Accel 5: Controller kdes7r
Acceleration (in/s^2)
10
5
0
-5
-10
0
5
10
15
20
25
30
Time (seconds)

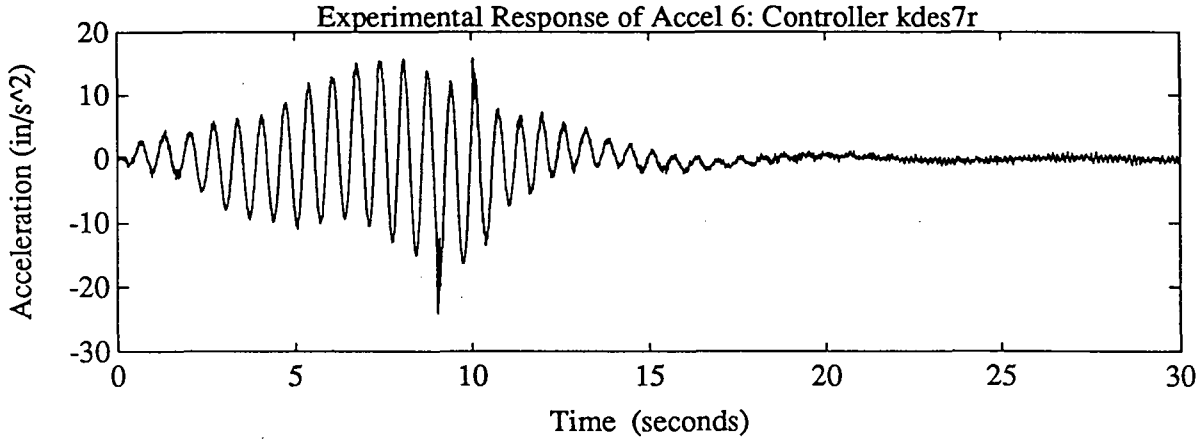
Experimental Response of Accel 6: Controller kdes7r
Acceleration (in/s^2)
20
10
0
-10
-20
-30
0
5
10
15
20
25
30
Time (seconds)

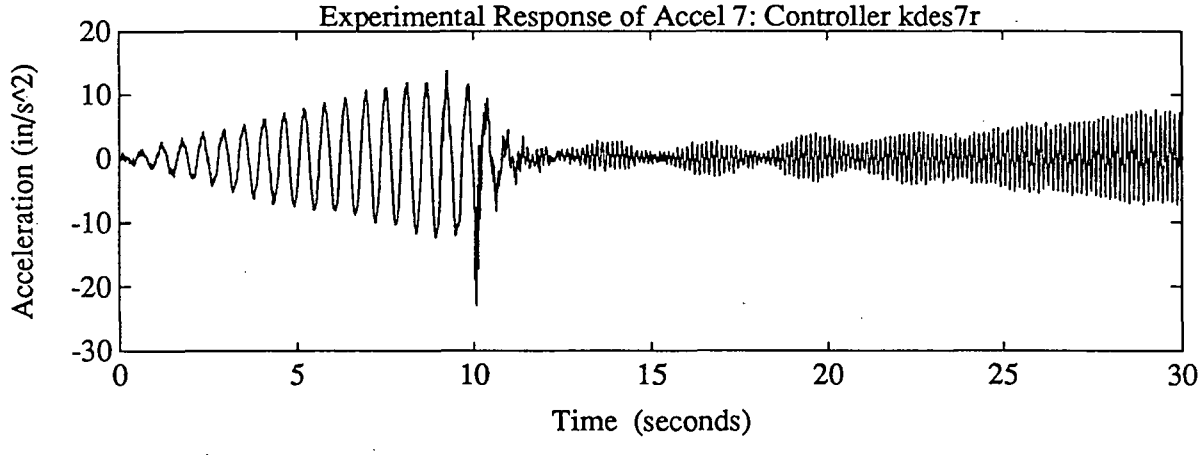
Experimental Response of Accel 7: Controller kdes7r
Acceleration (in/s^2)
20
10
0
-10
-20
-30
0
5
10
15
20
25
30
Time (seconds)

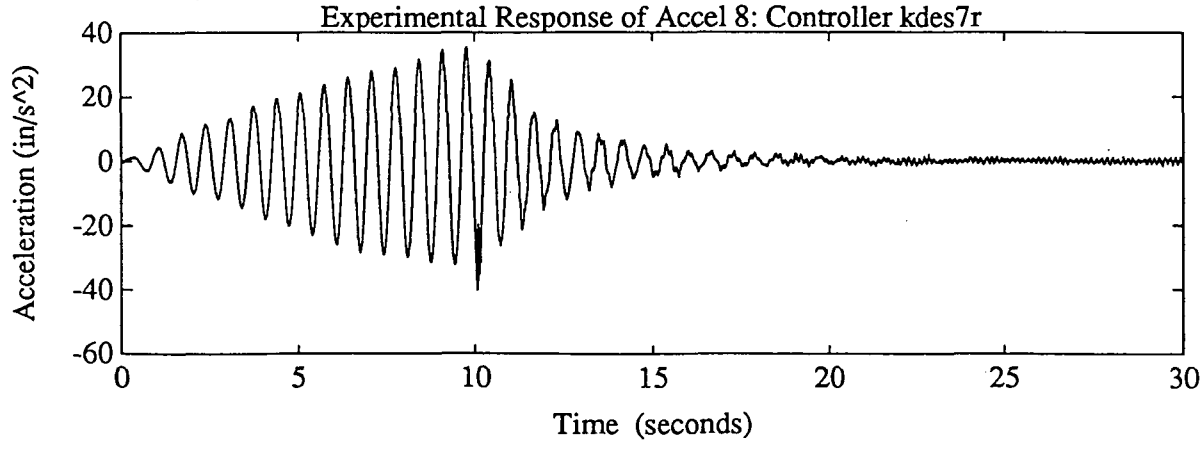
Experimental Response of Accel 8: Controller kdes7r
Acceleration (in/s^2)
40
20
0
-20
-40
-60
0
5
10
15
20
25
30
Time (seconds)

Figure A32

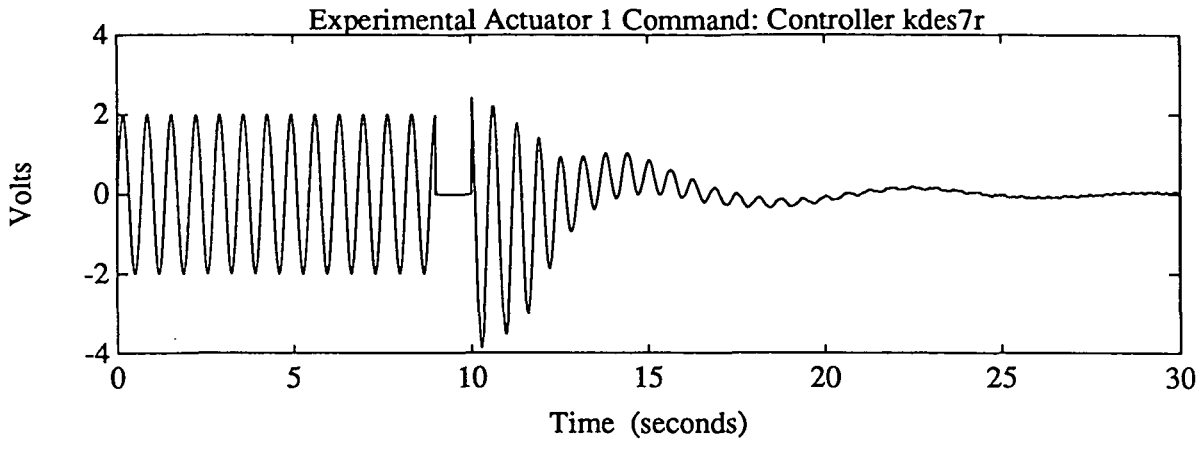
Experimental Actuator 1 Command: Controller kdes7r
Volts
Time (seconds)

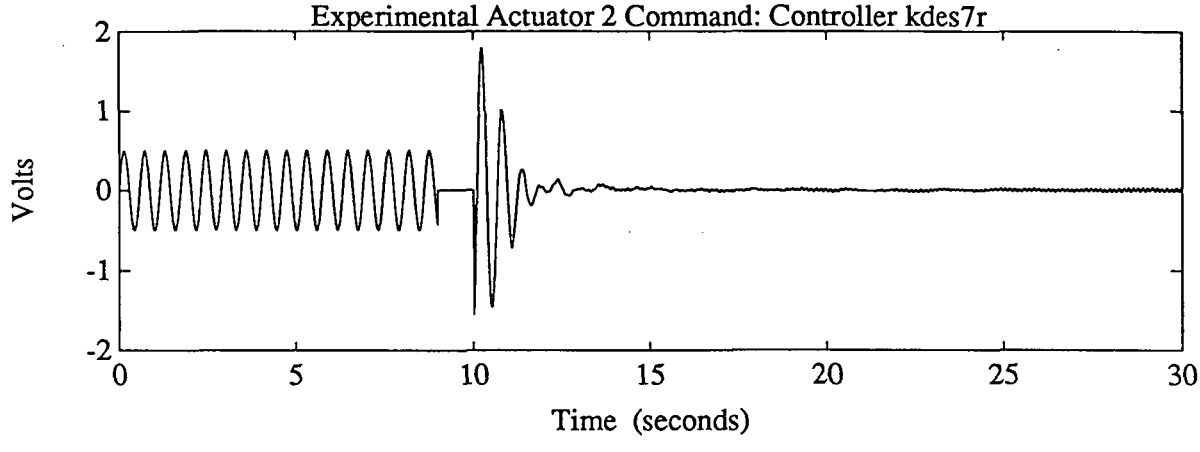
Experimental Actuator 2 Command: Controller kdes7r
Volts
Time (seconds)

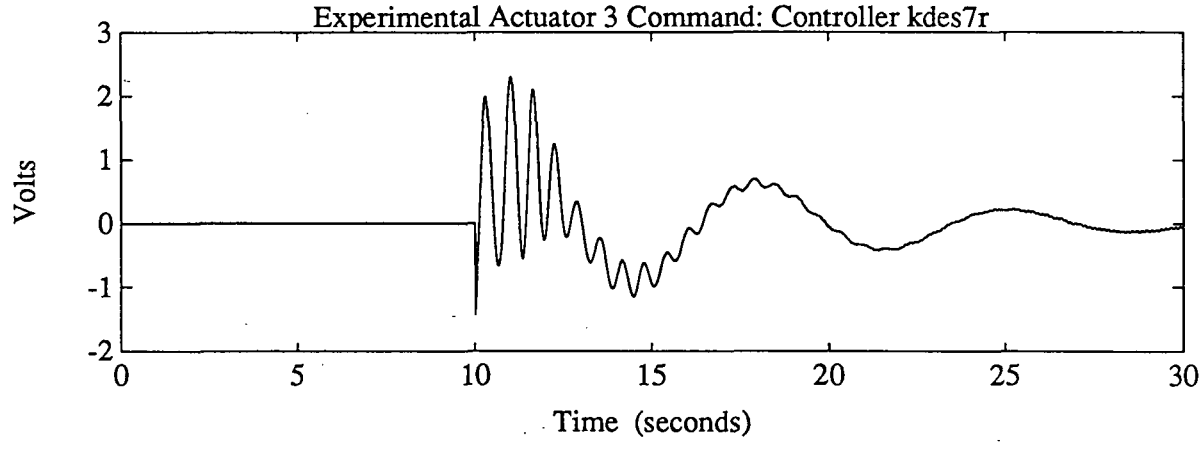
Experimental Actuator 3 Command: Controller kdes7r
Volts
Time (seconds)

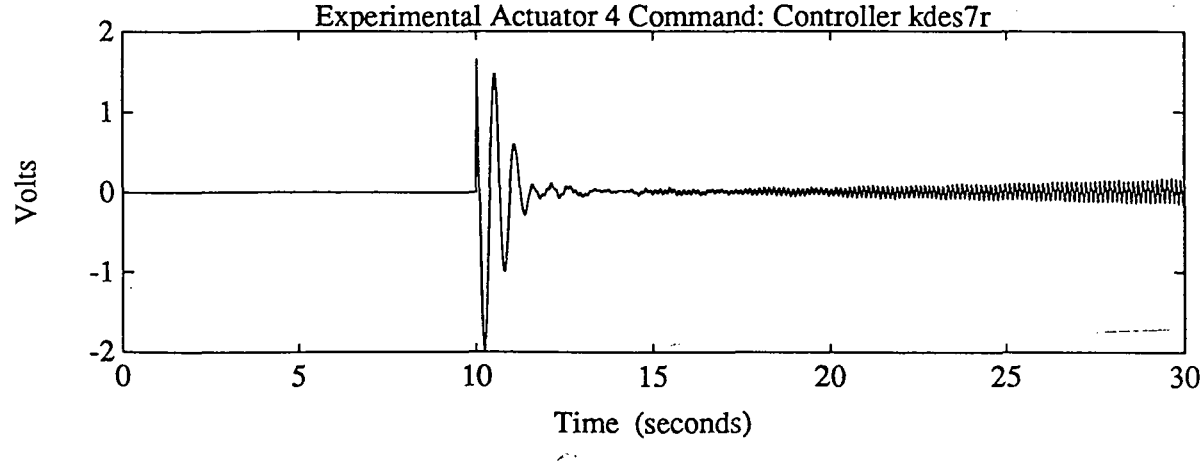
Experimental Actuator 4 Command: Controller kdes7r
Volts
Time (seconds)

Figure A33

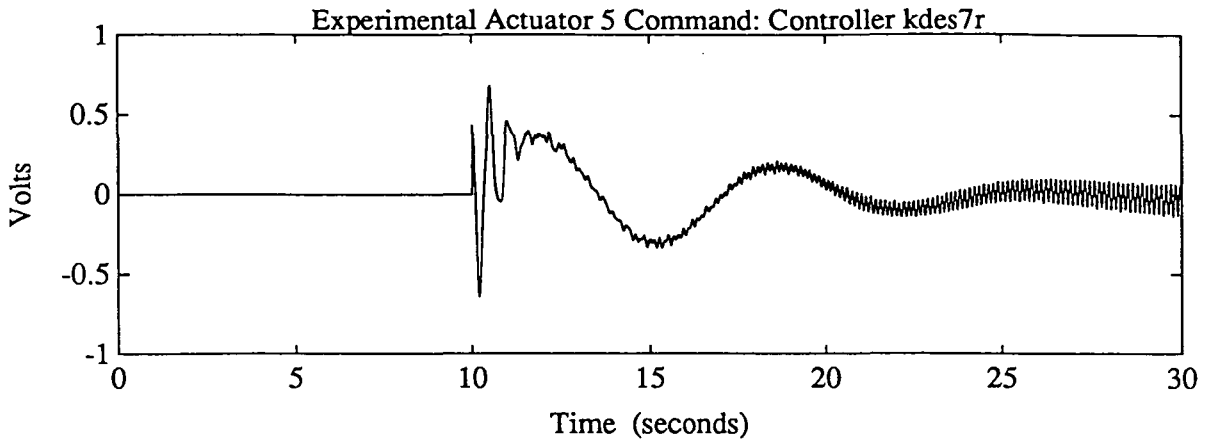
Experimental Actuator 5 Command: Controller kdes7r
Volts
Time (seconds)

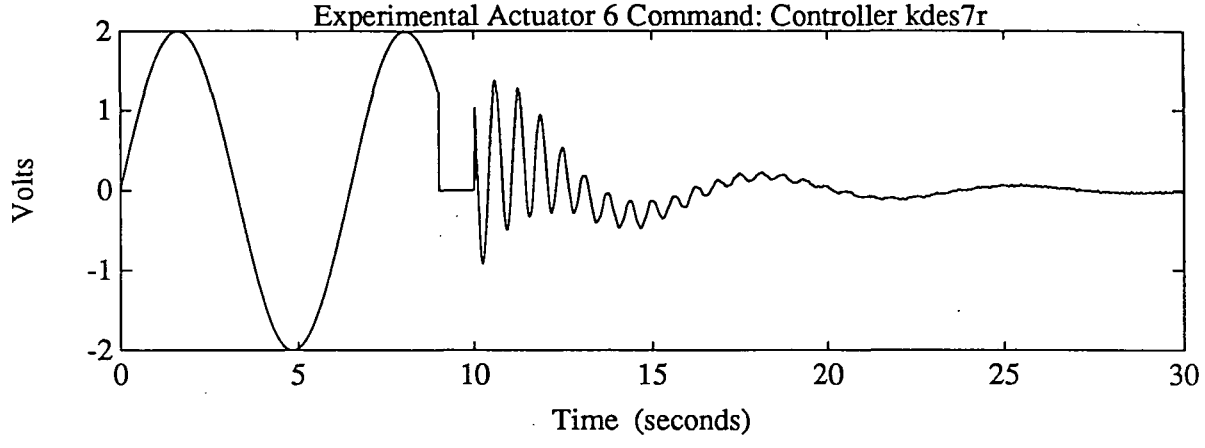
Experimental Actuator 6 Command: Controller kdes7r
Volts
Time (seconds)

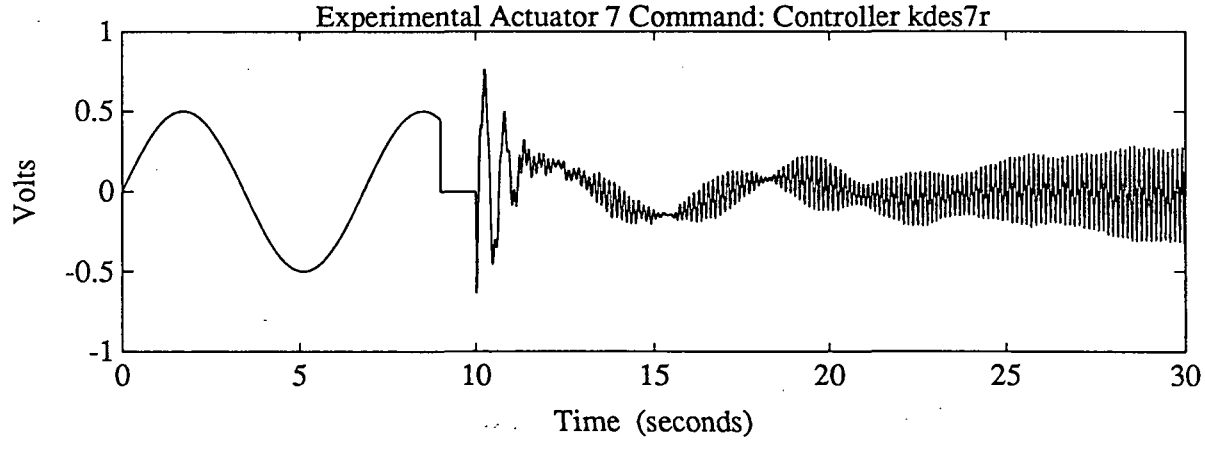
Experimental Actuator 7 Command: Controller kdes7r
Volts
Time (seconds)

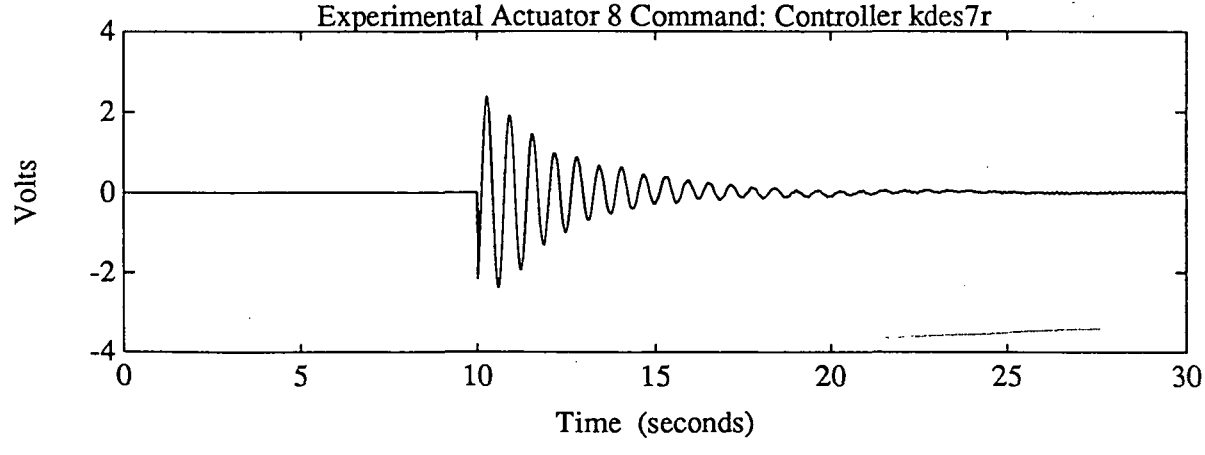
Experimental Actuator 8 Command: Controller kdes7r
Volts
Time (seconds)

Figure A34

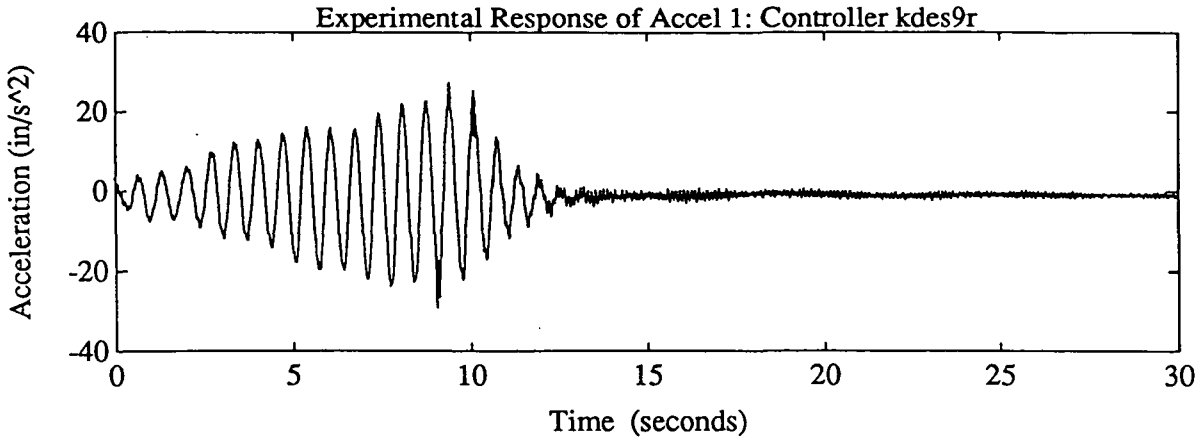
Experimental Response of Accel 1: Controller kdes9r
Acceleration (in/s^2)
40
20
0
-20
-40
0
5
10
15
20
25
30
Time (seconds)

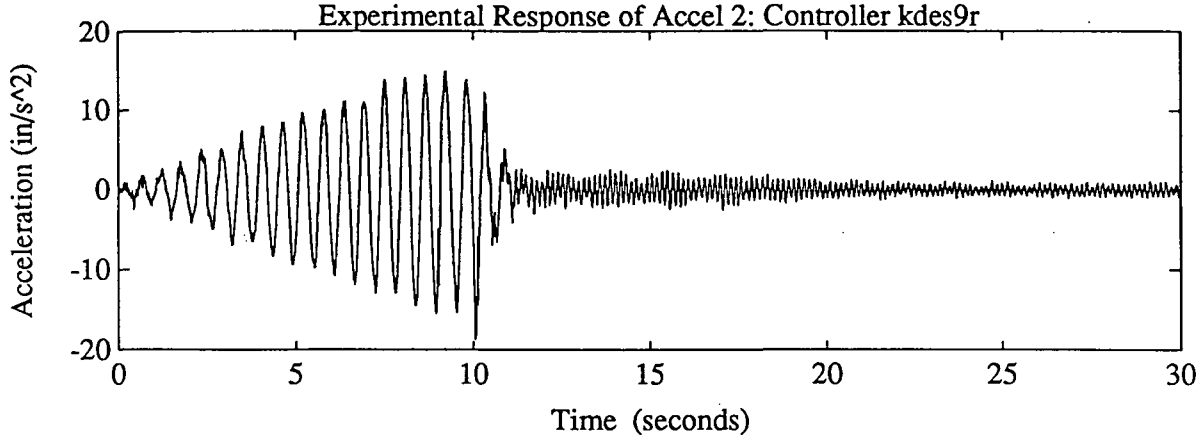
Experimental Response of Accel 2: Controller kdes9r
Acceleration (in/s^2)
20
10
0
-10
-20
0
5
10
15
20
25
30
Time (seconds)

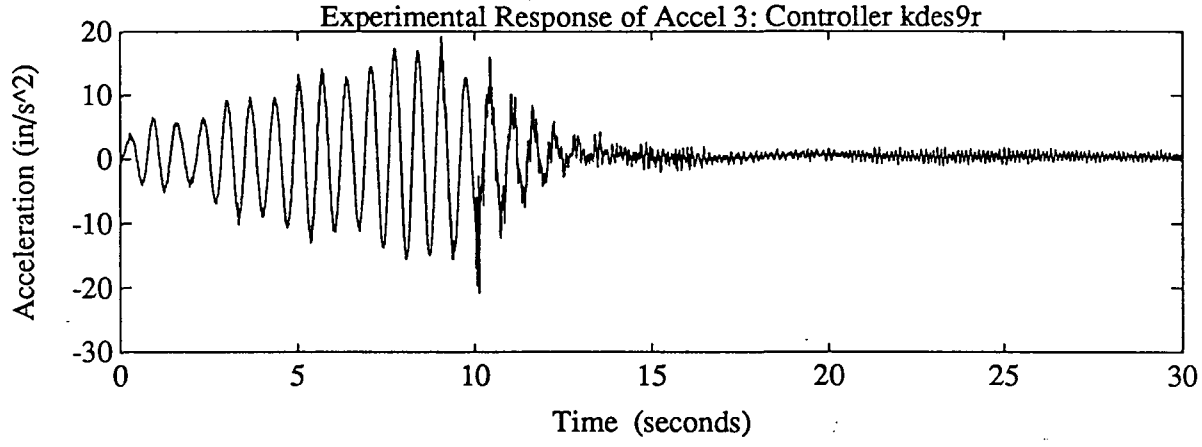
Experimental Response of Accel 3: Controller kdes9r
Acceleration (in/s^2)
20
10
0
-10
-20
-30
0
5
10
15
20
25
30
Time (seconds)

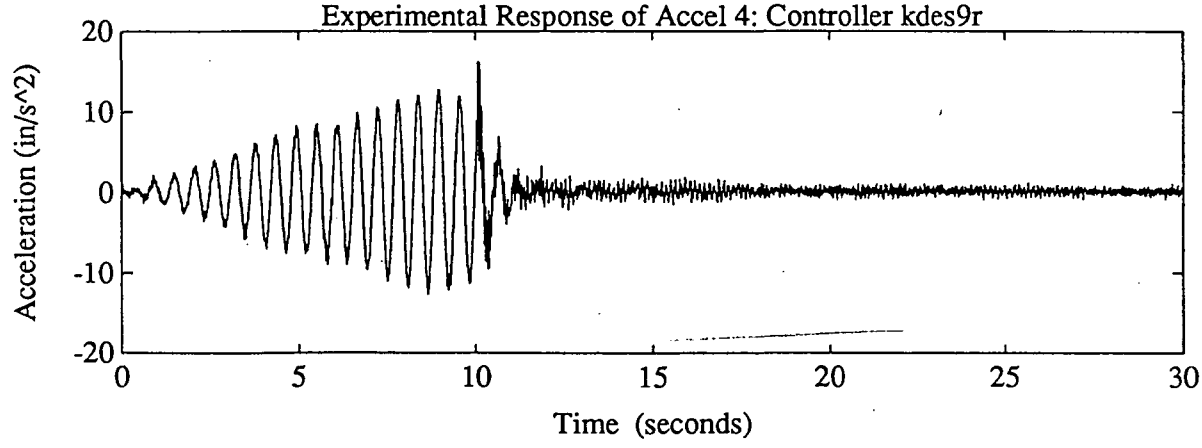
Experimental Response of Accel 4: Controller kdes9r
Acceleration (in/s^2)
20
10
0
-10
-20
0
5
10
15
20
25
30
Time (seconds)

Figure A35

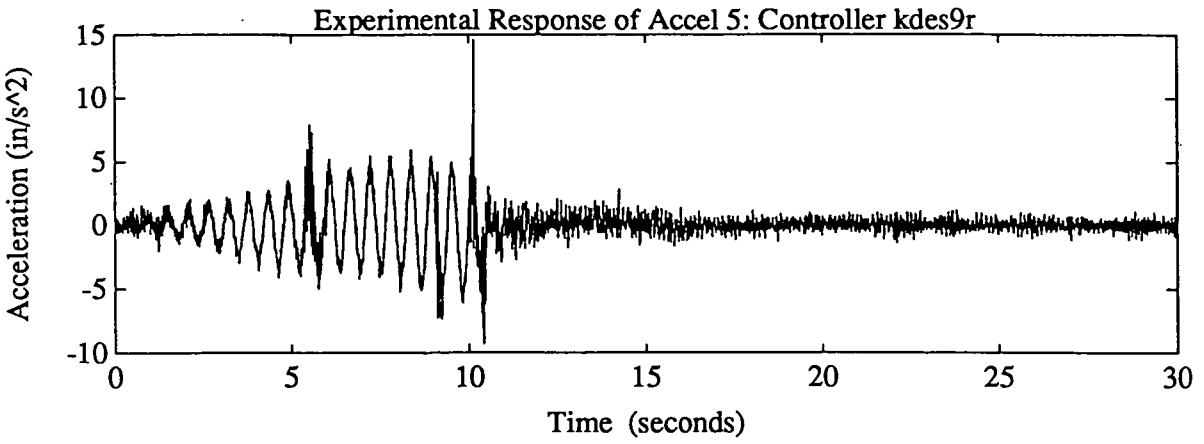
Experimental Response of Accel 5: Controller kdes9r
Acceleration (in/s^2)
15
10
5
0
-5
-10
0
5
10
15
20
25
30
Time (seconds)

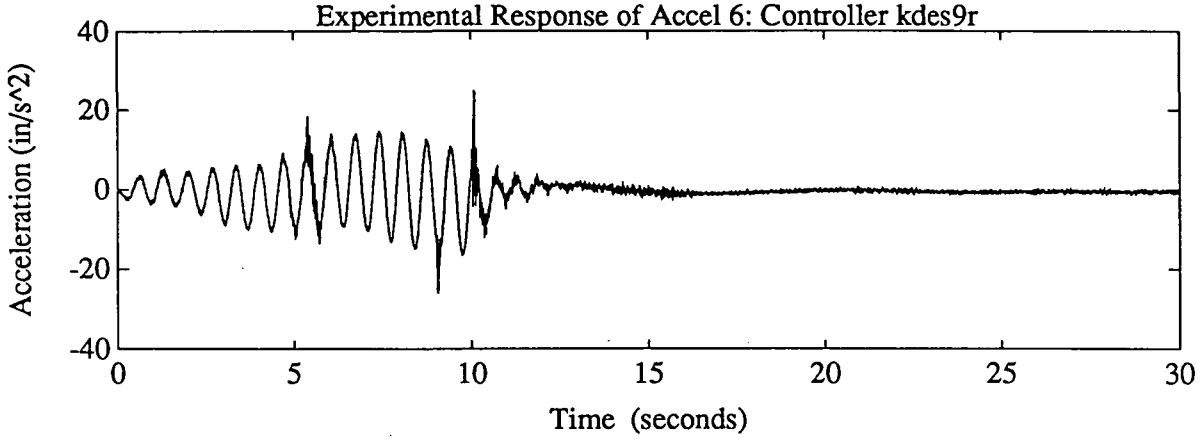
Experimental Response of Accel 6: Controller kdes9r
Acceleration (in/s^2)
40
20
0
-20
-40
0
5
10
15
20
25
30
Time (seconds)

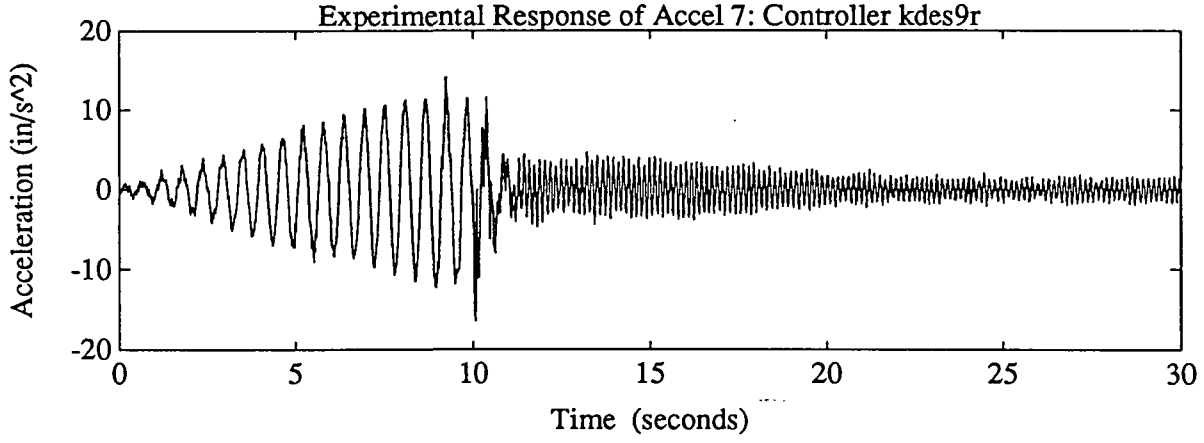
Experimental Response of Accel 7: Controller kdes9r
Acceleration (in/s^2)
20
10
0
-10
-20
0
5
10
15
20
25
30
Time (seconds)

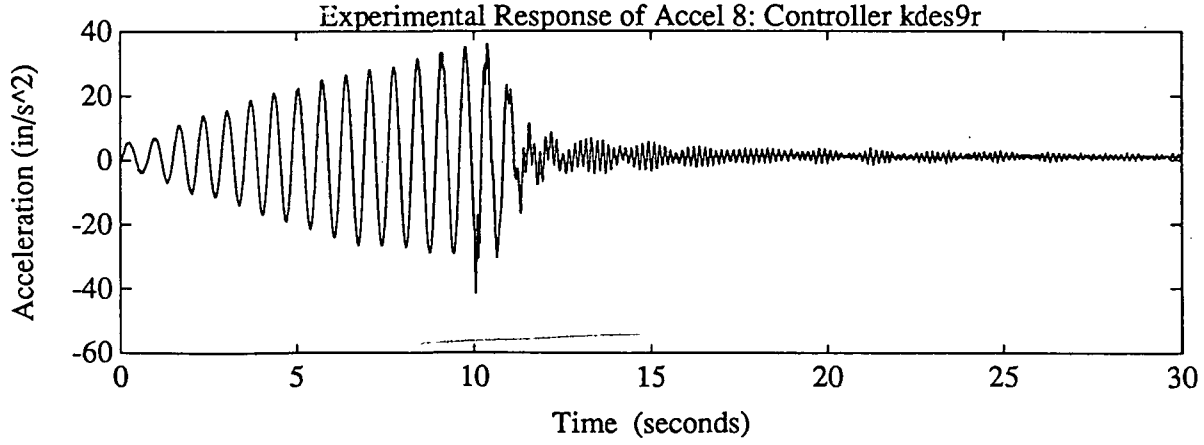
Experimental Response of Accel 8: Controller kdes9r
Acceleration (in/s^2)
40
20
0
-20
-40
-60
0
5
10
15
20
25
30
Time (seconds)

Figure A36

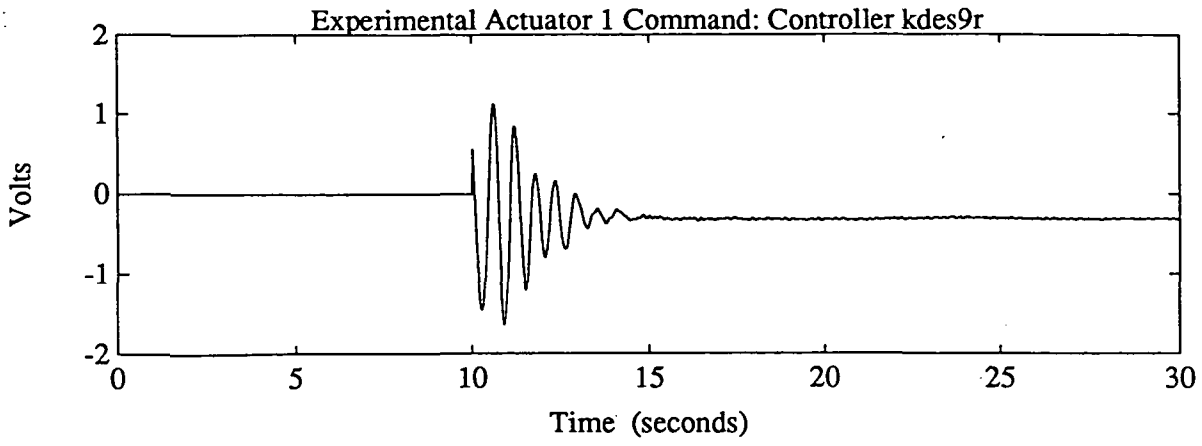
Experimental Actuator 1 Command: Controller kdes9r
Volts
Time (seconds)

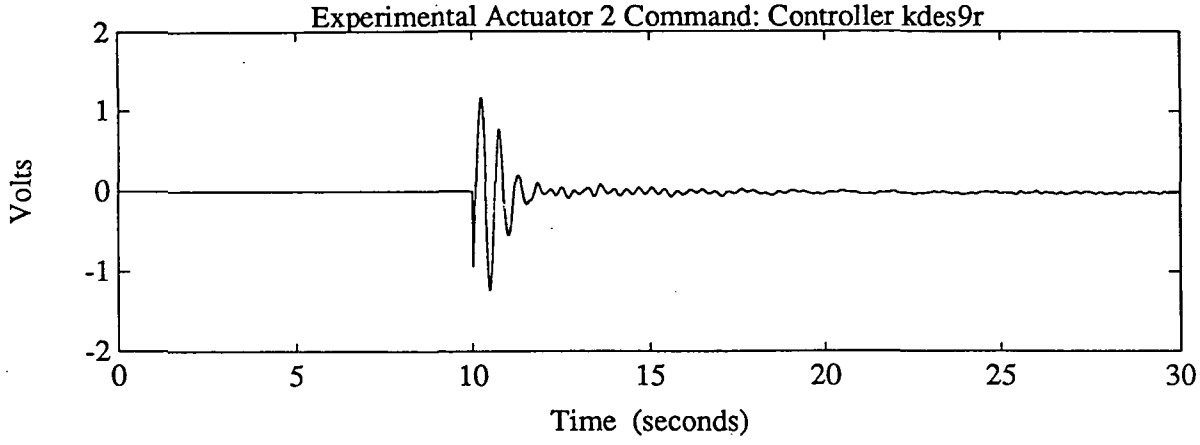
Experimental Actuator 2 Command: Controller kdes9r
Volts
Time (seconds)

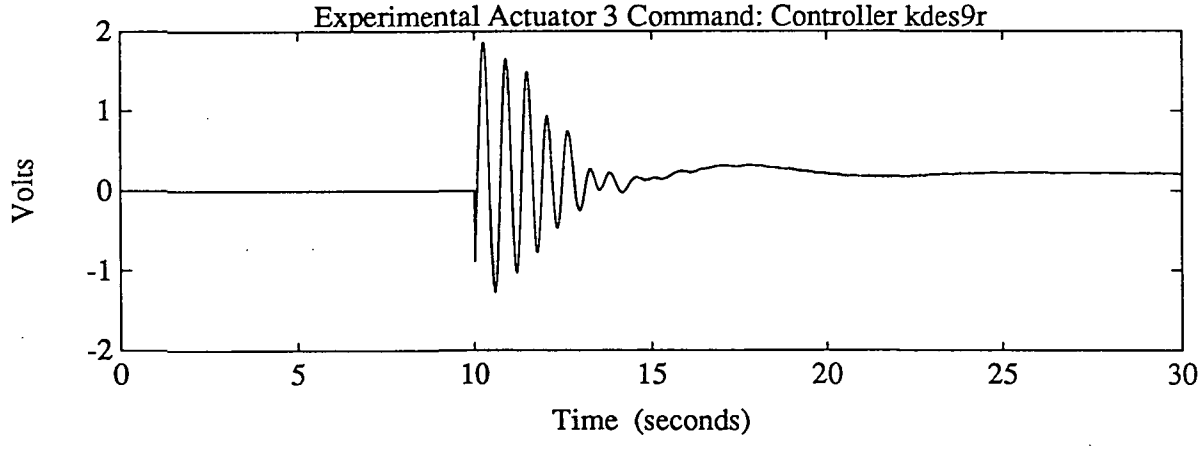
Experimental Actuator 3 Command: Controller kdes9r
Volts
Time (seconds)

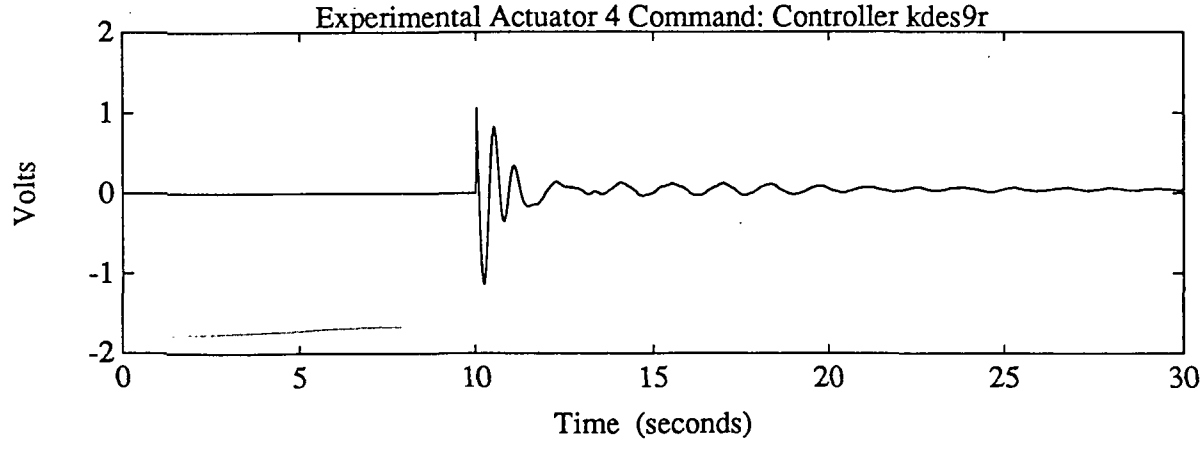
Experimental Actuator 4 Command: Controller kdes9r
Volts
Time (seconds)

Figure A37

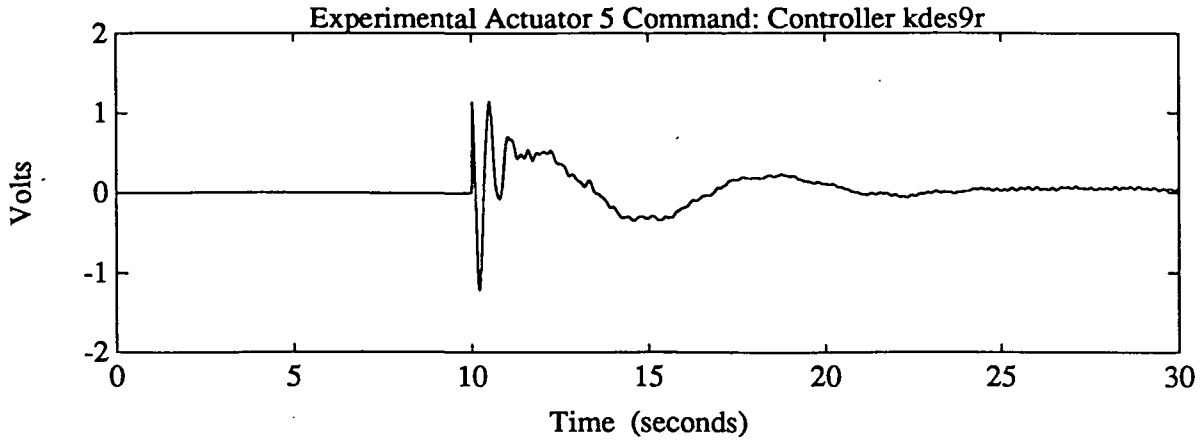
Experimental Actuator 5 Command: Controller kdes9r
Volts
2
1
0
-1
-2
0
5
10
15
20
25
30
Time (seconds)

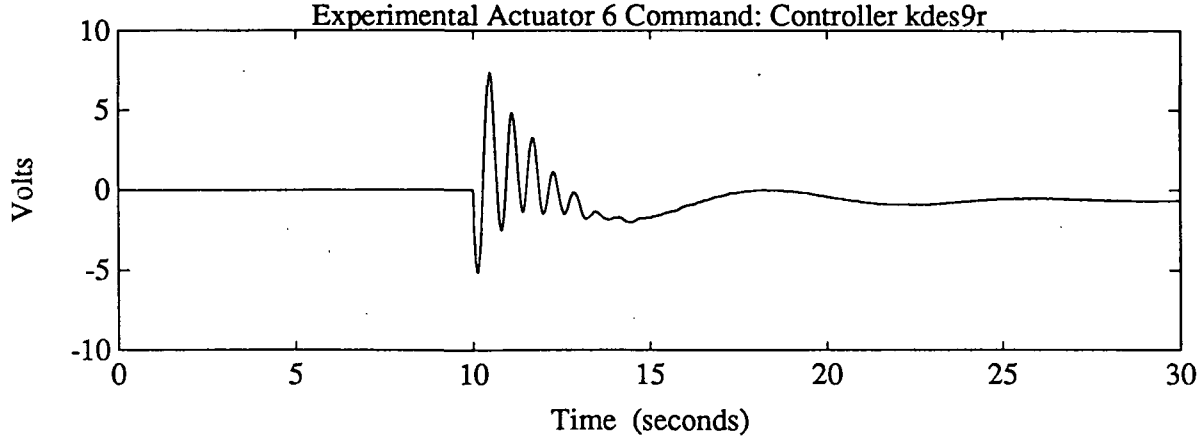
Experimental Actuator 6 Command: Controller kdes9r
Volts
10
5
0
-5
-10
0
5
10
15
20
25
30
Time (seconds)

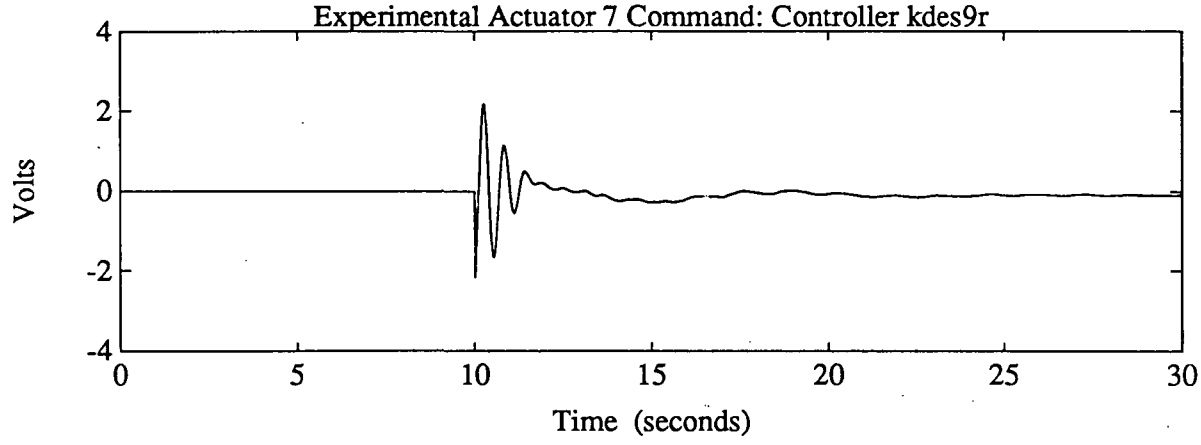
Experimental Actuator 7 Command: Controller kdes9r
Volts
4
2
0
-2
-4
0
5
10
15
20
25
30
Time (seconds)

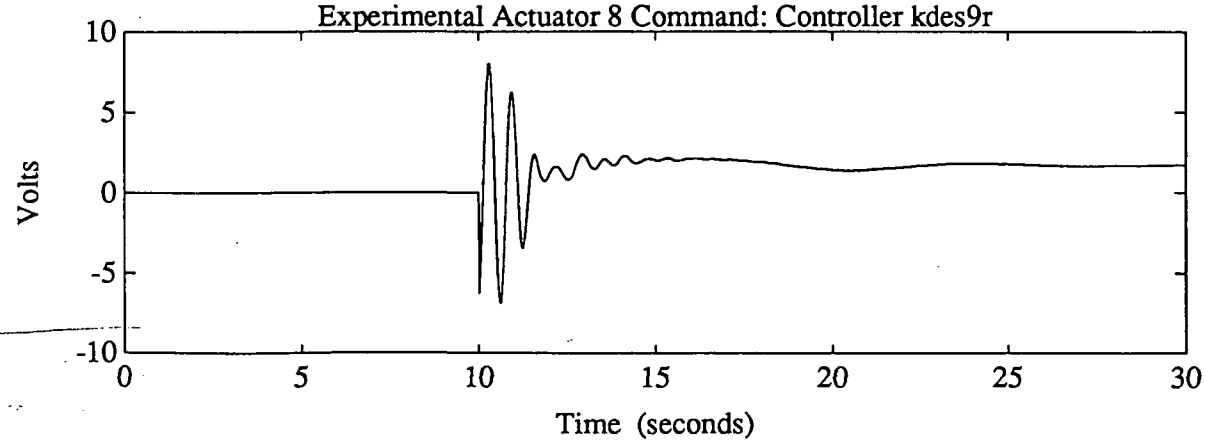
Experimental Actuator 8 Command: Controller kdes9r
Volts
10
5
0
-5
-10
0
5
10
15
20
25
30
Time (seconds)

Figure A38